ASD TECHNICAL REPORT 61-73

EFFECT OF CREEP-EXPOSURE ON MECHANICAL PROPERTIES OF RENE' 41

Jeremy V Gluck
James W. Freeman
The University of Michigan

June 1961

Materials Central
Contract No. AF 33(616)-6462
Project No. 7381

AERONAUTICAL SYSTEMS DIVISION
AIR FORCE SYSTEMS COMMAND
UNITED STATES AIR FORCE
WRIGHT-PATTERSON AIR FORCE BASE, OHIO

FOREWORD

This report was prepared by The University of Michigan, Department of Chemical and Metallurgical Engineering under USAF Contract No. AF 33(616)-6462. This contract was conducted under Project No. 7381, "Materials Application", Task No. 73810, "Exploratory Design and Prototype Development". The work was administered under the direction of the Materials Central, Deputy for Advanced Systems Technology, Aeronautical Systems Division, with Mr. W. H. Hill acting as project engineer.

This report covers work conducted from April 1, 1959 to March 31, 1960.

The research is identified in the records of The University of Michigan as Project No. 02902.

ABSTRACT

An investigation of the influence of creep-exposure on the mechanical properties at room temperature of Rene' 41 alloy is in progress. The objectives are to delineate the conditions causing changes in these properties and to develop general principles for predicting the influence of creep on such properties of nickel-base superalloys. The results obtained to date for exposures at 1200° to 1800°F and for 10 to 200 hours show that thermally-induced structural changes reduce room temperature strength and ductility when the exposure temperatures are 1500°F or higher. Limited data indicate that surface reactions also reduce properties with the temperature range of the effect extending to lower temperatures than 1500°F.

Creep accelerated the structural changes to some extent. In addition, it raised yield strength by a Bauschinger effect. Strain hardening, possibly in combination with strain-induced precipitation hardening raised tensile strength for exposure below 1500°F. In addition, ductility was reduced more in the presence of creep than by thermally-induced structural changes. Creep strains approaching the ultimate ductility of the alloy at 1200° and 1300°F induced deep cracking which reduced properties. This type of an effect was not found at higher temperatures.

The loss in strength from thermally-induced structural changes appeared to be due to overaging of the gamma prime precipitate. The loss in ductility was associated with agglomeration of carbides and gamma prime in the grain boundaries. The surface effects were associated with surface intergranular oxidation and/or cracking plus depletion of alloying elements. The role of creep remains to be further clarified and more study of the surface reactions is required before general principles can be established for the influence of creep on ordinary temperature mechanical properties.

PUBLICATION REVIEW

This report has been reviewed and is approved.

FOR THE COMMANDER:

W. J. TRAPP
Chief, Strength and Dynamics Branch
Metals and Ceramics Division
Materials Central

TABLE OF CONTENTS

LIST OF TABLES

LIST OF ILLUSTRATIONS

LIST OF ILLUSTRATIONS (continued)

LIST OF ILLUSTRATIONS (continued)

INTRODUCTION

An investigation is in progress under sponsorship of the Materials Central, ASD, United States Air Force, to obtain information and develop general principles for the influence of exposure to creep conditions on the normal temperature mechanical properties of alloys. This report presents data on this subject for Rene' 41 alloy for exposure to creep conditions over the temperature range of 1200° to 1800°F. The research is continuing to obtain additional mechanical property and microstructural information to supplement that being reported, and particularly to investigate the marked influence of surface reactions during exposure and study the feasibility of restoring properties by re-heat treatment.

Creep can alter subsequent mechanical properties at ordinary temperatures through the effects of the creep process and by altering thermally-induced structural changes. The thermally-induced structural changes in complex engineering alloys are, in themselves, usually a major factor in altered mechanical properties. Surface reactions including oxidation, depletion of alloying elements, introduction of contaminants, and cracking at the surface, can also be important sources of damage.

In earlier research (Refs. 1-4), studies of the influence of creep on short-time mechanical properties were carried out for a number of established alloys used in sheet form in aircraft structures. The exposure conditions were generally limited to those of known suitability for the alloys. Consequently, the results showed little creep damage. Because the major objective of the present research is to establish the general principles for predicting when creep-exposure can cause damage to subsequent mechanical properties at ordinary temperatures, exposure conditions causing such damage were sought without restriction to engineering limits commonly used to avoid damage.

Rene' 41 is a nickel-base superalloy which would normally be used at temperatures up to at least 1650°F. It has not been extensively used for aircraft structures. There is, however, considerable interest in alloys of this type for structures subjected to aerodynamic heating. Rene' 41 was selected to provide specific data for the alloy and to develop general principles for the numerous nickel-base alloys of the same metallurgical type which might be used for this type of application.

Evaluation of the influence of creep-exposure on normal temperature mechanical properties was primarily based on tensile tests at room tempera-

---

Manuscript released for publication April 4, 1961 as an ASD Technical Report.

ture. Some compressive testing was also carried out. The program originally included notch bar impact testing due to the known sensitivity of this property to structural changes, however, this was dropped due to such low initial impact strength that changes would not be evident. Most of the research eliminated surface effects by remachining specimens after creep exposure. Microstructural studies were carried out to identify changes associated with the property changes.

EXPERIMENTAL MATERIAL

The main requirement of the experimental material was that it be a complex high strength heat-resistant alloy expected to have considerable future applicability in Air Force applications. After discussion with representatives of the Materials Laboratory, a few preliminary experiments were conducted on small amounts of Rene' 41 and Udimet 500 alloys which were on hand at the University. When these indicated little technical difference on which to base a choice, it was requested that Rene' 41 be used.

Approximately 107 pounds of Rene' 41 alloy were then procured from the Metallurgical Products Department, General Electric Company, in the form of 0.516-0.520-inch diameter centerless ground bar stock from vacuum induction-melted Heat R-134. The material was reported to have the following chemical composition:

Element	Weight Percent
Nickel	55.32
Chromium	19.27
Cobalt	11.06
Molybdenum	9.06
Titanium	3.28
Aluminum	1.44
Carbon	0.12
Boron	0.004
Iron	0.30
Sulfur	0.006
Manganese	0.07
Silicon	0.07

The producer reported the grain size to be ASTM 3-6 and the Brinell Hardness to be 241-269. The material was shipped in the mill annealed condition (1975°F solution treatment plus water quench).

For the preliminary investigations leading to the selection of the test material, the Rene' 41 on hand at the University was heat treated in accordance with a treatment recommended by the General Electric Company at that time: solution treatment of one hour at 2150°F plus oil quench, then aged 4

hours at 1650°F and air cooled. A later perusal of a survey article by Jahnke and Frank (Ref. 5) indicated that although the above treatment produced a high level of rupture strength at temperatures above 1300°F, it was at a sacrifice of lower temperature yield strength in comparison with a treatment utilizing a 1950°F solution treatment followed by aging at 1400°F. As shown in Figure 9, the latter treatment, on the other hand, resulted in somewhat lower elevated temperature rupture strength. It appeared that the latter treatment offered a better all-round combination of mechanical properties over the range down to room temperature and, consequently, it was adopted as the primary condition for the studies of creep damage to mechanical properties using the newly procured material.

Batches of 24 specimen blanks, 4 inches long by 0.516-inch diameter, were then heat treated in 4 bundles of 6 blanks each according to the following schedule:

1) Solution treatment: 1950°F - 1/2 hour plus air cool.

2) Aging treatment: 1400°F - 16 hours plus air cool.

For the purposes of this investigation, this treatment was coded "R". The Vickers Hardness after treatment was 367 (equivalent to a Brinell Hardness of 347).

Some time after the adoption of this treatment was mentioned in a progress report, a communication was received from General Electric (Ref. 6) stating that the use of a 2150°F solution temperature was no longer recommended in combination with the aging treatment of 4 hours at 1650°F. The revised treatment, which was suggested for rupture-limited applications, substituted a solution temperature of 2050°F.

Several additional specimens were then treated according to the revised treatment for rupture-limited applications:

1) Solution treatment: 2050°F - 1/2 hour plus air cool.

2) Aging treatment: 1650°F - 4 hours plus air cool.

This treatment, coded "R2", resulted in a Vickers Hardness of 348, and was later shown to produce substantially the same short-time rupture properties as the "R" treatment.

TEST SPECIMENS

Details of the test specimens employed in this investigation are shown in Figure 1. The creep exposures were conducted on specimens having a 0.350-inch gage section diameter and a reduced section of approximately 2

inches. The specimens for subsequent tests of mechanical properties were designed to be machined from the gage sections of the creep-exposure specimens.

For the subsequent tensile tests in which the effect of surface damage was to be eliminated, approximately 0.025-inch was machined from the diameter of the gage length after creep exposure.

The 0.325-inch diameter by 1 5/8-inch long compression specimens were designed to maintain a 5:1 ratio of length to diameter. After machining to remove surface effects from the creep specimen gage section, the specimens were cut to length, polished, and then the ends were ground flat and parallel. Care was taken to ensure that the end surfaces were normal to the specimen axis.

The impact specimen adopted was the ASTM Type-W notched subsized specimen. The dimensions, 0.197-inch square by 2.16-inches long, were such that it could be conveniently machined from the reduced section of a creep specimen. The notch was roughed in with a special notch cutter to establish the angle and root radius and then ground out to final dimensions.

EQUIPMENT AND PROCEDURES

CREEP-EXPOSURE TESTS

The creep-exposure tests and preliminary creep-rupture tests were conducted in individual University of Michigan creep-testing machines. In these units, the stress is applied through a third-class lever system having a lever arm ratio of about 10 to 1. The specimen was gripped by threaded holders that fitted into a universal joint-type assembly for uniaxial loading. Heating was provided by a wire-wound resistance furnace fitting over the specimen and holder assembly.

Strain measurements were made with a modified Martens optical extensometer system. Extensometer bars in pairs were attached to collars threaded to the top and bottom shoulders of the creep specimen. Sandwiched between the pairs of extensometer bars were the stems of small mirror assemblies which reflected an illuminated fixed scale located about five feet in front of the creep unit. The differential movements of the top and bottom pairs of extensometer bars caused a rotation of the mirrors that was observed through a telescope mounted next to the scale. As the specimen elongated, a very small movement of the extensometer bars was magnified by the resulting optical lever arm and converted into a large change in the reflected scale reading observed against the cross-hairs in the telescope. This system permitted the detection of a specimen elongation of about 10 millionths of an inch.

Because the extensometer bars were attached to the threaded section adjacent to the specimen shoulders, it was necessary to correct the observed

deformation to account for the diminished contribution of the fillets and shoulders. "Effective gage lengths" were computed, both for the strain during loading and for the subsequent creep, and incorporated into the constants used to convert the scale readings into deformation. The factor for loading was based on the specimen geometry, while the factor for creep depended both on the specimen geometry and the relative deformation characteristics of the material at the test temperature. The derivation and use of these factors has been given previously (Ref. 1) and will not be repeated here. The Martens extensometers were also used in the unstressed exposure tests as an expedient in order to obtain information on dimensional changes due to structural reactions.

Three thermocouples were attached to each of the creep specimens at the center and at either end. All thermocouples were shielded from direct furnace radiation. Prior to starting a test, the furnace was heated to within 50°F of the desired test temperature. The specimen was then placed in the hot furnace and brought up to the test temperature and distribution in a period of not more than four hours. ASTM Recommended Practices were followed in controlling the test temperature and distribution.

Strain measurements were made as each weight was applied during loading. Creep strain was read periodically throughout tests. At the end of the exposure period, a final reading was made and the power to the furnace turned off. The specimen then cooled under load to minimize the effects of creep recovery. In the tests exposed without stress, the same procedure was followed in order to make the total time at temperature equivalent to the case of a stressed exposure. In the case of rupture, an automatic timer was actuated by the fall of the specimen holder measuring the rupture time to one-tenth of an hour.

TENSION AND COMPRESSION TESTS

The short-time tension and compression tests at room temperature were conducted in a hydraulic testing machine equipped with a strain pacer. The holders for the tension tests were similar to the type used in creep testing, while the compression tests were conducted in a special assembly.

Elongation in both the room temperature tension and compression tests was measured with microformer strain gages. An automatic stress-strain recorder was used. A two-inch gage length microformer was used in the tension tests, while the specimen dimensions required the use of a one-inch gage length microformer in the compression tests.

In the compression tests, the force was applied by a loading ram held in position by a special assembly incorporating a hollow cylindrical head. The assembly was mounted at the center of the tensile machine base and the loading ram was actuated by pressure against the cross-head of the tensile machine.

The tension tests were paced at a rate of 0.005 inches per inch per minute. In the compression tests, the extensometer system was actually operated in reverse and thus the pacing equipment could not be used directly. To approximate the desired strain rate, the testing machine was operated at the head speed setting that had given the same strain rate in tension over the elastic portion of the stress-strain curve. In the tension tests, the load was applied until fracture occurred, while in the compression tests the load was released when the 0.2 percent offset yield strength was exceeded.

In the elevated temperature tension tests, the modified Martens optical extensometer system was used for strain measurements. Temperature measurement and control practices were the same as those used in the creep-exposures.

The data determined in the tension tests were the ultimate tensile strength, the 0.2 percent offset yield strength, the elongation, the reduction of area, and the modulus. In the compression tests, the 0.2 percent offset yield strength and modulus were determined.

IMPACT TESTS

The Izod notched bar impact tests were used. In the Izod test, the specimen is mounted vertically and gripped at one end. A special holding fixture was constructed to accommodate the subsized specimen. The pendulum fall produced an impact energy of 120 foot-pounds. Prior to running a test, the measuring scale of the machine was zeroed by allowing the pendulum to swing through its cycle with no specimen in place and noting the height to which the indicating disc was raised.

In addition to measuring the impact energy, the ductility characteristics of the fractured specimens were determined by measuring the lateral contraction at the base of the notch and the lateral expansion at the surface opposite to the notch.

STRUCTURAL EXAMINATION

The techniques used in this investigation for structural examination included optical microscopy, electron microscopy, x-ray diffraction of extracted residues, and hardness tests.

Specimen Preparation

All specimens for microscopic examination and hardness testing were sectioned longitudinally with a water-cooled cut-off wheel and then mounted in Bakelite. The mounted specimens were wet ground on a rotating lap through a series of silicon carbide papers finishing at 600-mesh grit. Final polishing was carried out first on a cloth-covered rotating lap using fine

diamond compound and then on a vibratory polisher in an aqueous media of Linde "B" polishing compound. The samples were cleaned in an ultrasonic cleaner.

Etchants

Similar etching techniques were used for both optical microscopy and electron microscopy. The specimens were etched electrolytically in "G" etch, an etchant developed by Bigelow, Amy, and Brockway (Ref. 7) at the University of Michigan. Etching was conducted at 6 volts and a current density of 0.8 amperes per square inch for a period of 5-7 seconds. The composition of the etchant was:

"G" Etch

H_2PO_4	(85%)	12 parts
H_2SO_4	(96%)	47 parts
HNO_3	(70%)	41 parts

Electron Microscopy

Electron microscopy was carried out in an RCA EML Electron Microscope. For examination in the microscope, collodion replicas mounted on nickel grids were prepared from the surface of the etched specimens. The replicas were shadowed with palladium to increase the contrast and reveal surface contours. Polystyrene latex spheres of either 2580 or 3400 Å diameter were placed on the replicas prior to shadowing to indicate the angle and direction of shadowing and to provide an internal standard for the measurement of magnification. The micrographs reproduced in this report are direct prints from the original negatives; consequently, the polystyrene spheres appear black and the shadows appear white. Since the spheres are raised from the surface of the replica, a particle casting a shadow opposite to that of the latex spheres is in relief on the metal specimen; conversely, areas casting shadows in the same direction as those cast by the latex spheres are depressions in the surface of the metal specimen and correspond to material that was attacked or eaten out by the etchant.

X-Ray Diffraction

The principal purpose of the x-ray diffraction studies was the identification of the minor phases observed in the microstructure.

The identification of minor phases was made by x-ray diffraction analysis of residues extracted from the alloy by immersion in a bromine-alcohol solution. This procedure has the advantage of concentrating the minor phases so that a greater amount is available for diffraction and also eliminating possible interference from matrix lines.

The specimens for extraction were thoroughly surface ground, soaked in pure bromine liquid, cleaned with distilled water, and then completely dried.

Each specimen was placed in an individual centrifuge tube that had been cleaned, rinsed with anhydrous methyl alcohol, and dried. Approximately 25 ml of a 10:1 mixture of anhydrous methyl alcohol and bromine was then added to the tube. Boiling occurred in approximately 15 minutes, after which the tube was cooled under tap water. When a sufficient quantity of extract had been obtained, the specimen was removed from the tube and rinsed with methyl alcohol. The tube was then centrifuged and the extract washed repeatedly with methyl alcohol until the supernatant liquid was clear. The extract was then dried and formed into a thin wire for exposure in a Debye camera to nickel-filtered copper radiation for four hours. Analysis of the patterns was made by comparison with standard patterns either available from the literature or calculated from the lattice parameters.

Hardness Tests

Diamond Pyramid Hardness measurements were made on a Vickers Hardness Machine using a 50 kilogram load. Both diagonals of each of three impressions were measured and the six measurements were averaged. A statistical analysis of this technique (Ref. 8) indicated that in the range of 300-340 DPH, a hardness difference of 7 DPH was significant. In the range of 340-400 DPH, the range of significant hardness increased to 9 DPH.

RESULTS AND DISCUSSION

The first step in the investigation was the selection of the particular alloy to be used. Following selection of Rene' 41 as the alloy, tests were carried out to define the initial properties at room temperature and to provide high temperature properties to be used to select creep-exposure conditions. Creep-exposures were then initiated over the temperature range of 1200° to 1800°F. The exposed specimens were subjected to tension and compression testing at room temperature. Only a limited number of impact tests were used because the initial impact strength was so low that additional reduction from creep exposure was not measurable. Exposed specimens were then subjected to metallurgical examinations to obtain information as to the cause of observed effects on mechanical properties.

SELECTION OF EXPERIMENTAL ALLOY

The criteria used in selecting the particular alloy for the investigation were twofold. The alloy had to be representative of good high temperature alloys expected to be widely used in the future. In addition, it would have to be subject to alteration in normal mechanical properties during creep-exposure, sufficient to help define the metallurgical principles for creep damage. As a

result of discussion with representatives of the Materials Central, it was decided to conduct survey tests on Udimet 500 and Rene' 41 alloys using material on hand.

The Udimet 500 was available in 5/8-inch diameter bar stock which had been double solution treated and double aged. These treatments were 2 hours at 2150°F, air cooled; plus 4 hours at 1975°F, air cooled; plus 24 hours at 1550°F, air cooled; plus 16 hours at 1400°F, air cooled.

The Rene' 41 was in the form of 3/4-inch thick plate which had been water quenched from 1950°F. Prior to testing this material was solution treated for one hour at 2150°F, oil quenched and then aged for 4 hours at 1650°F and air cooled.

Two specimens of each alloy were exposed at 1200°F and two at 1700°F for 100 hours under a stress which was 75 percent of the 100-hour rupture strength. One specimen was subjected to tensile testing at room temperature and the other was machined into impact specimens.

The creep curves for the 100-hour exposure periods (Fig. 2) indicated that slight shrinkage occurred at 1200°F and that the creep had just reached the third stage at 1700°F. Exposure at 1200°F for both alloys resulted in an increase in yield strength (Table 1), while exposure at 1700°F reduced ultimate tensile strength and ductility. Exposure at 1200°F may have slightly reduced the ultimate tensile strength and increased the ductility of Rene' 41, while Udimet 500 was not affected.

The impact tests showed very low initial impact strength (Table 1) for both alloys. Thus, any decrease as a result of creep-exposure could not be measured by the test.

Creep-exposure at 1200°F had no discernible effect on the microstructure of the strengthening gamma prime precipitate in both alloys (See Figures 3 through 8). Exposure at 1700°F caused considerable growth of the gamma prime particles and gamma prime agglomerated at the grain boundaries.

From a technical viewpoint, there was little to choose between the two alloys insofar as creep-exposure influenced room temperature mechanical properties. Both indicated that changes would be induced and that they would be of sufficient magnitude for the objectives. Moreover, the structural changes accompanying the altered mechanical properties offered considerable promise for correlation to delineate causes of changed mechanical properties. When this was reported to the Materials Central, it was requested that Rene' 41 alloy be used for the investigation.

STUDIES OF RENE' 41 ALLOY

Base Properties

The as-treated properties of the Rene' 41 alloy were determined to provide the necessary comparative data for the evaluation of the effect of creep on mechanical properties and to provide the information needed for selection of the creep-exposure conditions. In addition, the information was used to confirm that the particular lot of test material had properties representative of the alloy.

Short-Time Properties. The basic properties at room temperature for the material used in this investigation are given in Table 2. Most of the research was carried out on stock heated 1/2-hour at 1950°F, air cooled, and then aged at 1400°F for 16 hours plus air cooled (condition "R"). Based on these somewhat limited data, this material had the following properties:

Ultimate tensile strength (psi)	190,000
0.2% offset yield strength in tension (psi)	130,000
Elongation (%)	20.5
Reduction of area (%)	28.0
Compression yield strength for 0.2% offset	131,000
Izod impact strength (0.197-inch square specimen) (ft-lbs)	3

Comparative tensile data are included in Table 2 from published values for the alloy (Refs. 9 and 10). The stock used in this investigation had tensile strengths higher than two of the comparative materials, but not as high as the third. Yield strengths were lower than the other values. Ductility values were considerably higher than the comparative materials. No comparative values for compression yield strength or impact tests were available. In general, these results showed a very acceptable level of properties for the purposes of the investigation. The comparative data were for several forms of the alloy and the solution treatment times varied. Both factors would be expected to cause variations in properties so that the lack of exact agreement was to be expected.

The agreement in yield strength for the tension and compression tests was considered an added virtue for the material. There apparently would be no marked directional property effects to complicate analysis. Unfortunately, the impact strength was so low that any detrimental effects from creep exposure would not be measurable.

Table 2 includes results of single tensile tests at 1200°, 1400°, and 1600°F conducted mainly to guide selection of stresses for creep-rupture testing.

The tensile properties for the "R2" condition, the condition subsequently suggested for rupture-limited applications (see page 3), showed a small reduction in the ultimate tensile and yield strengths and an increase in ductility from the "R" condition.

Creep-Rupture Properties. Creep-rupture tests were conducted to gain familiarity with the type of creep to be encountered in Rene' 41, to provide data for the selection of exposure conditions, and to confirm that the test material had representative properties.

A small number of initial survey tests were run at temperatures between 1200° and 1800°F at stresses picked to produce fracture in less than 100 hours. The test conditions were selected with the aid of a master-rupture curve derived from the data given by Jahnke and Frank (Ref. 5) for the 100-hour rupture strength of sheet material as a function of test temperature. The survey test data were then used to construct an approximate master-rupture curve for the present wrought material. As the investigation progressed, creep-exposure tests were occasionally run at stresses that turned out to be too high for the contemplated exposure time. The data from these inadvertent rupture tests were used to supplement the initial data and a more complete master-rupture curve was eventually constructed. An additional comparative master-rupture curve was also later derived from the supplier's "typical" property data of Reference 9.

All the rupture data from the present investigation are summarized in Table 3. The master-rupture curve is plotted in Figure 10 together with the curves derived from References 5 and 9. The time-elongation data are included with the creep curves for the creep-exposure tests (Figs. 19 through 25).

As previously cited, material solution treated at 1950°F and aged at 1400°F (condition "R") was used for most of the investigation. Tests were, however, also carried out on material heat treated at 2050°F and aged at 1600°F (condition "R2"). The data for both treatments fitted the same master-rupture curve. This was a mild surprise inasmuch as the "R2" condition was designated for rupture-limited applications. Conventional plots in Figure 11 of stress versus log rupture time at 1400°, 1600°, and 1800°F confirmed the similarity of properties. Perhaps a difference might have been noted between the two conditions if testing had been extended to cover longer time periods.

Examination of the master-rupture curves plotted in Figure 10 showed that the present experimental material had generally higher rupture strengths, i.e., displaced towards higher time-temperature parameter values at a given stress level than were indicated by either of the comparative curves. These results, together with the tensile data, further confirmed that the lot of test material had acceptable properties for the aims of the investigation and was representative of the alloy.

The master rupture curves were also used to aid in the selection of the creep-exposure conditions by the following process which is described in greater detail on page 15. Approximate stress versus time for rupture curves covering the period from 10 to 100 hours were derived for each test temperature. The first creep-exposures were conducted for 10 hours at the stress estimated to cause fracture in 20 hours, i.e., a 50-percent expenditure of rupture life. The creep-deformation obtained in this exposure was then used as the point of departure in planning subsequent tests.

The time-elongation curves for the tests conducted at 1300°F and above (Figs. 20 through 25) indicated that the creep rate, in most cases, increased continuously from the start of the test. In most of the tests at 1200°F (Fig. 19), there was evidence of decelerating creep ("first-stage" creep) at the beginning of the test period. In order to achieve an appreciable creep rate in the 1200°F tests, it was necessary to use such a high stress that an appreciable amount of plastic deformation by yielding was produced during loading. Where comparisons were possible, there appeared to be no difference between the creep curves of the "R" and "R2" conditions.

Effect of Unstressed Exposure

Changes in mechanical properties as a result of creep-exposure can be due to either or both creep and thermally-induced structural changes. The influence of thermally-induced changes was determined by studying specimens that had been exposed without stress. Tension and compression tests were conducted at room temperature on specimens that had been exposed at temperatures between 1200° and 1900°F for various time periods up to 200 hours. In order to eliminate surface effects, most specimens were remachined after exposure, although a few tests were conducted on specimens with as-exposed surfaces in order to confirm the need for remachining. The limited study of surface effects is discussed here and also in a later section of the report. Data for the tensile tests of remachined exposure specimens are included with the creep-exposure test data in Table 4. Plots of the short-time properties after unstressed exposure showing the effect of exposure temperature and exposure time are presented in Figures 12 and 13, respectively, while comparative data for a few tests of the "R2" heat treatment are plotted in Figure 14.

In conducting these tests, the specimens were loaded into the hot furnace and held at temperature for 4 hours before the exposure time was counted. This procedure was used so that these specimens could be compared directly with the stressed exposures in which the 4-hour period was necessary for the adjustment of temperatures before load application. The nominal 10-hour unstressed exposures were thus actually 14-hour exposures, and the longer-time exposures covered periods of 104 and 204 hours. All discussion of the results will be made in terms of the nominal exposure times.

Exposure at 1200° or 1400°F had little or no effect on the mechanical properties (Fig. 12). When the exposure temperature was increased above 1400°F for the 100-hour exposures or 1600°F for the 10-hour exposures, both the ultimate tensile strength and the tensile and compressive yield strengths were decreased below the base condition. The effect of temperature appeared to be similar on both the tensile and compressive yield strengths.

In contrast to the strength behavior, the elongation and reduction of area were not reduced significantly following a 10-hour exposure at any temperature studied between 1400° and 1900°F. Ductility values were decreased after the higher temperature exposures for periods of 100 hours or longer, with the only exception being a slight reversal for a 200-hour exposure at 1800°F. The minimum ductilities observed were in the range of 4-5 percent.

The effect of exposure time is more clearly shown by Figure 13, a cross-plot of short-time properties versus log exposure time. At 1600°F, the 10-hour exposure caused no decrease in ultimate strength, while the 100 and 200-hour exposures produced a 10-percent decrease. At 1700°F, a 6-percent drop in strength occurred in 14 hours and continued with increasing exposure time to eventually reach a 32 percent decrease in 204 hours. At 1800°F, a decrease of about 6 percent was reached in the first 6 hours. This increased to 27 percent in 104 hours, but then was reversed so that the strength after a 204-hour exposure was reduced only about 18 percent from the base value.

The tensile yield strength behaved in a manner similar to the ultimate strength following exposure at 1400° and 1600°F. In both the 1700° and 1800°F exposures, however, the minimum tensile yield strength was reached in 100 hours and was followed by a slight increase as the exposure time was increased to 200 hours. In addition, the curve for the 1800°F exposures fell between those of the 1600° and 1700°F exposures. The behavior of the compressive yield strength was similar to that of the tensile yield strength although the data only cover exposure periods up to 100 hours.

The elongation and reduction of area curves of Figure 13 show again that 10 hours exposure had little or no effect. As the exposure time and temperature were increased beyond 100 hours and 1600°F, respectively, the longer the exposure time and the higher the temperature, the lower was the ductility.

Limited data covering the effect of initial heat treatment (Table 4 and Fig. 14) show that the initial differences in properties were largely removed by 10-hour exposures at 1600° and 1800°F or for 100 hours at 1800°F. The "R" treatment (solution at 1950°F and aging 16 hours at 1400°F) had initially resulted in higher tensile and yield strengths and slightly lower ductility than

the "R2" treatment (solution at 2050°F and aging 4 hours at 1650°F). While the "R2" condition suffered less reduction in properties than the "R" condition, the results imply that the initial differences in structure were largely eliminated by the exposure.

The tests carried out on specimens which were not remachined after unstressed exposure at 1400°, 1600°, and 1800°F for 10 hours show that the tensile strengths and ductility values (Table 4 and Fig. 12) were substantially below those of the remachined specimens. This confirmed the need in these studies for remachining and also indicated that there were major effects occurring from surface reactions as well as those due to structural changes.

The extensometer system used to measure creep was attached to the unstressed specimens and readings were taken routinely during the exposures. As would be expected from the characteristics of the extensometer, which requires a load on the specimen to achieve perfect alignment, there were variations in the readings between duplicate tests. However, exposure at 1200° and 1400°F showed little change in length. All of the exposures at higher temperatures did show shrinkage and it appeared that the shrinkage increased with exposure temperature above 1400°F. The major change occurred in the first 10 to 20 hours and the shrinkage then proceeded at a slower rate throughout the remainder of the exposure. The fact that the temperatures at which the apparent shrinkage was observed coincided with those causing changes in room temperature properties indicates that the structural changes influencing properties caused a decrease in volume. From the available data, it appeared that the maximum amount of shrinkage was of the order of 0.03 to 0.04 percent. This is, however, very uncertain due to the errors in measurement. The measurements were also limited to exposure after the 4-hour period for temperature adjustment.

In summary then, unstressed exposures demonstrated that structural changes occurring in 10 hours at 1600°F or in less than 2 hours at 1700° and 1800°F caused reduction of properties at room temperature. The degree of reduction increased with exposure time. Similar total reductions were attained in 100 to 200 hours with the properties generally being slightly higher for exposure at 1600°F. Exposure at 1200° or 1400°F for times up to 100 hours did not significantly change properties. Initial differences in properties for the two heat treatments considered were eliminated by exposure to temperatures of 1600° and 1800°F. Evidence was obtained to indicate marked reduction in tensile strength and ductility from surface attack during exposures at 1400°, 1600°, and 1800°F.

Effect of Creep-Exposure

Creep-exposure tests were conducted primarily on material solution treated at 1950°F and aged at 1400°F (condition "R" material) for 10, 100, or 200 hours at temperatures between 1200° and 1800°F followed by room temperature tension tests on remachined specimens. Compression tests at

room temperature were run on a group of specimens and a few tension tests were also run on specimens exposed in the "R2" condition. The data from these tests are tabulated in Table 4 together with the results of the unstressed exposure tests. Individual plots showing the subsequent mechanical properties versus the total plastic strain are presented in Figures 15 and 16 for each temperature investigated. Cross plots of these data are presented in Figure 17 together with the data for unstressed exposures to show the effects of 1 and 3 percent total plastic strain reached in 10 or 100 hours as a function of exposure temperature.

A limited comparison of the "R" and "R2" conditions is presented in Figure 18.

The initial creep-exposures were conducted for 10 hours at stresses estimated to cause rupture in 20 hours. That is, approximately 50 percent of the rupture life was expended. This generally produced creep on the order of one percent. In order to produce as much creep as possible in subsequent exposures, the stresses were then increased, in some cases, to as close as 1000 psi to the rupture stress. Depending on the test temperature, this resulted in the expenditure of 80 percent or more of the rupture life, and in two cases 99 percent of the rupture life was theoretically expended. By the use of such high stresses, creep ranging from 3 percent to 14 percent was obtained in 10 hours. Exposure periods of 100 and 200 hours were also studied in a comparable manner, although somewhat smaller amounts of creep were obtained due to the limitation of the rupture elongation at the low stress levels used.

The time-elongation curves from the creep-exposures and preliminary creep-rupture tests are plotted in Figures 19 through 25. As indicated in Table 4, only during exposure to 1200°F was short-time plastic strain during loading an appreciable component of the total plastic strain. At 1300°F and above, virtually all the plastic strain was accumulated by creep.

Exposure under stress at 1200°, 1300°, and 1400°F, caused the tensile strength and particularly the yield strength to increase with increasing amounts of plastic strain (Fig. 15). The ductility values scattered considerably after exposure at 1200°F but were either the same or lower than the initial values. Small strains at 1300°F resulted in a slight decrease in ductility, while ductility fell off slowly with increasing amounts of strain at 1400°F. Because unstressed exposure at these temperatures did not change mechanical properties at room temperature, the observed changes are due to the plastic strain and not to thermally-induced structural changes.

For the 1200° and 1300°F creep-exposures, the changes in mechanical properties at room temperature were apparently independent of the time to attain a given amount of plastic strain. When exposed at 1400°F, however, the increase in tensile and yield strength was less for a given amount of strain

in 100 hours than in 10 hours. The reduction of area was also less for 100 hours of exposure.

One of two specimens strained 3.5 percent at 1200°F and a specimen strained 4.6 percent at 1300°F in 10 hours exhibited poor properties, particularly with respect to ductility. This was associated with part of the fracture being oxidized (Fig. 30). A crack or intergranular oxidation had occurred during creep which was not removed by machining 0.0125-inch off the surface.

When exposed to creep at 1500°F, tensile strengths (Fig. 15) were unchanged. Yield strengths did increase but not as much as at lower temperatures of exposure. Ductility values were reduced somewhat, with practically all the decrease being associated with less than 1-percent plastic strain. The reduction was more for 100-hours than for 10 hours of exposure to creep.

Creep at 1600°, 1700°, and 1800°F reduced tensile strengths (Fig. 16) slightly more than did the unstressed exposures for equal time periods. Increasing amounts of creep slightly intensified the effect. Yield strengths in tension were, however, increased somewhat over the values obtained for unstressed exposure. The data are not conclusive but indicate that the compressive yield strength was increased in the presence of creep during 10-hour exposures and reduced in the 100-hour exposures. After creep of up to several percent, ductility tended to be reduced below the values for unstressed exposures. As in unstressed exposures, the reduction in ductility was more for the longer exposures.

The lower ductility after the longer time exposures appeared in every case to be due mainly to the thermally-induced effects measured in unstressed exposure tests.

The influence of exposure temperature on tensile properties after creep-exposures of 1 and 3 percent is shown more clearly by the cross-plotted data of Figure 17. Three percent was chosen as the higher deformation parameter in this plot because it was about the maximum deformation for which data were available for the lower temperatures and when this amount was reached in the higher temperature exposures, the changes in properties had fairly well levelled off.

It will be noted that creep during exposure had a considerable effect on tensile and yield strengths for temperatures up to 1400°F. For higher temperatures, while creep did result in higher yield strengths and lower ductility in comparison to the unstressed exposure, the main changes from original properties were due to the thermally-induced structural changes measured by the unstressed exposure tests.

To recapitulate, for creep-exposures at 1200° to 1400°F, plastic strain

was the main cause of the observed changes in properties. In general, yield strength was influenced far more than the other properties. This indicates, as was found in Reference 4, that the major factor was the introduction of Bauschinger effects. The increase in tensile strength and reduction in ductility suggest that strain hardening and/or precipitation hardening also occurred.

Combinations of these latter factors are the principal causes for differences in the behavior of the ultimate tensile strength and the ductility beyond those caused by the exposure to temperature alone. For instance, the ultimate strength, after 10 hours of creep-exposures in the range from 1200° to 1500°F, was slightly raised above that following unstressed exposure. After 10 hours creep-exposure at temperatures greater than 1500°F, the ultimate strength curve was reduced below the curve for the unstressed exposures. This cross-over behavior was not observed in the 100-hour creep-exposures where curves for the stressed exposure lay above the curve for unstressed exposure at temperatures up to 1600°F but above this temperature fell only to the level of the unstressed exposure. This suggests stress-accelerated overaging in the 10-hour creep-exposures conducted above 1500°F. The aging process was probably complete under the effect of temperature alone in the 100-hour exposures.

The curves for the elongation and reduction of area following creep-exposure fell below those established for unstressed exposure for both the 10 hour and 100-hour exposures. This again probably resulted from a combination of strain hardening and stress-accelerated overaging. In general, it appears on the basis of the information contained in Figure 17 that exposure for 100 hours at temperatures above 1500-1600°F resulted in property changes governed primarily by the time at temperature. In the temperature range below 1500-1600°F, the effect of creep was significant in not only inducing the Bauschinger effect but in causing strain hardening and possibly additional precipitation hardening.

The compression test data obtained for creep exposures at 1600°, 1700°, and 1800°F and included in Figure 16 offer further evidence of the varying nature of the roles of stress-accelerated aging, strain hardening, and the Bauschinger effect. The presence of the Bauschinger effect, i.e., increase of tensile yield strength and reduction of compressive yield strength after prior tensile strain, indicates that conditions favorable to strain hardening are also present. However, in this case, creep-exposure for 10 hours increased both the tensile and compressive yield strengths after 1600° and 1800°F exposures, while after the 100-hour exposures at 1600°, 1700°, and 1800°F, the tensile yield strength was increased and the compressive yield strength decreased, i.e., the "normal" Bauschinger behavior. Since this should also have been observed after the 10-hour creep-exposure, the simultaneous increase in both yield strengths indicated that the Bauschinger effect was overridden by a metallurgical reaction of sufficient extent to cause a net increase in compressive yield strength. Presumably, in the 100-hour

exposures, the material became overaged and the Bauschinger effect was dominant in the subsequent compression test.

Within the limits of data scatter, there was no apparent difference in response to 100 hours creep-exposure at 1600° or 1800°F between the "R" and "R2" conditions (Table 4 and Figure 18).

The creep curves for the rupture and creep-exposure tests (Figs. 19 through 26) show that the creep rate increased from the start of the tests except at 1200°F. The stresses used were all below the yield strength except the higher stress tests at 1200°F. In the tests at 1300°F and above, there was generally either a period of constant rate creep (second-stage creep) followed by an acceleration in creep rate (third-stage creep) in the lowest stress tests, or else the creep rate accelerated continuously from the beginning of the exposure period. Only a slight increase in stress was required to produce an accelerating rate throughout the entire exposure period. The creep curves also indicate considerable variation between specimens in creep resistance. Apparently, the stock used was not particularly uniform in its creep characteristics. This is not an unusual finding in alloys of the type considered when the heat treating temperatures are below 2000°F.

Effect of Surface Reactions During Exposure

Previously, tests on specimens exposed without stress for 10 hours at 1400°, 1600°, and 1800°F had shown substantially lower ultimate tensile strength and ductility when tensile tested at room temperature without remachining the surface (page 14 and Fig. 12). These results not only confirmed the need for remachining in order to separate the effects of structural changes, but also indicated that there were major effects occurring from surface reactions as well. This pointed out the need for investigating surface damage after creep and a study was undertaken which is still in progress. Preliminary data are summarized in Table 5 and Figures 26 and 27 together with the results from the unstressed exposures. The results show that about the same differential in properties at room temperature due to remachining was maintained for the specimens exposed to creep as existed for the unstressed exposures. In both cases, yield strengths were similar whether or not the surface was remachined. The differential between remachined and unmachined surfaces on the specimens generally increased (Fig. 27) as the exposure temperature was increased from 1400° to 1800°F.

Since these results indicate that the yield strength was relatively unaffected while the ultimate tensile strength and ductility were reduced by surface attack, it can be assumed that the attack did not operate by reducing the section size. Apparently, the surface attack introduced effects that did not operate until after yielding started.

Although these data are indicative, the influence of surface reactions

during creep has not been adequately covered in this investigation to date. No data were obtained below 1400°F, the exposure times were limited to 10 hours, and the amount of creep was rather small. Attention is also directed to the data in the preceding section showing that all cracks originating at the surface were not removed by machining off 0.025-inch from the diameter of specimens which had been strained approximately 3 to 5 percent at 1200° and 1300°F. This is exemplified by Figure 30 which illustrates the appearance of the fracture surface of specimen R-63 which had been exposed to 4.6 percent total plastic strain in 10 hours at 1300°F. The area of oxidation is evidence of a deep crack exposed to the furnace atmosphere during the creep-exposure. A smaller oxidized area was noted on the fracture surface of specimen R-66 which had been exposed to 3.5 percent total strain in 10 hours at 1200°F.

No evidence of such oxidation could be detected on the fracture surfaces of any of the specimens exposed at temperatures above 1300°F to comparable or even much greater amounts of creep. Where low ductilities were observed following the longer exposures above 1600°F, the effects appeared to be mostly due to the exposure to temperature alone. Since surface attack itself should be greater the higher the temperature, and yet the material was able to withstand much larger total creep strains at the higher temperatures without evidence of deep cracking, it follows that at 1200° and 1300°F the deformation characteristics of the alloy were important. This suggests the possibility that exposure to smaller amounts of creep at these temperatures would show damage from unmachined surfaces. There is also need for data for larger amounts of creep at all temperatures before more definite conclusions can be drawn regarding the roles of stressed and unstressed exposure in influencing surface damage. Evidently, cracks penetrated far deeper at 1200° and 1300°F for a given amount of creep strain than at higher temperatures. The amazing feature of these specimens was that the cracks could have penetrated so deeply without causing rupture. They must have been growing rather slowly in spite of their depth. At this stage of the investigation, the data suggest that the cause of the deep cracks was associated with the fact that the creep deformation at the time the tests were discontinued was very near the strain at rupture.

A specimen exposed to creep at 1400°F exhibited intergranular cracking or oxidation (Fig. 28) about one grain deep for some of the grain boundaries. Figure 29 shows that remachining removed metal far below this visible attack. Because unstressed exposure resulted in about the same loss in properties as the stressed exposure (Fig. 27), it is probable that the surface attack was mainly time-temperature dependent and that creep had little effect. Exposure at 1800°F without stress for 10 hours resulted in intergranular oxidation, general fissuring from oxidation, and depletion of the precipitates (Fig. 31). These effects were only about one grain deep and machining again removed metal to a considerably greater depth than the visible attack.

The inference from these very limited studies of surface attack is that intergranular oxidation and depletion of alloying elements initiated cracking during tensile tests which limited ductility sufficiently to reduce tensile strength. There is, however, the possibility that surface reactions not evident in the microstructures could have been involved. Certainly, the alloy is subject to deep cracking when exposed to a sufficient amount of creep at 1200° and 1300°F under the combined effect of oxidation and creep strain.

Microstructural Studies

Microstructural studies of Rene' 41 were conducted for the purpose of relating the observed changes in mechanical properties during exposure to creep to the structural causes other than surface effects. In undertaking these studies, it was recognized that not only was it important to define the causes, but it was equally important to identify those cases where structural changes occurred with no apparent mechanical property effects, or where mechanical property effects occurred with no apparent structural changes.

Optical Metallography. Optical examination of the material solution treated at 1950°F and aged at 1400°F (condition "R") (Figs. 32 and 33) showed the microstructure to consist of fairly equi-axed matrix grains interspersed with minor-phase particles occurring both at the grain boundaries and within the grains. The particles in the grain boundary appeared to be somewhat larger and more numerous. Characteristic bronze-colored particles of the titanium carbonitride type occurred throughout the structure and were readily distinguishable from the remaining smaller particles. This structure had an excellent combination of both strength and ductility.

Following 100 hours stressed exposure to approximately 5 percent creep at 1800°F, the tensile and yield strengths, and particularly the ductility of sample R-45, were reduced considerably below the as-treated values. Examination at 100x of specimen R-45 (Fig. 34) revealed a thickening of the grain boundaries accompanying reduced ductility. The 1000x micrograph of sample R-45 (Fig. 35) resolved a heavy precipitate within the grains. In the grain at the upper right hand corner of this figure, the precipitate shows indications of being oriented along crystallographic planes. At this magnification, the grain boundary thickening of the specimen is seen to consist of an increase in the number of discrete particles and several of the original particles are apparently surrounded by a second phase. No evidence of internal cracking was observed.

The samples illustrated in Figures 33 and 35 represented not only extremes of mechanical properties encountered in the investigation of remachined specimens but extremes of microstructures as well. Optical examination of a number of other samples indicated that loss of tensile ductility and ultimate and tensile yield strength was accompanied by increasing complexity of the grain boundaries and the eventual appearance of the heavy precipitate within the grains.

In general, specimens exposed at temperatures below 1600°F had the appearance of Figure 33, while exposures of more than 100 hours at 1600°F tended to produce structures with an increasing amount of the precipitating phase readily observed in Figure 35.

Creep-exposure had no apparent effect on the matrix grain size. No evidence of internal microcracking was observed in any of the specimens examined of either condition "R" or "R2" material.

More information regarding the structural features which might be related to mechanical factors was obtained by turning to the greater resolving power of the electron microscope.

Electron Microscopy. The major portion of the electron microscope studies of Rene' 41 was conducted at 8200x magnification. As mentioned in the section on Experimental Procedures (page 7), polystyrene latex balls were placed on the replicas to indicate the shadowing direction and to provide an internal standard of magnification. At various times during the investigation, balls of 2580 or 3400 Å diameter were used and this fact should be kept in mind when examining the electron micrographs, inasmuch as the variation of ball sizes in the figures might be taken as apparently indicating differences in the magnification.

In the as-treated condition (Figs. 36 and 37), a phase in the matrix was just barely resolved at 8200x (Fig. 36) and which appears at 16,000x (Fig. 37) as small round particles is the gamma prime precipitate characteristic of titanium plus aluminum-hardened nickel-base alloys. These micrographs also show that the grain boundaries contained chains of discrete particles.

Figures 38 through 50 were selected to show the effects of increasing exposure times and/or temperatures as they affected both the room temperature tensile ductility and the appearance of the gamma prime phase and grain boundaries.

Creep-exposure for as long as 100 hours at temperatures from 1200°F up to and including 1400°F resulted in little, if any, change in the microstructure. Since Figure 17 shows that the tensile properties were affected by creep-exposure in this range, the stable structure indicates that the mechanical property effects were primarily caused by creep strain.

A 10-hour exposure at 1500°F resulted in a slight increase in the size of the gamma prime phase, while a 100-hour exposure at 1500°F (Fig. 38) resulted in approximately doubling the diameter of the gamma prime phase and an indication that a second phase was surrounding the grain boundary particles. This specimen exhibited reduced values of both strength and ductility from the as-treated condition.

A specimen aged for another purpose for 436 hours at 1550°F (Fig. 39) exhibited a continuation of the growth of the gamma prime phase in the matrix. The grain boundary material also appears to have grown and the occurrence of a second phase outlining the boundary material is more evident.

Figures 40, 41, and 42 show that the effects of exposure for 10, 100, and 200 hours, respectively, at 1600°F consisted of considerable growth and agglomeration of both the gamma prime phase and the boundary phases as the exposure time was increased. Figure 42 shows that one of the large particles within a grain was also enveloped by a second phase. The reduction in ductility followed both the growth of the gamma prime and the increasingly complex nature of the grain boundaries.

Parallel effects on structure and mechanical properties were also observed in samples exposed at 1700°F (Figs. 43 through 46) and 1800°F (Figs. 47 through 49). In Figures 45 and 48, massive plate-like material is seen to occur at the grain boundaries. This is a considerable departure from the as-treated condition and correlates with the lowest ranges of ductility observed after creep-exposure.

Of interest in the specimens exposed at 1800°F (Figs. 47, 48, and 49) are numerous very fine particles within the grains in addition to the large agglomerated gamma prime phase. The fine particles are gamma prime phase which dissolved during exposure and re-precipitated when the specimen cooled. The large gamma prime particles are those permitted to exist at the exposure temperature by the phase relationships of the alloy.

Beattie (Ref. 11) indicated the temperature for complete gamma prime solution for Rene' 41 to be between 1900° and 1950°F. This agrees fairly well with the temperature of 1875°F indicated by the phase diagram (Fig. 51) of Bettridge and Franklin (Ref. 12) for simple 80 Ni - 20 Cr alloys containing titanium and aluminum. Thus, specimens during creep-exposure at 1900°F would contain very little gamma prime. Much of the extensive amount of gamma prime in the specimen of Figure 50 after exposure, therefore, probably precipitated and grew while the specimen was furnace cooling from the exposure temperature. The mechanical properties of this specimen, R-46, were quite similar to those of specimen R-42 (Fig. 43) which had an almost identical appearance, particularly with respect to the gamma prime size and distribution, although exposed at a lower temperature.

The observations to this point have indicated that changes in mechanical properties followed creep-exposure at temperatures below 1500°F but were accompanied by no apparent structural changes. Therefore, the major factor causing these property changes was the creep process -- particularly as it resulted in the Bauschinger effect and strain hardening.

Mechanical property changes following creep-exposures at the higher temperatures were accompanied by three identifiable structural changes.

The gamma prime particles became larger and fewer in number; there was an increase in the number and size of the particles in the grain boundaries; and finally, there was evidence of a second phase enveloping the grain boundary material.

It is also obvious from the electron micrographs of the samples exposed without stress for 10 hours at temperatures up to 1900°F that a radical change in the appearance of the gamma prime phase could take place without causing a significant change in the ductility. On the other hand, the yield strength and, to a lesser extent, the ultimate strength were decreased following these exposures. This suggests that the amount of the gamma prime phase, its size, and its location controlled the strengths.

The identity of the phase enveloping the intergranular and intragranular particles after the longer-time high temperature exposures was determined with the aid of a selective etching technique. By varying the etching conditions, it was possible to etch out the gamma prime phase. This technique was applied to specimen R-26 which had been subjected to a 100-hour creep-exposure at 1800°F. In the normally etched condition, Figures 52 and 54, the structure consisted of massive grain boundary material surrounded by an unknown phase, large particles of the gamma prime which remained undissolved at the exposure temperature, fine gamma prime that formed during cooling, and several isolated particles surrounded by the unknown phase. After selective-etching, it can be seen in Figures 53 and 55 that the unknown "enveloping" phase was attacked in the same manner as both forms of the matrix gamma prime. This indicated that the "enveloping" phase was gamma prime.

The gamma prime was thus subject to several processes during creep exposure above 1400°F. First, there was a tendency to go into solution in order to satisfy the phase relationships at the exposure temperature. Secondly, there was a tendency for it to agglomerate into larger particles and also to envelope the particles of another phase present in the boundaries and also as isolated intragranular particles. There was also a tendency for the reprecipitation of gamma prime as fine particles on cooling. The net effect of these processes was to reduce the number of gamma prime particles in the matrix as the exposure time and temperature were increased. There was no evidence to indicate if the total amount of gamma prime in the overall structure was changed. It can be seen that as the amount of "enveloping" gamma prime was increased, the amount of "free" matrix gamma prime was decreased. Some tendency was observed for the large particles of "free" gamma prime to be aligned on crystallographic planes of samples subjected to stressed exposure at the higher temperatures.

Similar structural changes were also observed in specimens heat treated at 2050°F ("R2" condition) when subjected to creep-exposure. Representative electron micrographs before and after 100 hours exposure are presented in Figure 56 (as-treated) and Figures 57 and 58 (after exposure).

In the as-treated condition, the "R2" material had a coarser gamma prime dispersion than the "R" condition. Changes in the amount, size, form, and distribution of gamma prime and increasing complexity of the boundary phases followed the exposures at 1600°F (Fig. 57) and 1800°F (Fig. 58). The mechanical properties of these specimens after exposure were the same as those of the "R" material similarly exposed and the microstructures were quite similar.

Up to this point in the discussion, no reference by name has been made to the other phases present in the material other than to point out the presence of titanium carbonitride. X-ray diffraction studies, to be discussed below, were carried out concurrently with the electron microscope investigations. These studies identified the other minor phases as metal carbides.

X-ray Diffraction. X-ray diffraction analysis was made with one exception on the residues from bromine-methyl alcohol extractions of a number of specimens. The purpose of these studies was to identify the minor phases so their occurrence could be correlated with the mechanical property and metallographic observations.

The diffraction data are summarized in Table 6 together with the creep-exposure conditions and subsequent room temperature tensile test elongation for each sample. Also included in Table 6 are the patterns for several phases suspected to be present in Rene' 41. Previous experience at the University indicated that likely minor phases included the metal carbides M_6C and $M_{23}C_6$ (where "M" could indicate Mo, Cr, Fe, etc.) and TiC and TiN. Later, during the investigation, access was gained to the studies of Beattie on the aging characteristics of Rene' 41 (Ref. 11). Depending on the aging temperature after solution treatment at 2150°F, and generally after 1000 hours of aging, Beattie identified the following constituents and their solution temperatures:

Constituent	Solution Temp.
$M_{23}C_6$	1700 - 1800°F
Mu phase (Co_7Mo_6)	
Ni_3 Ti (possibly)	
Gamma Prime	1900 - 1950°F
M_6C	2150°F
TiC, TiN	Not defined

Since the emphasis of the present investigation was on the study of creep damage to mechanical properties rather than structural studies per se,

no attempt was made to determine individual lattice parameters for the phases present in each sample. The "d" values and intensities given in Table 6 for standard patterns are best compromise values and are primarily a synthesis of the data of Rosenbaum (Ref. 13) and Goldschmidt (Ref. 14).

Since gamma prime was identifiable by electron microscopy, no rigorous attempt was made to include it in the x-ray diffraction studies of minor phases. Its occurrence was, however, also confirmed by a diffraction study of the residue from a phosphoric acid extraction of sample R-26 (not reported in Table 6). The bromine extractions had the advantage of concentrating the minor phases, thus allowing diffraction patterns to be obtained that were free of extraneous reflections from gamma prime and the matrix.

A careful study of the data of Table 6 led to the following conclusions:

1) M_6C and TiC were identified in all samples.

2) $M_{23}C_6$ was identified in all the extracted samples except the as-treated "R" condition and sample R-23 which had been exposed 100 hours at 1400°F.

3) Mu phase (Co_7Mo_6) could not be identified in any of the samples.

With respect to the identification of TiC, it should be noted that TiC and TiN form a continuous solid solution. The phase identified optically had the characteristic appearance of Ti(C, N), however, the lattice parameter with the best fit of the observed data was that of TiC. The phase is, therefore, probably a carbon-rich Ti(C, N).

A considerable effort was made to determine if Mu phase developed because Beattie described it as causing secondary long-time hardening. Its metallographic appearance was said to be a general distribution of platelets. No platelets similar to those reported by Beattie were found in any of the metallographic samples of the present investigation. Examination of the pattern given in Table 6 indicates the difficulty of distinguishing Mu phase by x-ray diffraction analysis. Almost without exception, every strong line for the Mu phase falls very near a strong line for one of the carbide phases. However, sufficient separation existed so that identification should have been made if Mu phase was present in any of the samples. The data of Das, Rideout, and Beck (Ref. 15), Hengelein and Kohsok (Ref. 16), Magneli and Westgren (Ref. 17), Das and Beck (Ref. 18), and Sykes and Graff (Ref. 19) were consulted to be sure that no possible diffraction lines had been overlooked. The pattern given in Table 6 was calculated from lattice parameters given by Hengelein and Kohsok.

It should also be recognized that isolated lines belonging to none of the above listed phases were occasionally observed. Attempts to identify these lines as belonging to various nitrides or oxides were unsuccessful.

Summary of Structural Observations and Mechanical Properties

Integration of the metallographic and x-ray diffraction studies, the mechanical property tests, and data from the literature produced the following hypothesis:

1) Solution treatment at 1950°F and aging at 1400°F (the "R" condition) produced a matrix of equi-axed grains containing a very fine dispersion of gamma prime phase. Throughout the structure, more or less at random, were particles of M_6C and TiC. Small M_6C particles were also present in the grain boundaries. This structure had an excellent combination of both strength and ductility. Exposure without stress at temperatures up to and including 1400°F and for times far beyond the normal aging time of 14 hours produced no significant change in properties. Changes in mechanical properties after creep at these temperatures were due to the residual strains from creep.

2) Solution treatment at 2050°F and aging at 1650°F (the "R2" condition) resulted in all the micro-constituents found in the "R" condition, plus the addition of $M_{23}C_6$. Due to the higher aging temperature, the gamma prime dispersion was coarser (i.e., fewer and larger particles) than the "R" condition. This probably accounted for the slightly lower ultimate tensile and yield strengths. The $M_{23}C_6$ apparently did not affect the properties.

3) As the exposure temperature was increased above 1400°F, there was an apparently time-dependent decrease in the number of dispersed gamma prime particles in the matrix and an increase in the amount of grain boundary material. The remaining dispersed gamma prime particles became larger and after the stressed exposures tended to line up along crystallographic planes, although this did not appear to affect properties. The coarsening of the gamma prime dispersion with increased exposure time and temperature probably accounts for the decrease in ultimate tensile and yield strengths.

Selective etching showed that gamma prime enveloped both the intergranular and intragranular carbides and also that much of the increased amount of grain boundary material consisted of carbides. In general, therefore, as the exposure temperature and time increased, the size and amount of the grain boundary carbides increased. $M_{23}C_6$ was identified as a micro-constituent in all samples examined by diffraction after exposure at 1550°F or above.

4) Beattie (Ref. 11) observed on Rene' 41 water quenched from 2150°F, aged at temperatures between 1300° and 1700°F and then subjected to impact tests, a sharp drop in the impact resistance of standard size Charpy specimens as the aging time and temperature were increased. This was correlated

with coherent nucleation of $M_{23}C_6$ at the grain boundaries. The grain boundary $M_{23}C_6$ was then said to ultimately transform to M_6C. Morris (Ref. 10) stated that Rene' 41 should not be annealed at a temperature (2150°F) which dissolves M_6C. He further stated that dissolved carbon from this source precipitated as brittle $M_{23}C_6$ films in the grain boundaries upon exposure at 1200° to 1500°F.

The present data indicated that after solution at 1950°F and aging at 1400°F, exposure temperatures above 1500°F were required for the appearance of $M_{23}C_6$ in relatively short times. Since $M_{23}C_6$ was identified in samples exhibiting good tensile ductility, its occurrence per se was not the cause of the poor ductility observed in other samples.

5) The explanation for poor ductility after creep exposure appears to lie in the increased amounts of grain boundary material which occurred both by build-up of carbides and the agglomeration of gamma prime. The observation by Beattie that the $M_{23}C_6$ transforms to M_6C indicates that the carbide build-up takes the form:

$$M_{(soln)} + C_{(soln)} \rightarrow M_{23}C_6 + M_{(soln)} \rightarrow M_6C$$

This suggests the total amount (and possibly the distribution) of the carbides as an important factor in controlling ductility. Apparently, 10 hours exposure without stress at temperatures up to 1900°F, while sufficient to change the gamma prime dispersion and cause a reduction in strength, was not sufficient to result in enough of a build-up of grain boundary material to reduce ductility.

However, any explanation for the behavior must also account for the additional observations of the volume shrinkage in the unstressed exposures and the apparent stress-accelerated reduction in ductility after the 10-hour creep-exposures.

6) Although this investigation has been concerned with damage to mechanical properties after creep-exposure, it should be recognized that to induce these changes it was necessary to subject the Rene' 41 stock to extremes of both stress and temperature. The material possessed good strength and ductility in the heat treated condition and retained these properties after most conditions of "normal" exposure. The material was particularly outstanding in its lack of susceptibility to internal micro-cracking after substantial amounts of creep at high temperatures. The deep cracking phenomenon after 1200° and 1300°F creep-exposures was obtained under conditions where most of the rupture ductility had been expended. Again, this was well outside the "normal" usage range for the alloy.

CONCLUSIONS

Rene' 41 alloy was subject to thermally-induced structural changes, surface attack, and to creep strain effects, all of which altered mechanical properties at room temperature. It is important, however, to recognize that this investigation deliberately used extreme exposure conditions which emphasized these effects in order to delineate principles governing alteration of mechanical properties by prior creep. The alloy was no more subject to damage from this source and was quite certainly less subject to it than most alloys of the same type.

The observed effects on room temperature properties and their causes, as defined by the investigation to date, were as follows:

1) When the temperatures exceeded 1400°F during unstressed exposure, strength and ductility were reduced by thermally-induced structural changes. The magnitude of the damage increased with temperature of exposure and, within limits, with the time of exposure. There were some alterations of the general trends for exposure at the highest temperatures.

2) Surface reactions also reduced tensile strength and ductility. This subject was not extensively studied for this report. Limited data for 10-hour exposures indicate that the surface effect was as large as the thermally-induced structural changes and probably operated at lower temperatures of exposure.

3) Creep during exposure resulted in higher tensile yield strengths than for unstressed exposure. It also apparently accelerated the structural changes which influence ultimate tensile strength and ductility. Increases in tensile strength also occurred after exposure in the range of 1200° to 1500°F. Above 1500°F, the tensile strengths were less after a 10-hour exposure than for unstressed exposure and after 100-hours exposure were no higher. Ductilities were generally lower for stressed than for unstressed exposure. In addition, a marked loss in ductility occurred in specimens exposed to 3 to 5 percent creep at 1200° and 1300°F.

4) Apparently, exposure to creep conditions removes differences in room temperature properties arising from different initial heat treatments. Internal micro-cracking was not detected and did not appear to be a factor in any of the observed property changes. The thermally-induced structural changes were associated with microstructural changes. Exposure above 1400°F resulted in increasing agglomeration of the gamma prime precipitate with increasing temperature and exposure time. This was apparently responsible for the decrease in strength. The loss in ductility was associated with agglomeration of carbides and gamma prime in the grain boundaries. The absence of such changes for the exposure conditions up to and including

1400°F appeared to be responsible for the absence of any effect on mechanical properties.

The increase in yield strength from creep-exposure appeared to be mainly due to a Bauschinger effect. The increase in tensile strength after exposure up to 1500°F indicates that strain hardening, perhaps augmented by strain-induced precipitation of gamma prime, had occurred. The creep appeared to accelerate the thermally-induced structural changes. The low ductility after 3 to 5 percent creep at 1200° and 1300°F was due to deep cracking associated with the creep strain being close to elongation at rupture.

REFERENCES

1. Gluck, J. V., Voorhees, H. R., and Freeman, J. W. "Effect of Prior Creep on Mechanical Properties of Aircraft Structural Metals", WADC TR 57-150, Parts I, II, III. Part I: 2024-T86 Aluminum (1957), Part II: 17-7PH (TH 1050 Condition) (1957), Part III: C110M Titanium Alloy (1958)

2. Gluck, J. V. and Freeman, J. W. "Effect of Prior Creep on Short-Time Mechanical Properties of 17-7PH Stainless Steel (RH 950 Condition Compared to TH 1050 Condition)", WADC TR 59-339 (1959)

3. Gluck, J. V. and Freeman, J. W. "Effect of Prior Creep on the Mechanical Properties of a High-Strength Heat-Treatable Titanium Alloy, Ti-16V-2.5Al", WADC TR 59-454 (1959)

4. Gluck, J. V. and Freeman, J. W. "Further Investigations of the Effect of Prior Creep on Mechanical Properties of C110M Titanium with Emphasis on the Bauschinger Effect", WADC TR 59-681 (1960)

5. Jahnke, L. P. and Frank, R. G. "High Temperature Metallurgy Today", Metal Progress, v. 74, No. 6, p. 88 (December 1958)

6. Letter from W. H. Couts, Jet Engine Dept., General Electric Co., dated January 7, 1960

7. Bigelow, W. C., Amy, J. A., and Brockway, L. O. "Electron Microscope Identification of the Phase of Nickel-Base Alloys", Prec. ASTM, v. 56, p. 945 (1956)

8. Decker, R. F., Rowe, J. P., Bigelow, W. C., and Freeman, J. W. "Influence of Heat Treatment and Microstructure on High Temperature Properties of a Nickel-Base Precipitation Hardening Alloy", NACA TN 4329 (July 1958)

9. General Electric Bulletin VM-107 "Engineering Data - Rene' 41" May 1958

10. Morris, R. J. "Rene' 41 ... New Higher-Strength Nickel-Base Alloy", Metal Progress, v. 76, No. 6, pp. 67-70 (December 1959)

11. Beattie, H. J. "Aging Reactions in Rene' 41", General Electric Co. Report No. DF59SL314, (May 1959)

12. Betteridge, W. and Franklin, A. W. "Les progres des alliages a base de nickel-chrome en service a haute temperature", Rev. Metallurgie, t. 53, pt. 4, pp. 271-284, (Apr. 1956)

13. Rosenbaum, B. M. "X-Ray Diffraction Investigation of Minor Phases of 20 High Temperature Alloys", NACA TN 1580, (July 1948)

14. Goldschmidt, H. J. "The Structure of Carbides in Alloy Steels", Part I: General Survey, J. Iron and Steel Inst., v. 160, p. 345 (1948), Part II: Carbide Formation in High Speed Steels, J. Iron and Steel Inst., v. 170, p. 218 (1952)

15. Das, D. K., Rideout, S. P., and Beck, P. A. "Intermediate Phases in the Mo-Co-Fe, Mo-Fe-Ni, and Mo-Ni-Co Ternary Systems", J. Metals, v. 4 (10), pp. 1071-1075 (1952)

16. Henglein, E. and Kohsok, H. "The Determination of the Phase Co_7Mo_6", Rev. de Metallurgie, v. 45 (9), pp. 569-571 (1949)

17. Magneli, A. and Westgren, A. "X-Ray Investigation of Cobalt-Tungsten Alloys", Z. anorg. Chem. 238(2/3), p. 268-272 (1938)

18. Das, D. K. and Beck, P. A. "Survey of Portions of the Iron-Nickel-Molybdenum and Cobalt-Iron-Molybdenum Ternary Systems at 1200°C", NACA Tech. Note 2896 (1953)

19. Sykes, W. P. and Graff, H. F. "The Cobalt-Molybdenum System", Trans. ASM v. 23, p. 249-285 (1935)

Table I

PRELIMINARY STUDIES OF EFFECT OF CREEP-EXPOSURE ON MECHANICAL PROPERTIES OF RENE' 41 AND UDIMET 500

Material and Specimen No.	Exposure Conditions: Temp (°F)	Stress (psi)	Time (hours)	% of Rupture Life (est)	Total Load Def. (%)	Plastic Load Def. (%)	Creep Def. (%)	Total Plastic Def. (%)	Total Def. (%)	Room Temperature Properties after Exposure: Ult. Tensile Strength (psi)	0.2% Offset Yield Str. (psi)	Elongation (%)	Reduction of Area (%)	Modulus E (10^6 psi)
*Rene' 41-1	As Heat Treated (a)	--	--	--	--	--	--	--	--	>163,000 (c)	98,400	>15.9	>16.4	29.9
*Rene' 41-2	1200	75,000	100.0	75	0.34	Nil	-0.01	-0.01	0.33	150,000	114,000	9.5	12.7	28.0
*Rene' 41-4	1700	12,000	100.0	75	0.06	Nil	0.11	0.11	0.17	114,400	102,800	1.6	1.6	24.4
Udimet 500-1	As Heat Treated (b)	--	--	--	--	--	--	--	--	168,000	121,000	6.8	7.9	29.7
Udimet 500-2	1200	75,000	100.0	75	0.29	0.01	0.003	0.013	0.293	170,500 (d)	131,000	6.7	6.8	30.9
Udimet 500-4	1700	12,000	100.0	75	0.06	Nil	0.56	0.56	0.61	104,000	98,600	0.8	2.3	30.4

										Izod Impact Strength (ft. lb.)
*Rene' 41	As Heat Treated (a)	--	--	--	--	--	--	--	--	1
*Rene' 41-3	1200	75,000	100.0	75	0.36	0.05	-0.01	0.04	0.35	1
*Rene' 41-5	1700	12,000	100.0	75	0.06	Nil	0.22	0.22	0.28	0
Udimet 500	As Heat Treated (b)	--	--	--	--	--	--	--	--	1
Udimet 500-3	1200	75,000	18.5 (e)	14	0.52	0.07	0.15	0.22	0.67	<1
Udimet 500-5	1700	12,000	100.0	75	0.06	Nil	0.30	0.30	0.36	<1

* Not the same heat of Rene' 41 used in intensive studies

< Less than

> Greater than

(a) 2150°F--1 hr + Oil Quench; 1650°F--4 hr + Air Cool

(b) 2150°F--2 hr + Air Cool; 1975°F--4 hr + Air Cool; 1550°F--24 hr + Air Cool; 1400°F--16 hr + Air Cool

(c) Broke in threads; elongation measurements made on unbroken gauge section

(d) Broke in fillet

(e) Threads stripped out of holder; test discontinued but not cooled under load

Table 2

SHORT-TIME MECHANICAL TEST DATA FOR AS-TREATED RENE' 41 ALLOY

Spec. No.	Test Temp. (°F)	Ult. Strength (psi)	0.2% Offset Yield Strength(psi)	Elongation (%)	Reduction of Area(%)	Modulus E x 10^6 (psi)
			TENSION TESTS			
Condition "R": 1950°F - 1/2 hr + AC; 1400°F - 16 hr + AC						
R-1	Room	187,400	125,800	19.6	26.2	31.0
R-2	Room	187,000	128,000	20.6	28.2	29.9
R-3	Room	195,000	135,400	21.6	29.4	30.7
Average		189,800	129,733	20.5	27.9	30.5
R-22	1200	182,000	--	18.1	18.0	25.3
R-16	1400	132,800	113,100	12.7	17.0	24.8
R-17	1600	82,000	79,800	25.8	47.4	24.1
Condition "R-2": 2050°F - 1/2 hr + AC; 1650°F - 4 hr + AC						
R2-1	Room	179,000	113,200	25.6	32.3	31.1
R2-13	Room	181,600	117,000	25.0	27.0	31.3
Average		180,300	115,100	25.3	29.6	31.2
			COMPARATIVE TENSION DATA			
Data from Ref. 10 Extrusion - 1/2" wall thickness - longitudinal direction Condition: 1950°F - 4 hr + AC; 1400°F - 16 hr + AC						
(avg of 2)	Room	177,200	134,250	10.9	10.0	--
(avg of 4)	1400	134,470	115,865	16.4	19.9	--
Data from Ref. 9 Bar Stock - section size unknown Condition: 1950°F - 4 hr + AC; 1400°F - 16 hr + AC						
	Room	206,000	154,000	14.	--	--
	1400	160,000	136,000	11.	--	--
Sheet Stock - 0.062-inch thickness 1950°F - 12 min + AC; 1400°F - 16 hr + AC						
	Room	185,000	148,000	9.	--	--
	1400	140,000	121,000	5.	--	--
			COMPRESSION TESTS			
Condition "R": 1950°F - 1/2 hr + AC; 1400°F - 16 hr + AC						
R-1C	Room	--	131,800	--	--	30.8
R-2C	Room	--	129,500	--	--	31.9
R-3C	Room	--	132,000	--	--	29.4
Average		--	131,100	--	--	30.4

Spec. No.	Test Temp. (°F)	Impact Str. ft. lb.	Lateral Expansion (%)	Lateral Contraction (%)	Specimen Dimensions
		IZOD IMPACT TESTS			
Condition "R": 1950°F - 1/2 hr + AC; 1400°F - 16 hr + AC					0.197-inches square 2.16 inches long 45° V-notch .039-inches deep at mid-point 0.010 notch root radius
R-1M	Room	3	3.5	2.0	
R-2M	Room	3	4.0	2.5	
Average		3	3.8	2.2	

Table 3

RUPTURE TEST DATA FOR RENE' 41 ALLOY

Spec. No.	Test Temp. (°F)	Stress (psi)	Rupt. Time (hrs)*	Elongation (%)	Reduction of Area (%)	Parameter **
			CONDITION "R"			
			(1950°F - 1/2 hr + AC; 1400°F - 16 hr + AC)			
R-18	1200	140,000	4.0	8.3	10.2	34.2
R-49	1200	133,000	9.0	5.3	12.4	34.8
R-67	1200	115,000	100.0	5.0	9.5	36.6
R-15	1300	100,000	28.2	2.6	11.3	37.8
R-68	1300	87,500	90.9	9.5	16.9	38.7
R-88	1400	83,000	9.6	11.4	21.0	39.1
R-82	1400	83,000	7.8	4.7	11.1	38.9
R-6	1400	80,000	17.3	25.5	28.9	39.9
R-39	1600	46,337	5.3	25.6	40.3	42.7
R-35	1600	41,000	9.4	25.0	40.0	43.3
R-7	1600	35,000	27.7	26.2	41.0	44.2
R-57	1700	13,000	99.7	27.1	46.9	47.5
R-56	1800	13,500	6.9	32.8	55.0	47.1
R-64	1800	13,000	9.6	35.4	55.0	47.5
R-14	1800	8,000	116.1	41.4	54.3	49.8
			CONDITION "R2"			
			(2050°F - 1/2 hr + AC; 1650°F - 4 hr + AC)			
R2-2	1400	90,000	5.0	22.1	35.2	38.6
R2-4	1400	67,000	83.5	16.1	37.6	40.8
R2-3	1600	42,000	9.5	24.0	44.4	43.3
R2-5	1600	28,000	81.0	19.8	43.8	45.2
R2-6	1800	17,000	3.1	27.2	67.0	46.4
R2-9	1800	8,500	97.3	23.2	38.6	49.7

* Plus 4 hr pre-heat prior to load application

** $P = T(20 + \log t) \times 10^{-3}$

Where T = temperature, °R

t = time, hours

Table 4

CREEP EXPOSURE TEST DATA FOR RENE' 41 ALLOY

(REMACHINED SPECIMENS)

Specimen No.	Temp (°F)	Time* (hrs)	Stress (psi)	% of Rupture Life (est)	Total Load Def. (%)	Plastic Load Def. (%)	Creep Def. (%)	Total Plastic Def. (%)	Total Def. (%)	Ult. Tensile Strength (psi)	0.2% Offset Yield Str. (psi)	Elongation (%)	Reduction of Area (%)	Modulus E x 10^6 (psi)
CONDITION "R": 1950°F - 1/2 HR + AIR COOL; 1400°F - 16 HR + AIR COOL														
TENSION TESTS														
As Treated (avg)	--	--	--	--	--	--	--	--	--	189,800	129,733	20.5	27.9	30.5
R-66	1200	10.0	133,000	80	2.94	1.86	1.63	3.49	4.57	200,000	185,500	4.7 [a]	5.3	31.9
R-28	1200	10.0	130,000	55	2.77	2.40	1.02	3.42	3.79	208,000	193,000	21.5	28.0	30.6
R-58	1200	100.0	114,000	91	0.54	0.08	0.38	0.46	0.92	198,800	160,400	10.9	12.0	32.3
R-34	1200	100.0	113,000	83	0.77	0.30	1.52	1.82	2.04	199,000	161,000	14.9	25.0	30.5
R-74	1200	116.0	None	Nil	--	--	--	--	--	193,200	133,000	21.8	25.8	31.7
R-63	1300	10.0	108,397	83	0.50	Nil	4.60	4.60	5.10	171,000	--	0.4 [a]	0.7	33.4
R-38	1300	10.0	106,000	67	0.50	0.04	0.46	0.50	0.89	191,000	143,000	20.1	26.4	32.2
R-24	1300	10.0	100,000	34	0.49	Nil	0.31	0.31	0.80	203,000	153,000	19.8	23.8	33.2
R-48	1300	100.0	86,500	87	0.40	Nil	1.24	1.24	1.64	203,000	158,000	19.3	23.2	31.8
R-33	1300	100.0	85,000	77	0.39	Nil	0.83	0.83	1.22	201,000	157,200	20.0	27.1	31.8
R-69	1400	11.6	84,000	99+	0.35	0.02	2.95	2.97	3.20	194,500	164,000	15.9	23.2	33.1
R-44	1400	10.0	83,000	80	0.35	Nil	2.69	2.69	3.04	203,000	172,000	16.7	27.7	31.2
R-65	1400	10.0	80,000	57	0.42	Nil	1.24	1.24	1.66	200,500	155,000	18.5	28.4	32.6
R-51	1400	10.0	None	Nil	--	--	--	--	--	195,100	138,300	20.9	29.5	33.7
R-54	1400	20.5	80,000	99+	0.36	Nil	7.5 (est)	7.5 (est)	7.86 (est)	207,000	181,200	8.6	27.6	30.5
R-40	1400	100.5	61,000	83	0.45	Nil	4.40	4.40	4.85	200,000	163,500	14.5	22.6	31.6
R-23	1400	100.0	56,000	48	0.35	Nil	1.32	1.32	1.67	200,000	148,000	18.1	23.6	35.0
R-30	1400	100.0	None	Nil	--	--	--	--	--	190,000	131,000	22.0	24.9	31.1
R-36	1500	10.0	60,000	91	0.37	Nil	3.45	3.45	3.92	190,500	151,000	18.4	20.8	32.7
R-55	1500	10.0	55,000	48	0.24	Nil	0.67	0.67	0.91	192,500	138,700	19.7	22.1	31.0
R-41	1500	100.0	39,500	80	0.17	0.05	7.3 (est)	7.35 (est)	7.47 (est)	192,000	145,000	12.1	13.2	32.6
R-24	1500	100.0	35,000	43	0.20	Nil	0.71	0.71	0.91	194,000	134,000	10.5	15.7	33.5
R-47	1600	10.0	39,800	80	0.18	Nil	8.6 (est)	8.6 (est)	8.78 (est)	185,000	143,400	10.8	13.6	30.6
R-43	1600	10.0	34,800	38	0.14	Nil	1.07	1.07	1.21	183,000	130,000	16.5	17.8	30.4
R-52	1600	10.0	None	Nil	--	--	--	--	--	190,500	129,000	20.4	25.9	30.8
R-71	1600	100.0	24,000	89	0.11	Nil	0.61	0.61	0.72	159,500	110,800	8.6	8.4	30.8
R-27	1600	100.0	23,000	77	0.13	Nil	1.35	1.35	1.48	170,000	114,100	10.3	11.7	31.8
R-25	1600	100.0	19,000	45	0.09	Nil	0.21	0.21	0.30	171,000	111,400	10.8	13.7	32.2
R-31	1600	100.0	None	Nil	--	--	--	--	--	170,000	106,000	15.1	16.6	30.1
R-60	1600	200.0	19,000	91	0.15	Nil	4.05	4.05	4.20	159,200	109,500	6.8	7.9	34.4
R-59	1600	200.0	None	Nil	--	--	--	--	--	172,100	106,000	13.5	15.0	31.3
R-37	1700	10.0	23,500	71	0.13	Nil	14.2 (est)	14.2 (est)	14.33 (est)	170,400	117,800	11.3	12.0	31.0
R-70	1700	11.6	22,500	68	0.11	Nil	4.4 (est)	4.4 (est)	4.51 (est)	167,500	115,300	10.8	11.4	31.9
R-20	1700	10.0	21,000	48	0.12	0.01	0.74	0.75	0.86	185,000	118,000	18.5	19.0	32.1
R-42	1700	10.0	None	Nil	--	--	--	--	--	179,000	108,200	22.9	26.5	32.6
R-62	1700	100.0	12,500	77	0.07	Nil	3.04	3.04	3.11	153,200	109,500	8.2	8.0	33.2
R-29	1700	100.0	12,000	69	0.08	Nil	0.84	0.84	0.92	147,800	101,500	7.3	7.9	31.2
R-50	1700	100.0	None	Nil	--	--	--	--	--	161,500	89,200	18.2	19.4	32.1
R-73	1700	100.0	None	Nil	--	--	--	--	--	145,200	94,500	8.3	8.7	31.2
R-77	1700	200.0	9,000	72	0.04	Nil	0.41	0.41	0.45	133,800	99,500	2.7	5.7	31.2
R-76	1700	200.0	None	Nil	--	--	--	--	--	128,000	96,400	3.8	6.0	32.2
R-53	1800	2.0	None	Nil	--	--	--	--	--	178,000	105,600	24.6	32.2	31.2
R-72	1800	10.0	12,800	95	0.08	Nil	9.8 (est)	9.8 (est)	9.88 (est)	165,000	114,000	11.2	11.6	30.6
R-19	1800	10.0	12,500	83	0.06	0.02	2.62	2.64	2.68	171,000	115,000	12.4	13.5	31.3
R-61	1800	10.0	None	Nil	--	--	--	--	--	176,000	102,500	22.6	26.5	29.4
R-45	1800	100.0	7,900	77	0.07	Nil	5.17	5.17	5.24	139,500	119,000	3.5	4.1	31.9
R-26	1800	100.0	7,500	62	0.04	Nil	1.70	1.70	1.74	130,200	106,800	3.4	11.7	29.5
R-32	1800	100.0	None	Nil	--	--	--	--	--	137,500	102,600	4.2	5.9	32.4
R-79	1800	200.0	6,000	67	0.03	Nil	1.80	1.80	1.83	--	--	2.2	5.7	--
R-78	1800	200.0	None	Nil	--	--	--	--	--	155,000	109,800	6.3	8.5	--
R-46	1900	10	None	Nil	--	--	--	--	--	180,300	110,500	20.6	26.0	32.5
COMPRESSION TESTS														
As Treated (avg)	--	--	--	--	--	--	--	--	--	--	131,100	--	--	30.4
R76C-1	1400	10.0	None	Nil	--	--	--	--	--	--	132,800	--	--	31.6
-2	1400	10.0	None	Nil	--	--	--	--	--	--	126,800	--	--	32.2
R-83	1600	10.0	38,000	62	0.17	Nil	2.40	2.40	2.57	--	125,000	--	--	33.2
R77C-1	1600	10.0	None	Nil	--	--	--	--	--	--	115,200	--	--	31.2
-2	1600	10.0	None	Nil	--	--	--	--	--	--	109,000	--	--	31.2
R-85	1600	100.0	24,000	89	0.11	Nil	0.45	0.45	0.56	--	98,000	--	--	32.8
R79C-1	1600	100.0	None	Nil	--	--	--	--	--	--	99,500	--	--	33.4
-2	1600	100.0	None	Nil	--	--	--	--	--	--	106,200	--	--	33.4
R-86	1700	100.0	12,500	77	0.05	Nil	0.41	0.41	0.46	--	92,800	--	--	31.5
R80-1	1700	100.0	None	Nil	--	--	--	--	--	--	101,200	--	--	31.4
-2	1700	100.0	None	Nil	--	--	--	--	--	--	96,400	--	--	31.2
R-84	1800	10.0	12,600	84	0.07	Nil	3.45	3.45	3.52	--	102,100	--	--	32.2
R78C-1	1800	10.0	None	Nil	--	--	--	--	--	--	96,000	--	--	30.0
-2	1800	10.0	None	Nil	--	--	--	--	--	--	99,000	--	--	32.0
R-87	1800	100.0	7,900	77	0.04	Nil	2.77	2.77	2.81	--	93,800	--	--	32.2
R81-1	1800	100.0	None	Nil	--	--	--	--	--	--	108,300	--	--	30.6
-2	1800	100.0	None	Nil	--	--	--	--	--	--	104,000	--	--	32.2
CONDITION "R2": 2050°F - 1/2 HR + AIR COOL; 1650°F - 4 HR + AIR COOL														
TENSION TESTS														
Treated (avg)	--	--	--	--	--	--	--	--	--	180,300	115,100	25.3	28.6	31.2
R2-10	1600	100.0	25,000	83	0.11	Nil	2.92	2.92	3.03	163,000	114,000	9.0	9.9	29.4
R2-7	1600	100.0	None	Nil	--	--	--	--	--	170,000	108,000	14.1	14.3	31.4
R2-12	1800	10.0	None	Nil	--	--	--	--	--	166,800	98,300	18.6	19.2	31.0
R2-11	1800	100.0	7,500	69	0.03	Nil	3.88	3.88	3.91	138,000	110,900	3.6	5.0	31.7
R2-8	1800	100.0	None	Nil	--	--	--	--	--	140,500	105,000	5.0	4.9	30.6

Plus 4 hr pre-heat prior to load application

) Small oxidized area on fracture

Table 5

EFFECT OF RE-MACHINING ON ROOM TEMPERATURE TENSILE PROPERTIES OF RENE' 41 SUBJECTED TO 10 HOURS CREEP-EXPOSURE AT ELEVATED TEMPERATURE

	Exposure Conditions									Room Temperature Tensile Properties After Exposure					
Spec. No.	Temp (°F)	Time* (hrs)	Stress (psi)	% of Rupture Life (est)	Total Load Def. (%)	Plastic Load Def. (%)	Creep Def. (%)	Total Plastic Def. (%)	Total Def. (%)	Amount Machined from Dia. (in)	Ult. Tensile Strength (psi)	0.2% Offset Yield Str. (psi)	Elongation (%)	Reduction of Area (%)	Modulus E x 10^6 (psi)
R-11	1400	10.0	None	Nil	-	-	-	-	-.006	NR	183,500	134,000	14.7	18.7	29.7
R-51	1400	10.0	None	Nil	-	-	-	-	-	0.027	195,100	138,300	20.9	29.5	33.7
R-8	1400	10.0	80,000	57	0.36	Nil	2% (est)	2% (est)	2% (est)	NR	192,400	152,600	16.0	17.2	30.1
R-65	1400	10.0	80,000	57	0.42	Nil	1.24	1.24	1.66	0.022	200,500	155,500	18.5	28.4	32.6
R-13	1500	10.0	55,000	48	0.30	Nil	1.24	1.24	1.54	NR	179,500	136,000	9.9	15.2	30.1
R-55	1500	10.0	55,000	48	0.24	Nil	0.67	0.67	0.91	0.025	192,500	138,700	19.5	22.1	31.0
R-10	1600	10.0	None	Nil	-	-	-	-	-.017	NR	175,800	125,500	10.1	13.7	30.1
R-52	1600	10.0	None	Nil	-	-	-	-	-	0.027	190,500	129,000	20.4	25.9	30.8
R-9	1600	10.0	35,000	38	0.18	Nil	1.13	1.13	1.31	NR	169,000	128,200	8.9	11.5	30.2
R-43	1600	10.0	34,800	38	0.14	Nil	1.07	1.07	1.21	0.022	183,000	126,000	16.5	17.8	30.4
R-12	1800	10.0	None	Nil	-	-	-	-	.02	NR	158,000	104,300	9.5	10.5	29.9
R-61	1800	10.0	None	Nil	-	-	-	-	-	0.027	176,000	102,500	22.6	26.5	29.4

* Plus 4 hour preheat prior to load application

NR: Not Remachined

Table 6

X-RAY DIFFRACTION DATA FROM EXTRACTION RESIDUES OF RENE' 41 ALLOY

EXTRACTION: BROMINE - METHYL ALCOHOL

DIFFRACTION: 4 HOURS - COPPER Kα RADIATION

(Data given are "d" values and relative intensity of the line)

Spec. No. / Exp. Temp / Time	R-1 As Treated	R-23 1400°-100	D-1 1550°-436	R-27 1600°-100	R-60 1600°-200	R-42 1700°-10	R-62 1700°-100	R-77 1700°-200	R-61 1800°-10	R-32 1800°-100	R-26 1800°-100	R-45 1800°-100	R-79 1800°-200	R-46 1900°-10	R2-1 As Treated	R2-10 1600°-100	R2-8 1800°-100	"M_6C" (K_1)	TiC	$M_{23}C_6$	Mu (Co_7Mo_6)
Total Plastic Def. - %	--	1.32	--	1.35	4.20	--	3.04	(0.41)	--	--	1.70	5.17	(1.80)	--	--	2.92	--				α=8.98 β=30° 48
Tensile Elongation	20.5	18.1	2	10.3	6.8	22.9	8.2	2.7	22.6	4.2	3.4	3.5	2.2	20.6	25.6	9.0	5.0	α=11.10	α=4.32	α=10.71	
"d" Range			2.89 mw			2.92 w+			2.91 mw	2.90 w				2.87 w			2.88 mw	3.20		3.105	2.84 20
2.70 - 2.79	2.79 mw	2.77 w+		2.77 mw	2.78 mw	2.76 w+	2.77 mw	2.77 mw	2.78 w+		2.76 mw	2.77 mw	2.77 w+	2.77 mw	2.77 mw		2.77 mw	2.77 m			
2.60 - 2.89																	2.67 mw			2.68 w	
2.50 - 2.59			2.55 mw		2.54 m-		2.54 m-	2.54 mw			2.54 mw	2.54 mw	2.54 mw	2.54 mw			2.545 mw	2.54 ms			2.52 40
2.39 - 2.49	2.48 vs	2.49 vs	2.49 m 2.40 m	2.485 vs 2.395 m-	2.485 m 2.40 mw	2.49 s 2.40 mw	2.485 m- 2.40 mw	2.49 m- 2.40 m	2.49 vs 2.39 w	2.49 vs 2.395 vw	2.49 vs 2.405 mw	2.485 m- 2.90 mw	2.485 mw 2.90 mw	2.49 s 2.395 mw	2.49 s 2.40 mw	2.49 s 2.40 mw+	2.49 s 2.40 m-	2.48	2.49s	2.46 vw 2.399 s	
2.30 - 2.39																					2.385 100
2.20 - 2.29	2.26 m-	2.26 mw 2.22 w	2.26 m-	2.26 m	2.26 ms	2.26 mw	2.26 m	2.26 m	2.235	2.24 vw	2.265 m 2.225 mw	2.255 ms	2.26 m-	2.255 ms	2.255 m-		2.26 m-	2.263 s			(2.29) (?)
2.10 - 2.19	2.16 vs	2.16 vs 2.125 w	2.19 m 2.13 ms	2.15 vs 2.125 m-	2.19 w+ 2.135 vs	2.155 vs	2.19 mw 2.16 mw 2.13 vs	2.19 m 2.13 s	2.155 vs	2.16 vs	2.16 vs	2.19 w+ 2.145 s	2.19 mw 2.13 s	2.19 mw 2.155 ms+ 2.125 vs	2.16 vs	2.20 mw 2.155 s	2.19 m- 2.135 ms 2.125 ms	2.135 vs	2.16 s	2.185 s	2.18 80 2.125 40
2.00 - 2.09			2.065 s	2.063 m-	2.065 m+	2.065 m-	2.06 m	2.07 s	2.06 w	2.07 mw	2.065 mw+	2.063 m-	2.065 ms	2.065 m+	2.063 m	2.065 ms	2.06 s			2.062 s	2.085 80 2.06 60
1.89 - 1.99	1.957 mw	1.957 mw	1.947 m- 1.895 m-	1.96 m- 1.90 mw	1.955 ms 1.895 mw	1.957 mw	1.955 m+ 1.895 mw	1.957 m- 1.895 m-	1.985 mw	1.90 w	1.96 m- 1.90 w+	1.955 m+ 1.90 mw	1.955 m 1.895 mw	1.955 m 1.895 mw	1.955 m- 1.895 mw	1.905 m-	1.935 m- 1.90 m-	1.959 m		1.892 m	2.04 60 1.965 40 1.905 40
1.80 - 1.88			1.815 m-	1.843 w+ 1.81 w+	1.843 mw 1.815 mw	1.825 mw	1.84 m- 1.81 mw	1.845 w+ 1.815 mw		1.815 w	1.845 w+ 1.82 mw	1.845 mw 1.815 mw	1.842 w+ 1.81 mw+	1.840 mw		1.813 mw	1.82 m-	1.875 w 1.850 w		1.810 s	1.822 40
1.69 - 1.79			1.70 m-				1.785 w+ 1.693 w	1.787 w+ 1.695 mw			1.793 m-	1.787 w	1.70 w+	1.787 mw+			1.79 mw 1.695 w+	1.753 vw 1.69 w		1.785 mw 1.692 vw	1.802 20 1.73 40
1.60 - 1.68			1.632 m		1.67 mw 1.615 w	1.66 mw 1.625 vw	1.67 mw+ 1.655 w+	1.67 w 1.62 mw			1.613 w	1.667 mw 1.615 w+	1.673 w+ 1.617 mw	1.667 mw 1.615 mw	1.66 w+	1.683 w 1.615 mw	1.667 w+ 1.617 mw	1.67 w 1.60		1.632 vw 1.615 mw	1.63 40
1.50 - 1.59	1.527 ms	1.525 s	1.55 w 1.525 m-	1.525 s	1.55 m- 1.525 m	1.525 ms	1.55 m- 1.52 m-	1.55 mw 1.523 mw	1.525 s	1.523 s	1.57 m- 1.55 w 1.525 ms	1.546 mw 1.520 m-	1.55 mw 1.52 mw	1.545 m- 1.52 m	1.523 ms	1.525 ms	1.55 w+ 1.523 m	1.552 mw 1.528 w	1.528 m	1.545	1.584 40 1.56 20 1.55 20 1.542 20
1.40 - 1.49	1.437 vw		1.44 w	1.44 s	1.443 mw		1.403 m-	1.443 w+			1.445 mw	1.440 mw	1.438 mw	1.438 mw+	1.443 w		1.440 mw	1.481 1.443 mw		1.500 vw 1.486 vw 1.431	1.42 20 1.405 20
1.30 - 1.39	1.38 vw 1.305 ms	1.300 ms	1.354 w 1.303 m	1.364 w 1.30 ms	1.355 m- 1.306 s	1.300 m	1.35 m-	1.354 w 1.342 w	1.30 ms	1.300 ms	1.354 mw 1.338 m- 1.302 ms	1.352 mw 1.303 m+	1.350 mw 1.302 m	1.35 mw 1.300 ms	1.353 w 1.300 w	1.300 m+	1.352 w+ 1.302 m	1.385 w 1.353 m 1.345 vw 1.307 s	1.302 mw	1.395 vw 1.340 w 1.310 1.300	1.39 20 1.38 60 1.34 60 1.32 60 1.30 60
1.20 - 1.29	1.250 m	1.246 m	1.28 w 1.266 m- 1.242 mw	1.284 ms 1.264 w 1.244 w	1.28 mw 1.264 mw 1.245 mw 1.217 w+	1.266 w 1.244 m-	1.278 m- 1.264 mw 1.242 w 1.212 w	1.279 mw 1.264 m 1.240 mw	1.244 m	1.295 m	1.280 m 1.267 m- 1.245 m	1.275 mw 1.263 mw 1.242 mw 1.214 w	1.275 mw 1.263 m- 1.238 mw	1.276 m- 1.267 m- 1.242 m- 1.215 w+	1.264 w 1.244 m-	1.264 mw 1.244 m-	1.279 w+ 1.266 m- 1.243 m-	1.280 ms 1.271 1.240 1.218 1.210	1.249	1.271 s 1.238 w 1.230 w	1.26 40 1.24 20 1.225 60 1.22 60
1.10 - 1.19	1.114 mw	1.16 w	1.179 mw 1.117 mw	1.175 mw	1.18 w+ 1.17 w+	1.113 mw 1.102 mw	1.178 w 1.112 mw	1.178 mw 1.113 mw			1.170 m- 1.12	1.178 w 1.14 m-	1.177 w+ 1.16 mw	1.178 w+ 1.16 m-	1.13 mw		1.18 mw 1.112 mw	1.182 w 1.115		1.198 m 1.175 1.170 1.142	1.19 80
1.00 - 1.09	1.078 m	1.032 m	1.099 m- 1.08 mw	1.076 m	1.094 w+ 1.088 mw 1.078 w+	1.079 m-	1.094 w+ 1.086 mw+ 1.07 mw	1.098 mw 1.087 w 1.078 mw	1.079 m-	1.098 vw 1.078 m-	1.098 1.074 m- 1.015	1.099 w 1.086 w 1.07 w 1.036 mw	1.097 mw 1.079 mw	1.097 w 1.085 w 1.076 w	1.093 vw 1.075 m- 1.03 m-	1.097 mw 1.078 mw	1.098 mw 1.079 mw		1.080 1.02		1.089 1.079 1.046 1.043 1.029 1.023
less than 1.00	additional 6 lines	additional 7 lines	additional 17 lines	additional 10 lines	additional 20 lines	additional 6 lines	additional >20 lines	additional >17 lines	additional 6 lines	additional 6 lines	additional 13 lines	additional 17 lines	additional 18 lines	additional 20 lines	additional 5 lines	additional 6 lines	additional >10 lines				
Phases Identified	M_6C TiC	M_6C TiC	M_6C TiC $M_{23}C_6$	M_6C TiC $M_{23}C_6$	M_6C TiC $M_{23}C_6$	M_6C TiC $M_{23}C_6$	M_6C TiC $M_{23}C_6$	M_6C TiC $M_{23}C_6$	M_6C TiC $M_{23}C_6$	M_6C TiC $M_{23}C_6$	M_6C TiC $M_{23}C_6$	M_6C TiC $M_{23}C_6$	M_6C TiC $M_{23}C_6$	M_6C TiC $M_{23}C_6$	M_6C TiC $M_{23}C_6$	M_6C TiC $M_{23}C_6$	M_6C TiC $M_{23}C_6$				

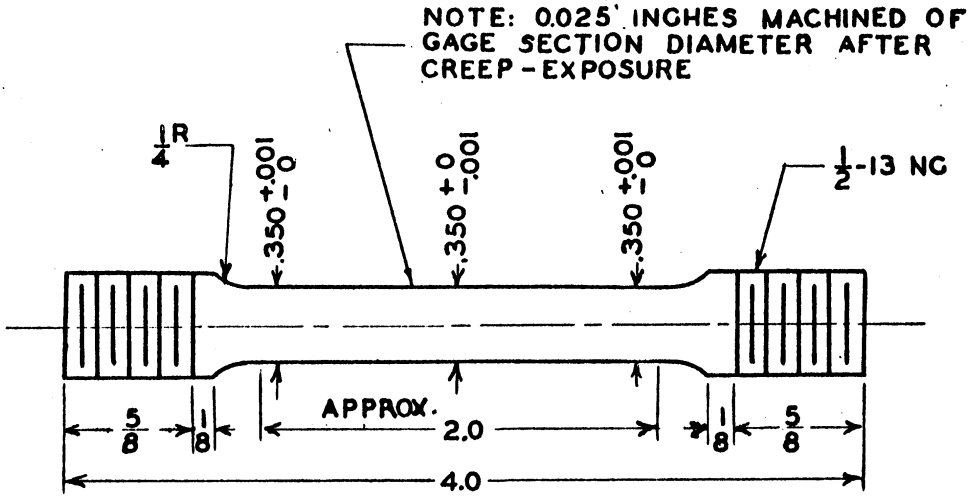

TENSILE AND CREEP SPECIMEN

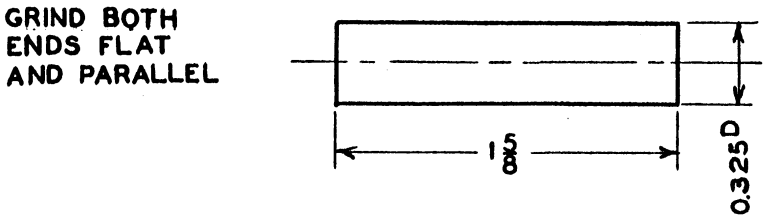

COMPRESSION SPECIMEN

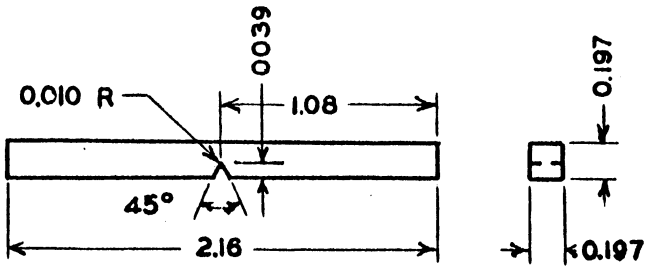

TYPE-W IMPACT SPECIMEN

Note: Center of the Compression and Impact Specimen to Coincide with the Center of the Creep Specimen.

FIGURE 1. Details of Test Specimens

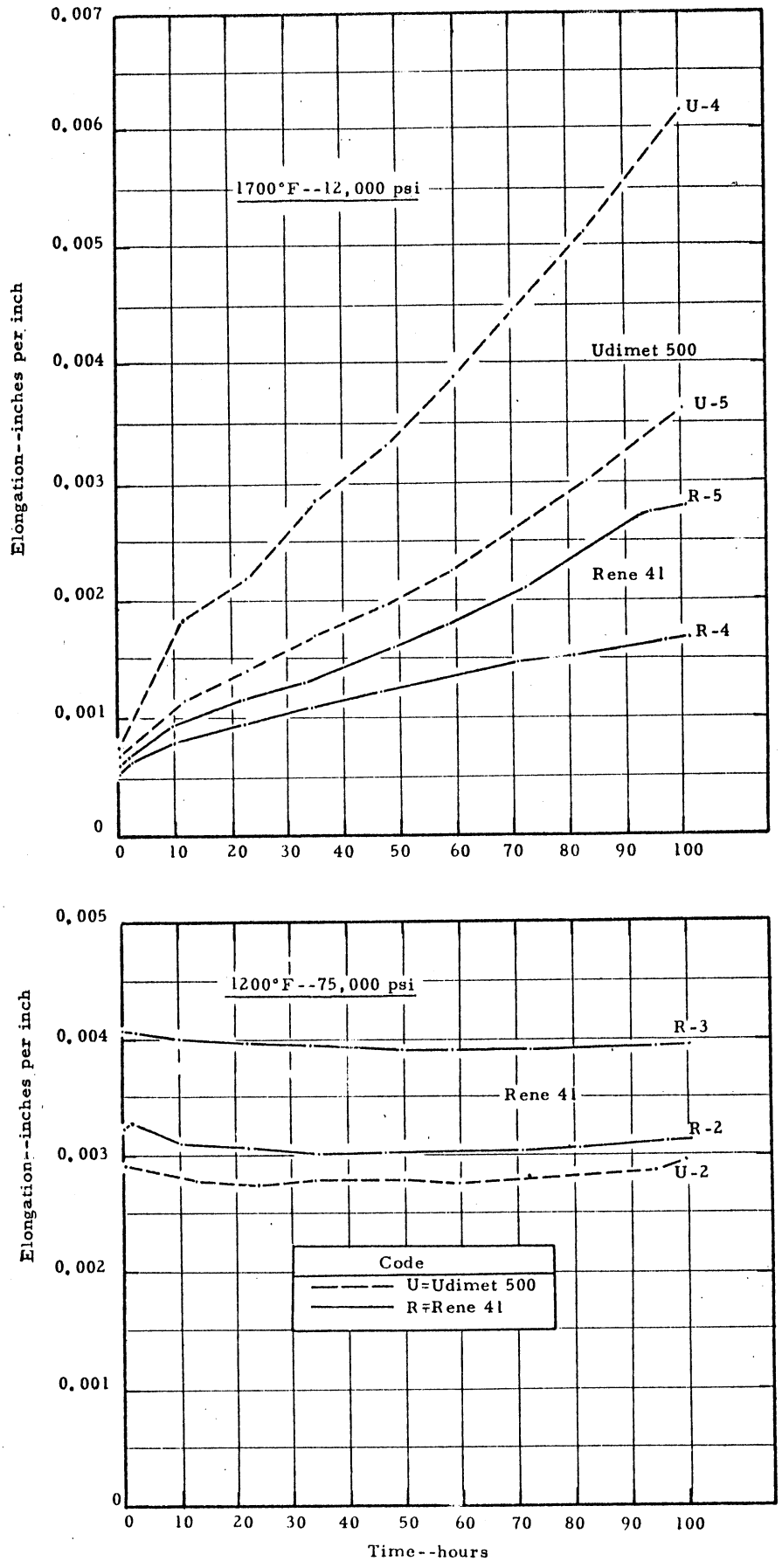

Figure 2 Time-Elongation Curves for Preliminary Creep-Exposures of Rene' 41 and Udimet 500 at 1200°F or 1700°F

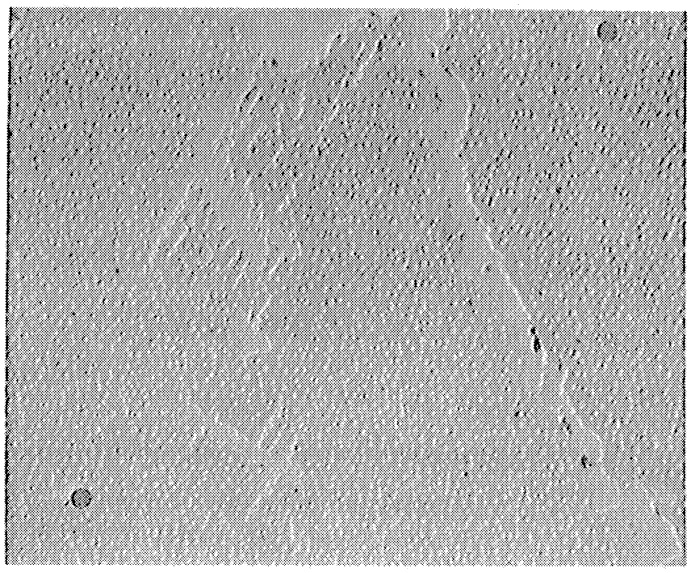

Figure 3 Rene' 41 - As Heat Treated (2150°F - 1 hr + Oil Quench 1650°F - 4 hr + Air Cool)

G-etch
8200x

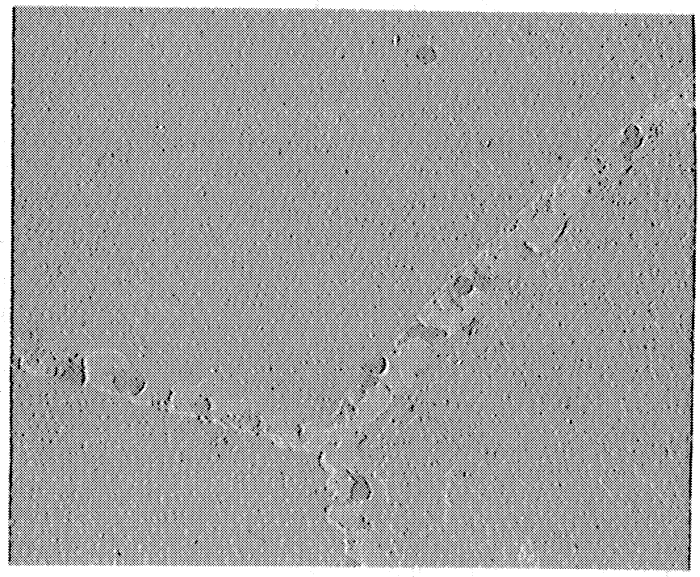

Figure 4 Rene' 41 - Exposed 100 Hours at 1200°F and 75,000 psi

G-etch
8200x

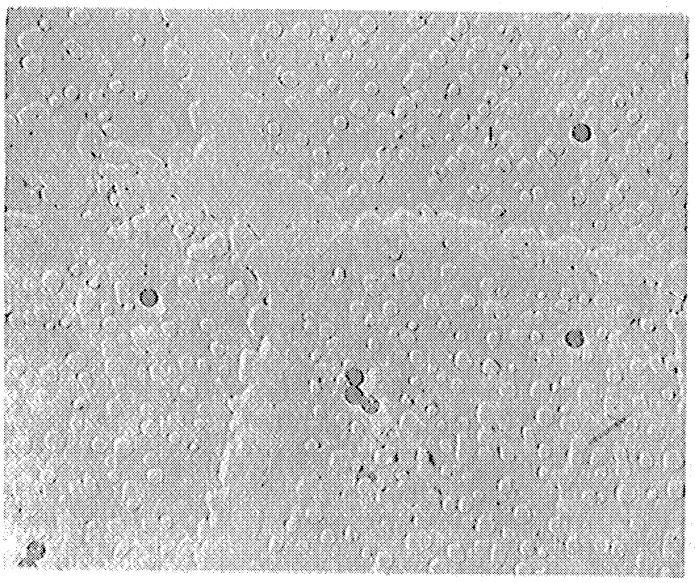

Figure 5 Rene' 41 - Exposed 100 Hours at 1700°F and 12,000 psi

G-etch
8200x

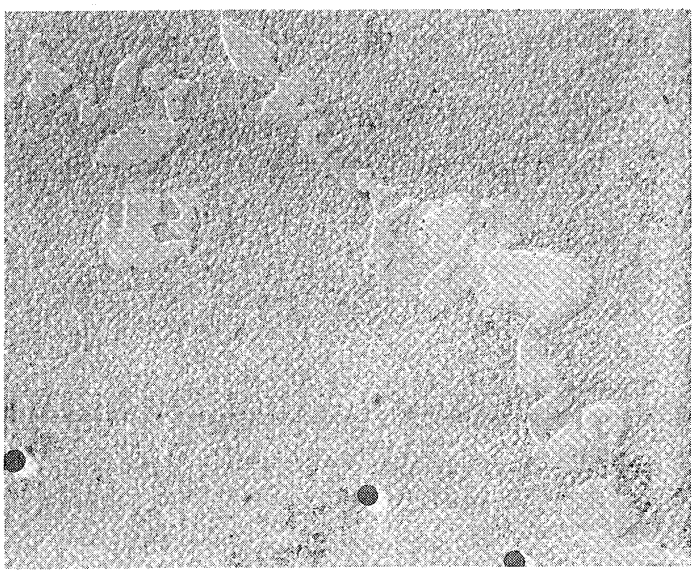

Figure 6 Udimet 500 - As Heat Treated
(2150°F - 2 hr + Air Cool
1975°F - 4 hr + Air Cool
1550°F - 24 hr + Air Cool
1400°F - 16 hr + Air Cool

G-etch
8200x

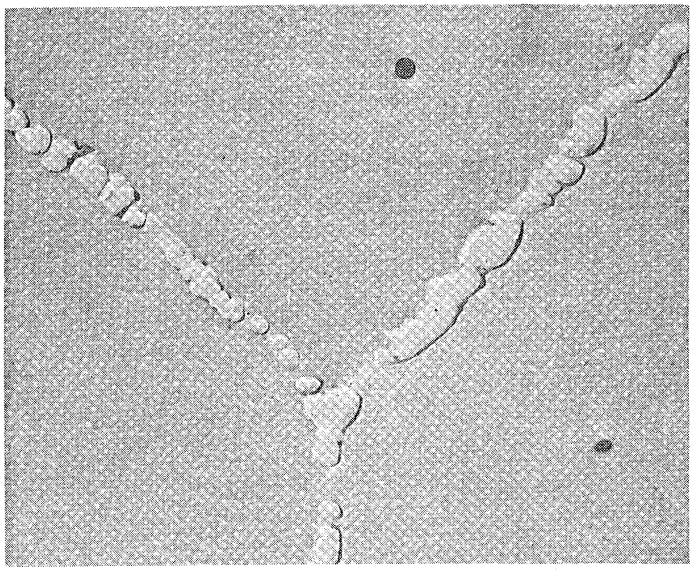

Figure 7 Udimet 500 - Exposed 100
Hours at 1200°F and 75,000 psi

G-etch
8200x

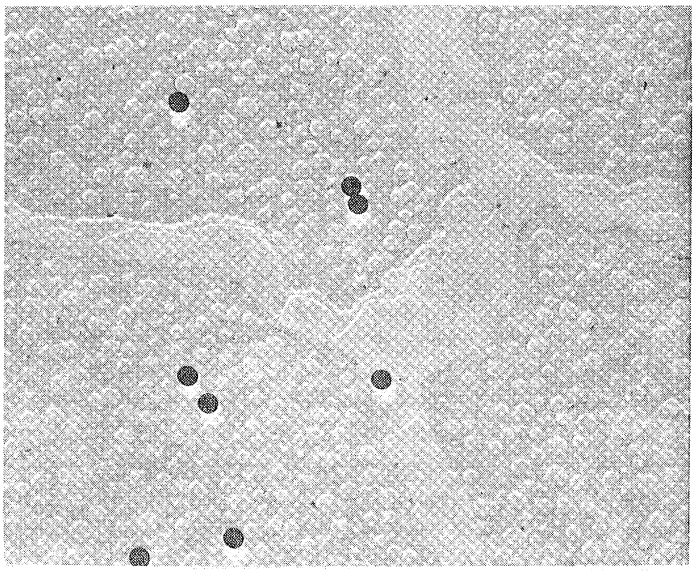

Figure 8 Udimet 500 - Exposed 100
Hours at 1700°F and 12,000 psi

G-etch
8200x

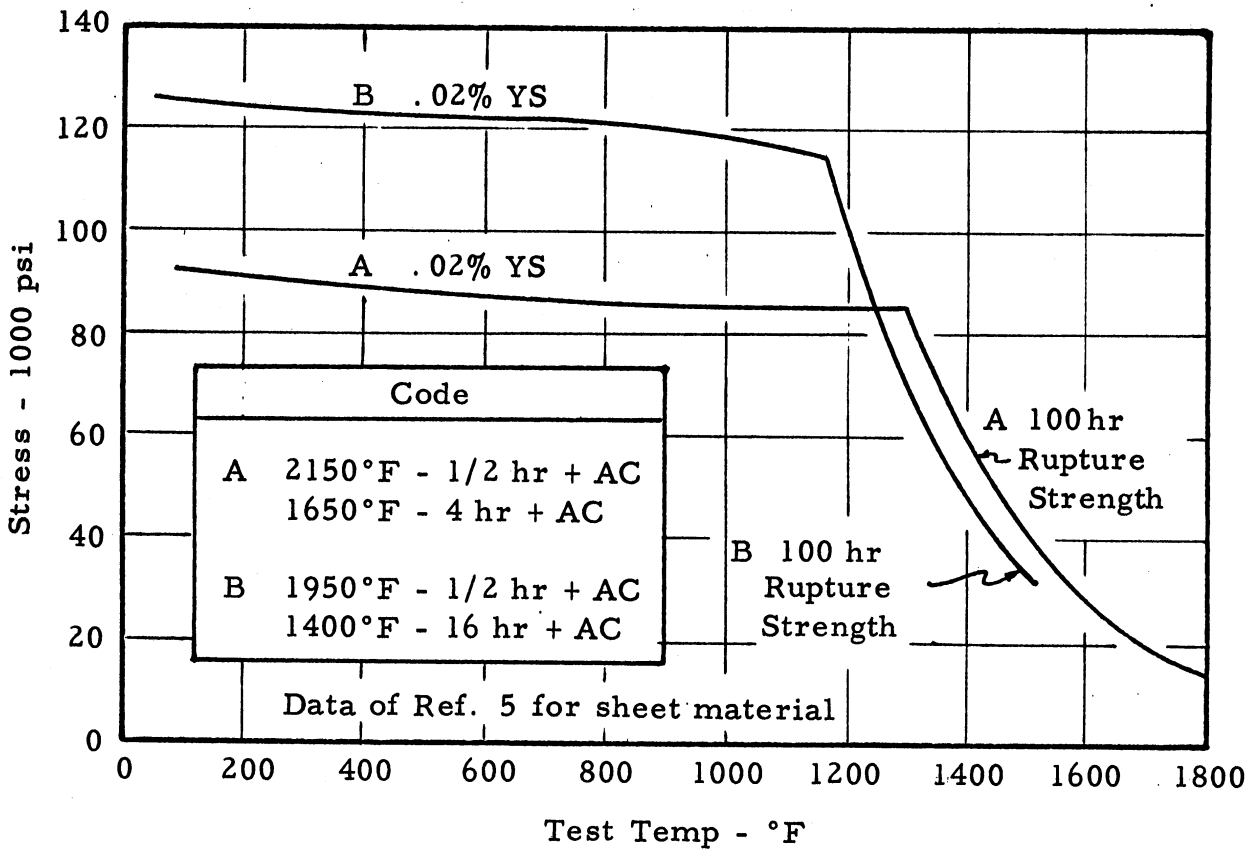

Figure 9 Data of Jahnke and Frank (Ref. 5) On Effect of Temperature and Heat Treatment On Properties of Rene' 41.

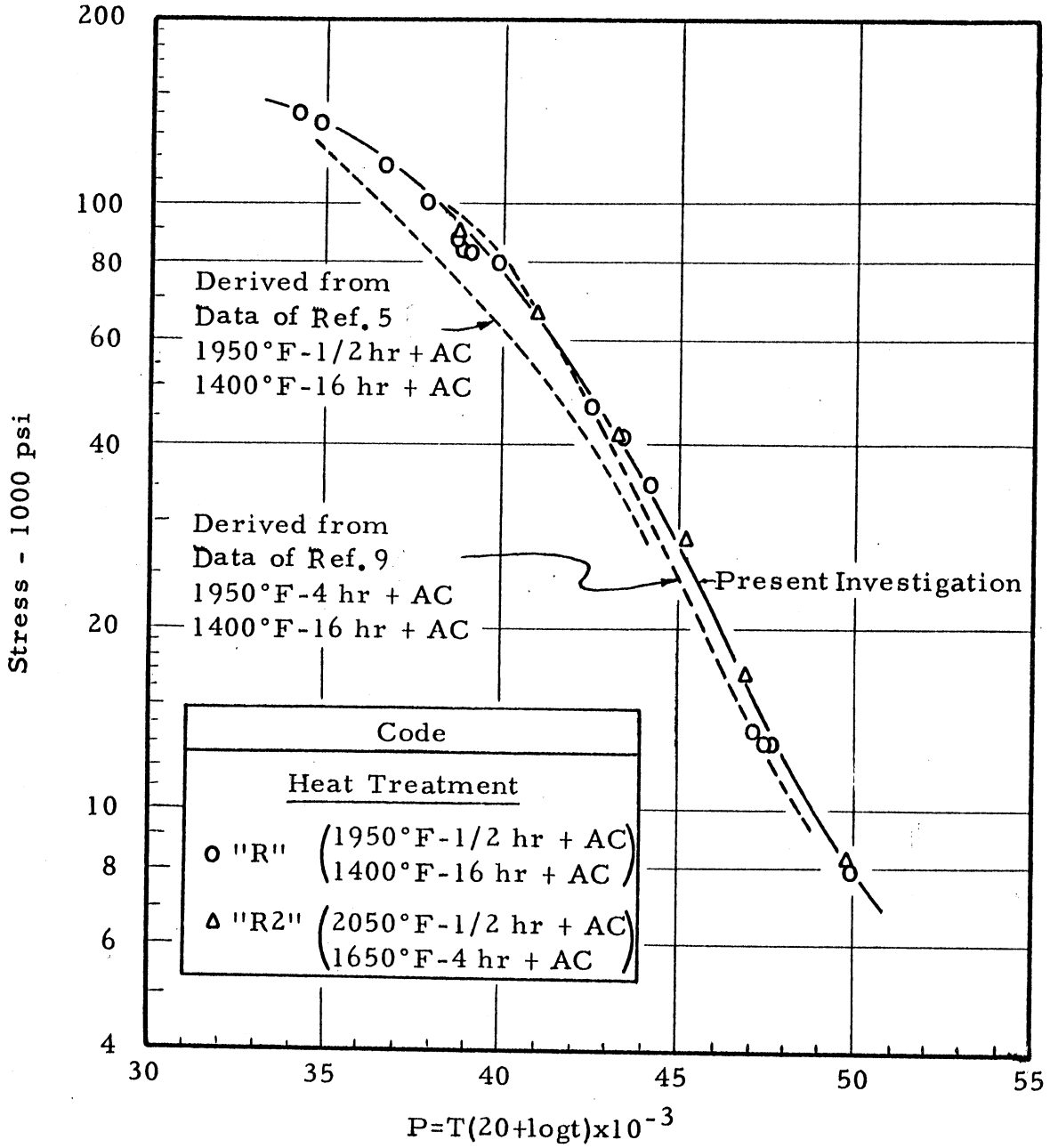

Figure 10 Master Rupture Curves for Solution Treated and Aged Rene' 41 Alloy

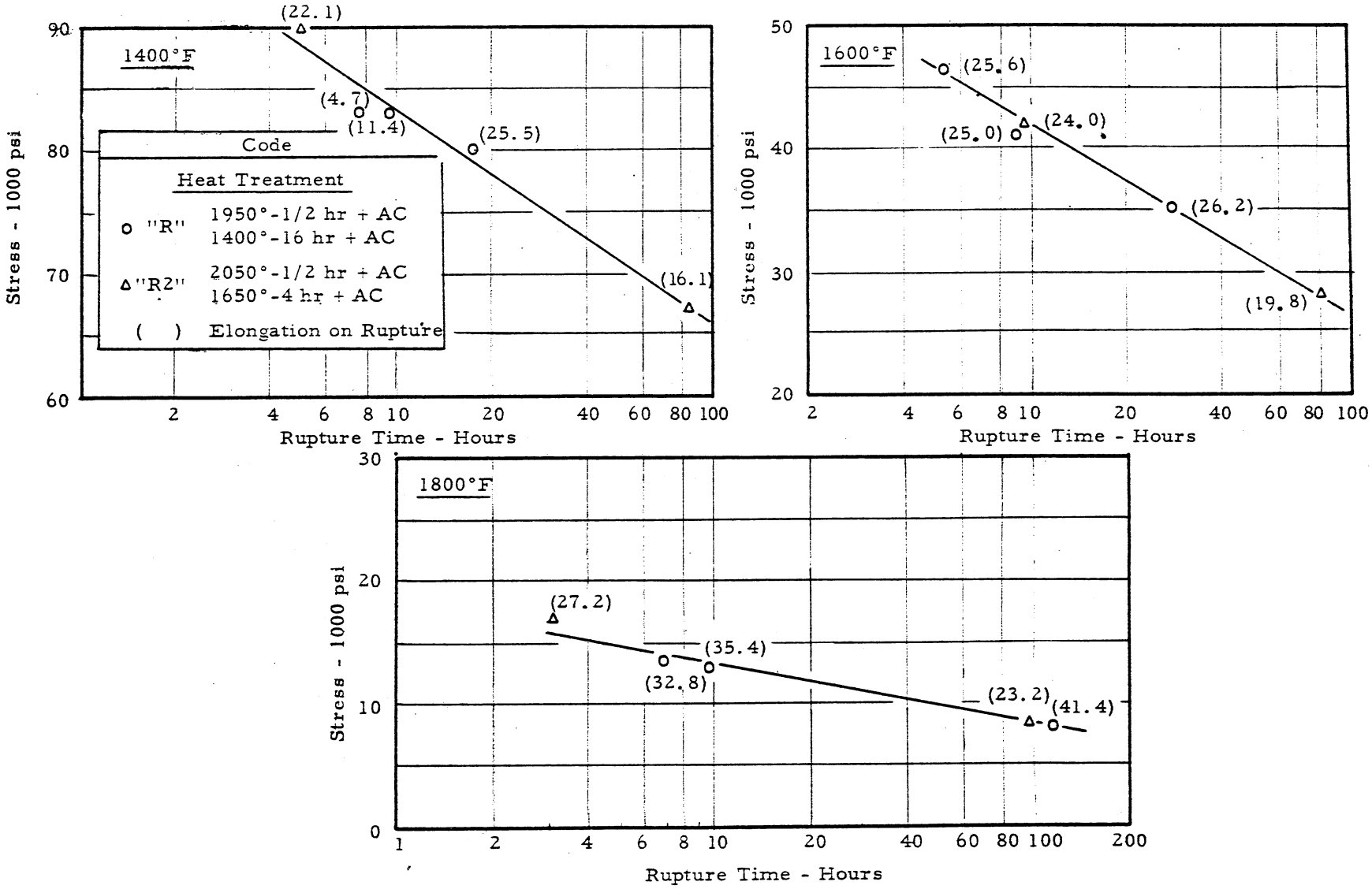

Figure 11 Comparison of Rupture Properties of Rene' 41 in Two Conditions of Heat Treatment

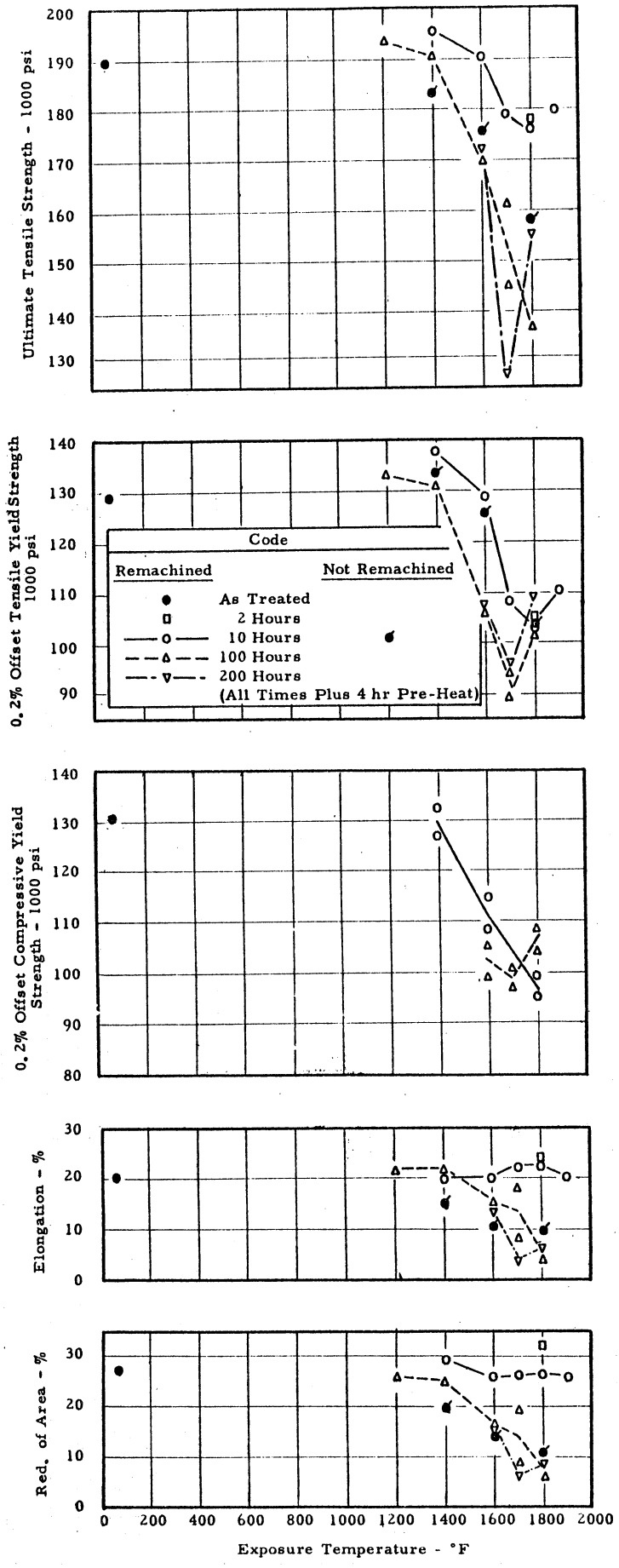

Figure 12 Effect of Exposure Temperature in Unstressed Exposures on Room Temperature Short-Time Properties of Rene' 41 Alloy

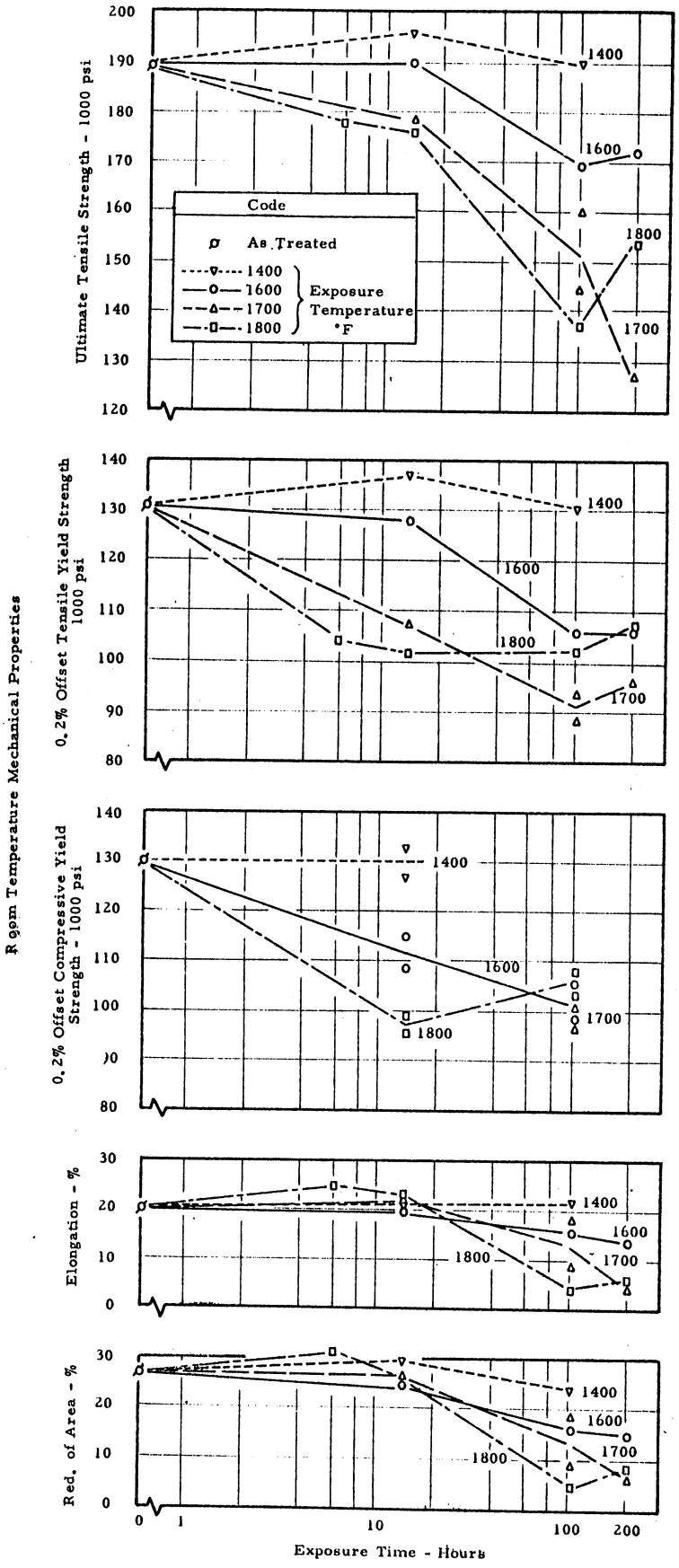

Figure 13 Effect of Exposure Time in Unstressed Exposures on the Room Temperature Short-Time Properties of Rene ' 41 Alloy

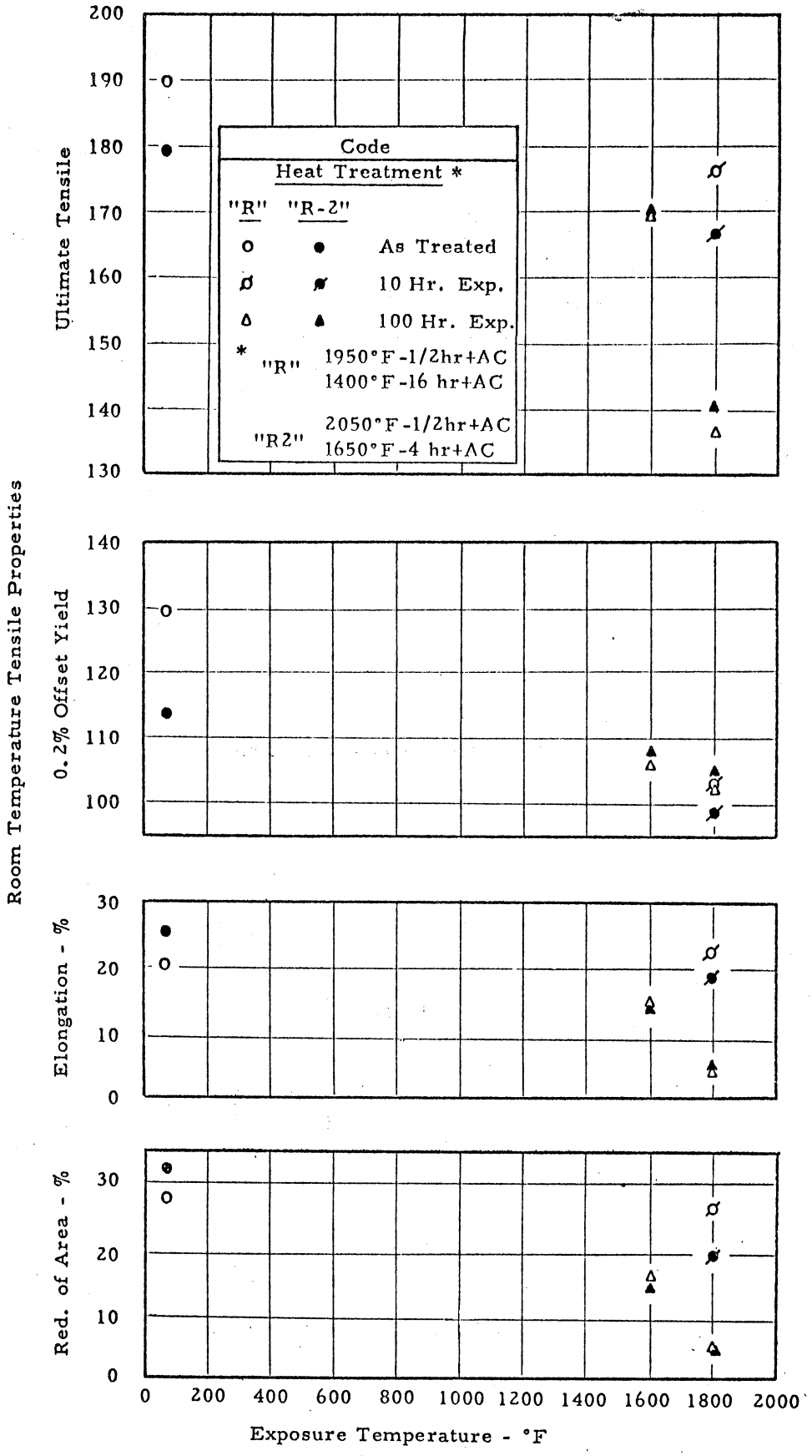

Figure 14 Effect of Prior Heat Treatment on Tensile Properties of Rene' 41 After Unstressed Exposure

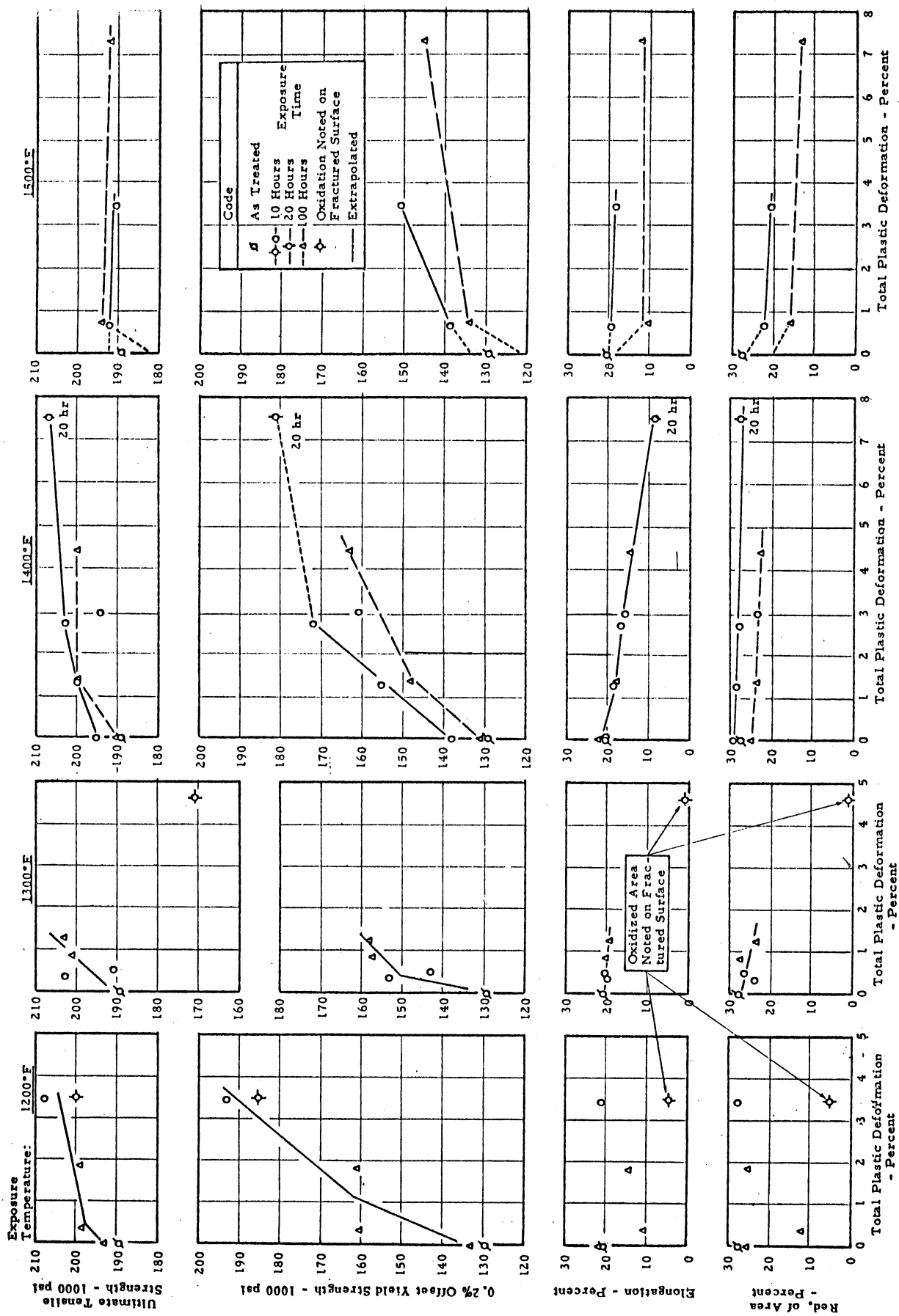

Figure 15 Effect of Prior Creep at 1200°-1500°F On Room Temperature Mechanical Properties of Rene' 41 (Condition "R")

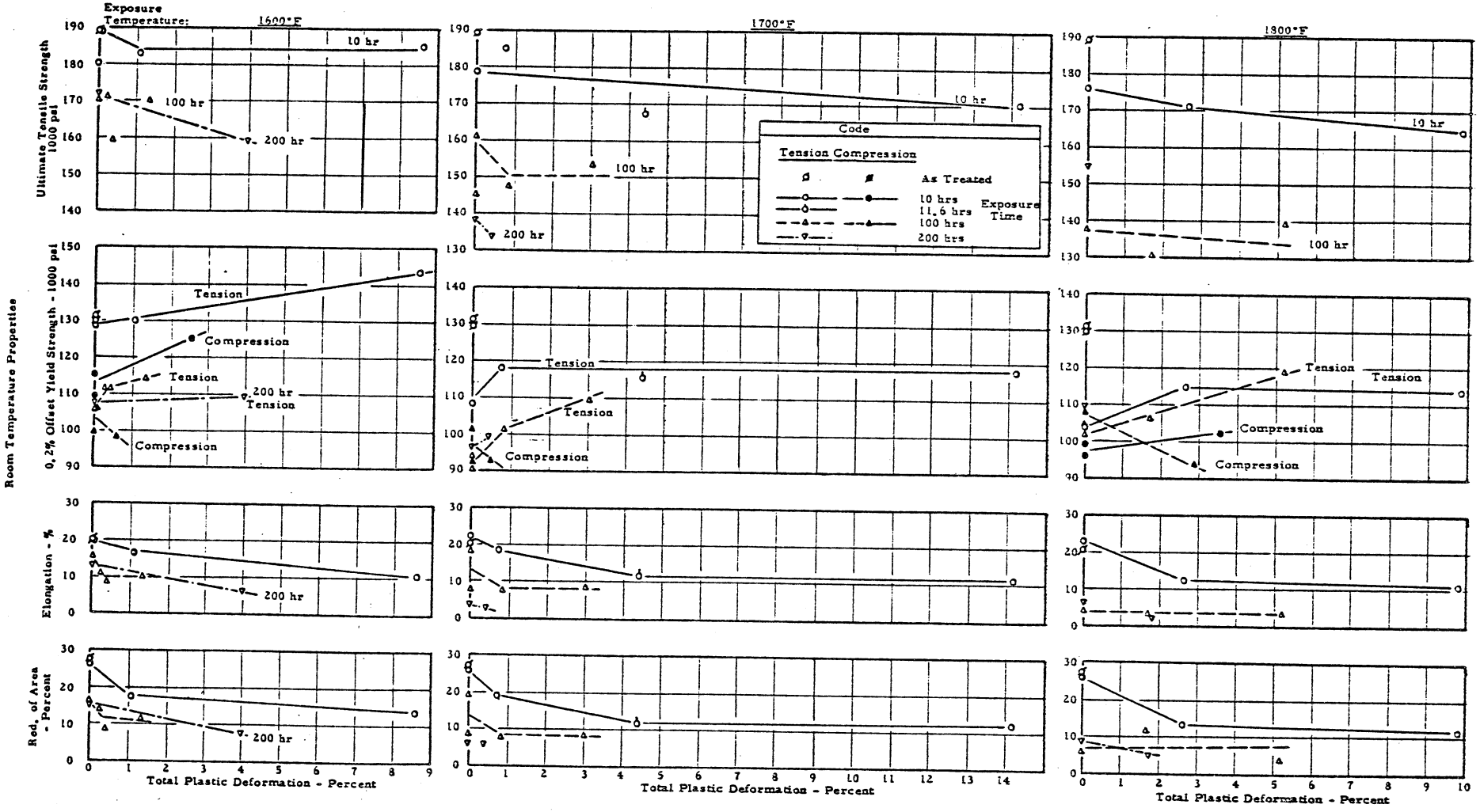

Figure 16 Effect of Prior Creep at 1600°-1800°F On Room Temperature Mechanical Properties of Rene' 41 (Condition "H")

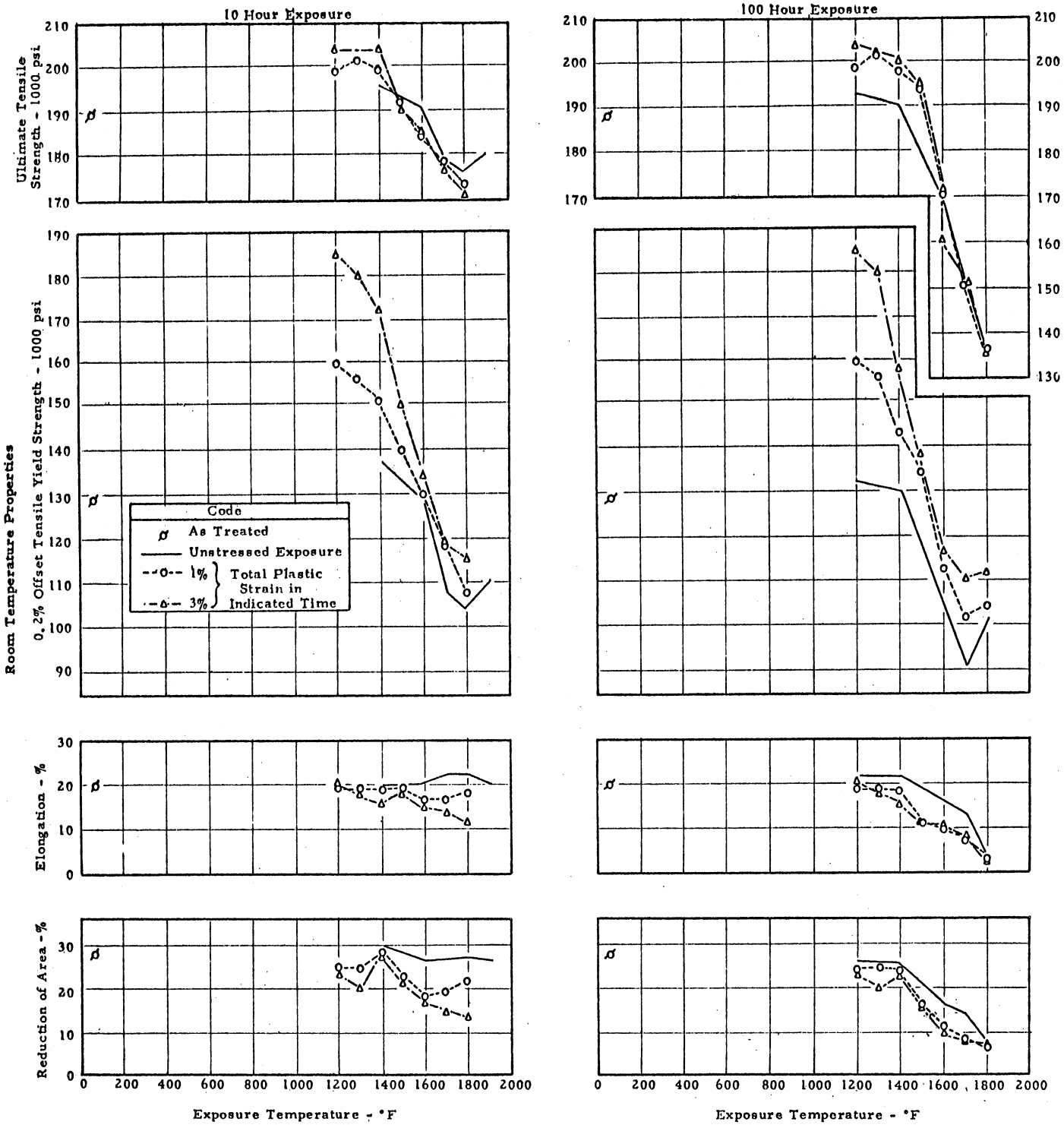

Figure 17 Effect of Exposure Temperature on Room Temperature Tensile Properties of Rene' 41 Alloy (Condition "R") Subjected to Creep-Exposures of 1 Percent or 3 Percent at 1200° to 1800°F

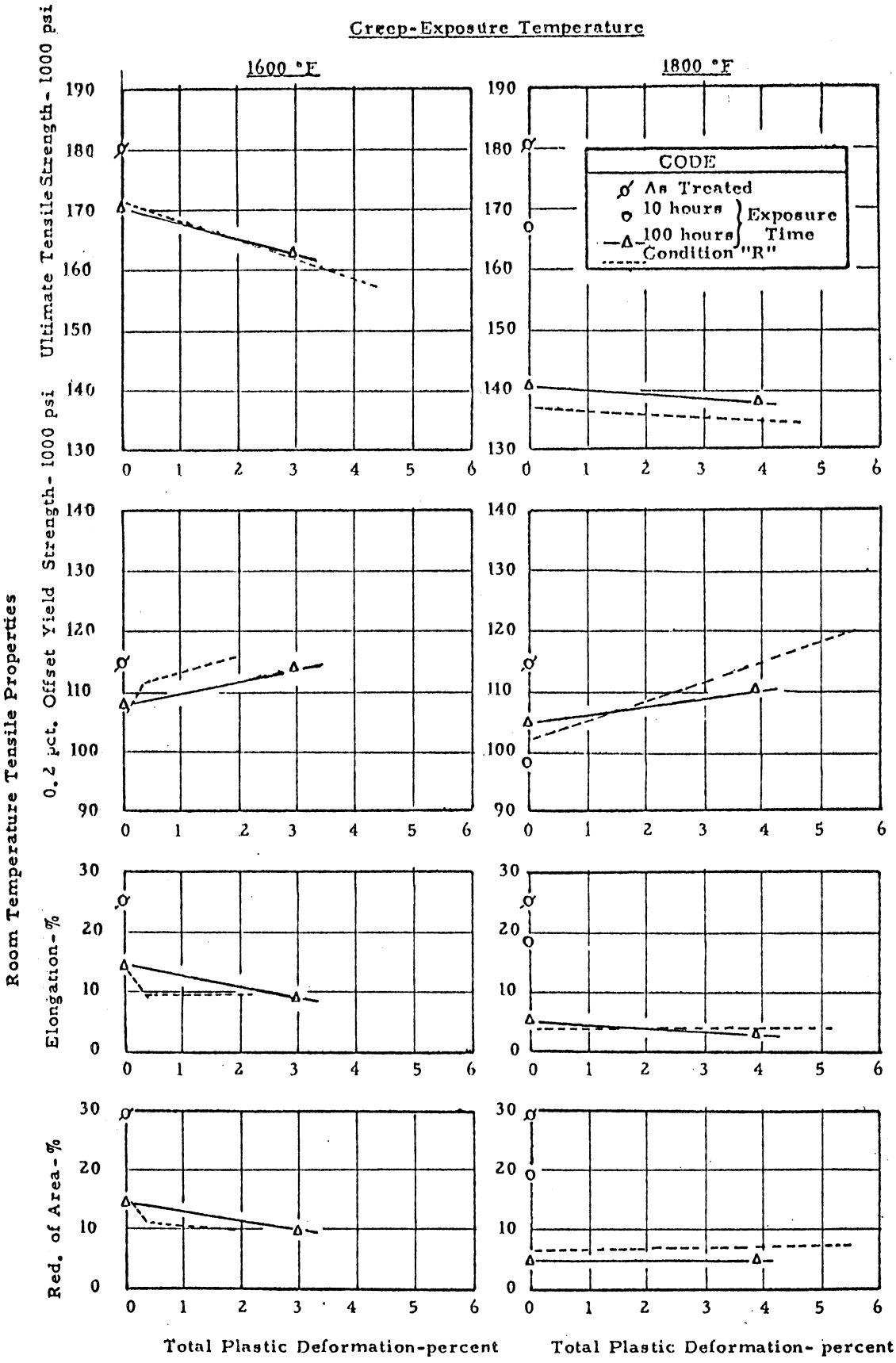

Figure 18 Effect of Heat Treatment and Prior Creep-Exposure at 1600° or 1800°F ire on Room Temperature Tensile Properties of Rene' 41 ("R2" Condition Compared With "R" Condition)

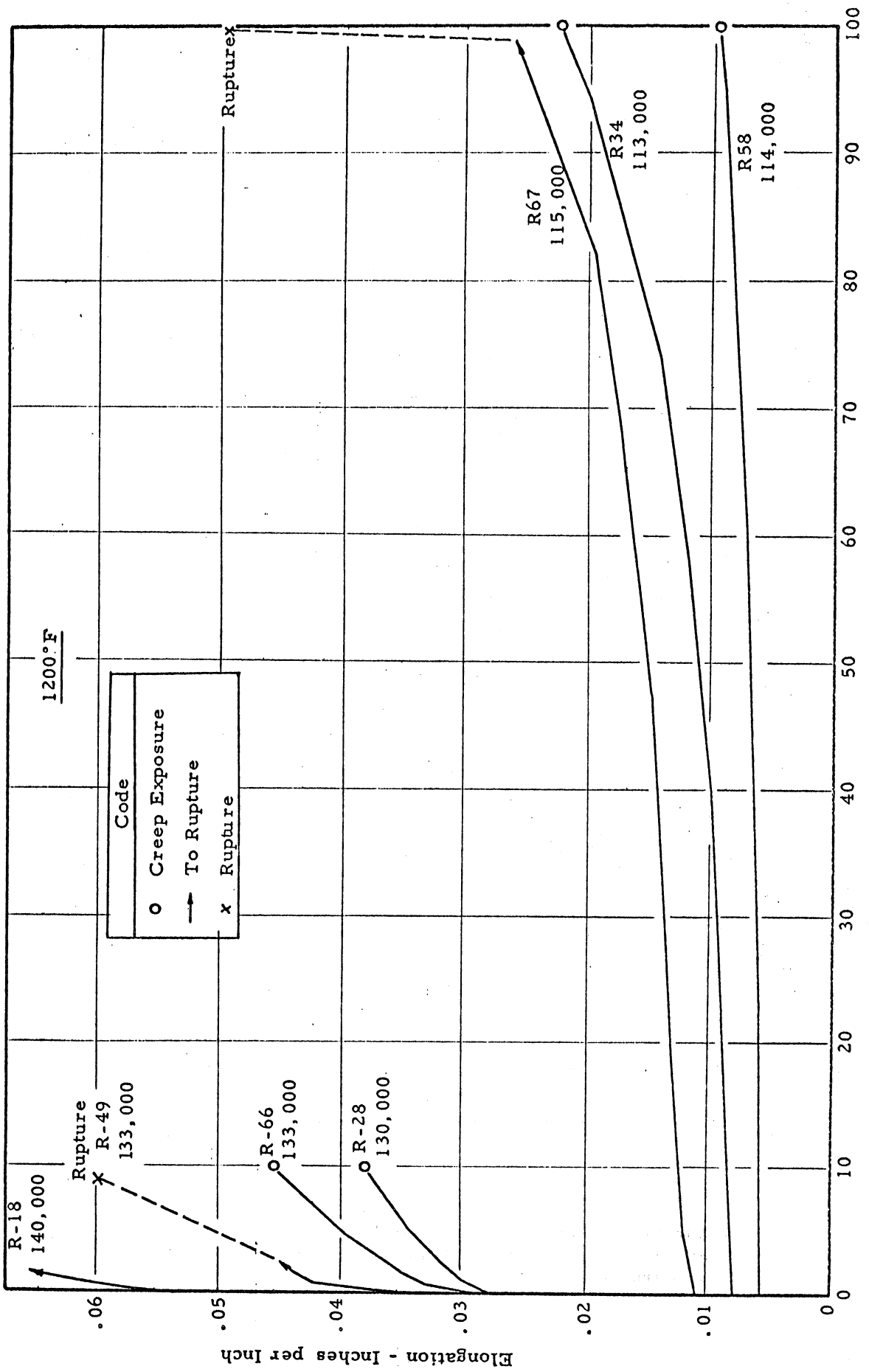

Figure 19 Time-Elongation Curves for Rene' 41 at 1200°F

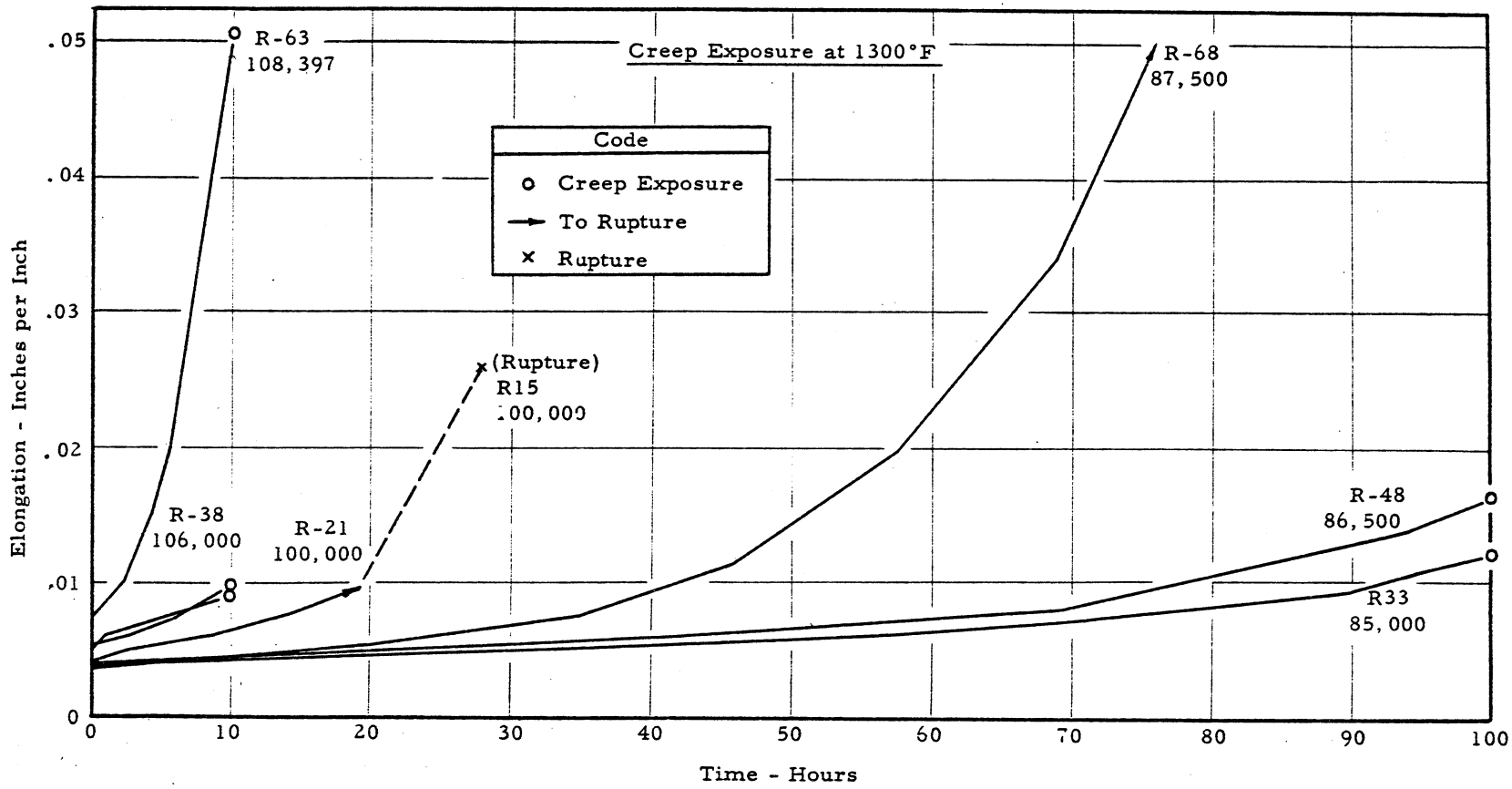

Figure 20 Time-Elongation Curves for Rene' 41 at 1300°F

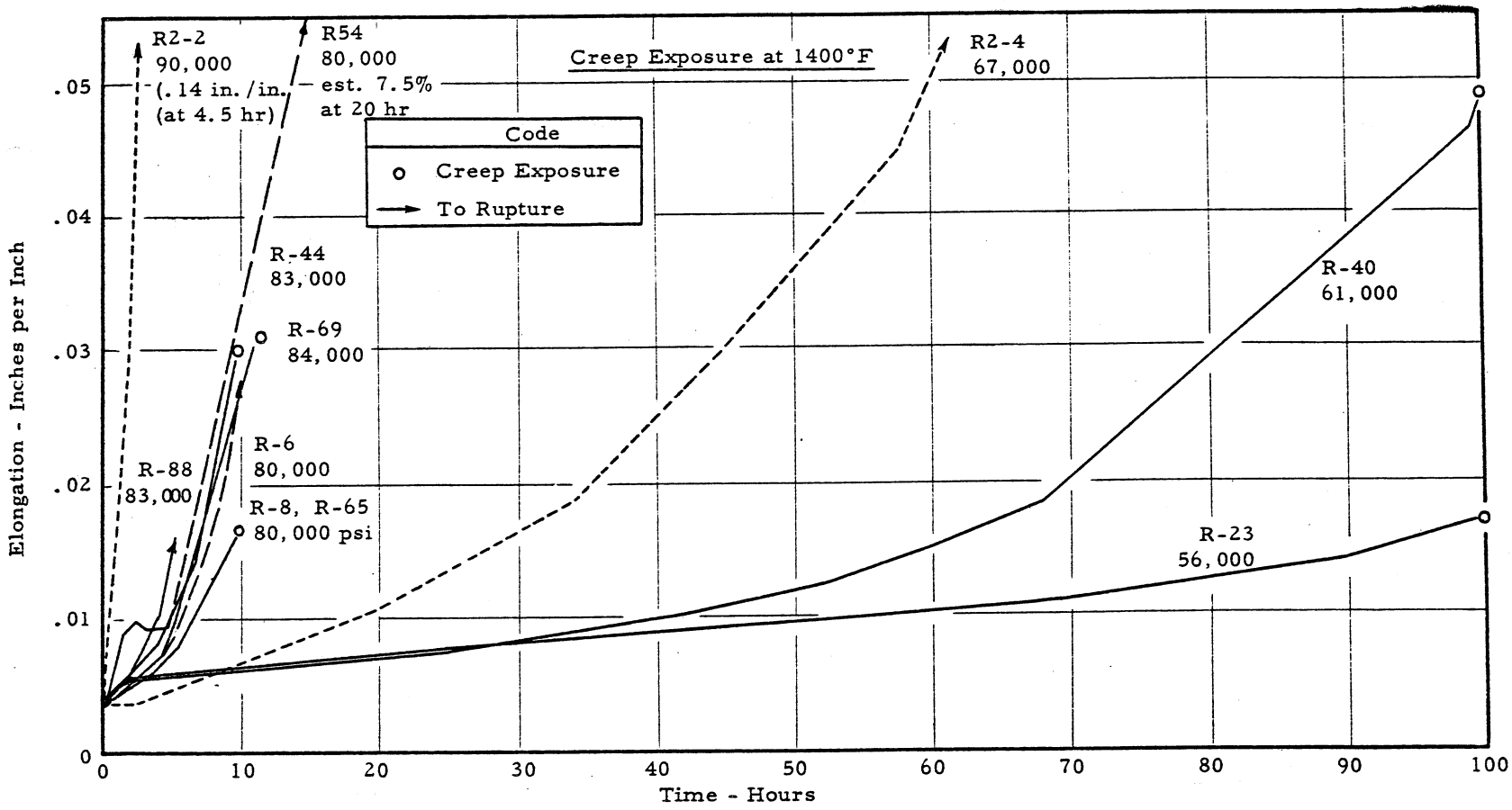

Figure 21 Time-Elongation Curves for Rene' 41 at 1400°F

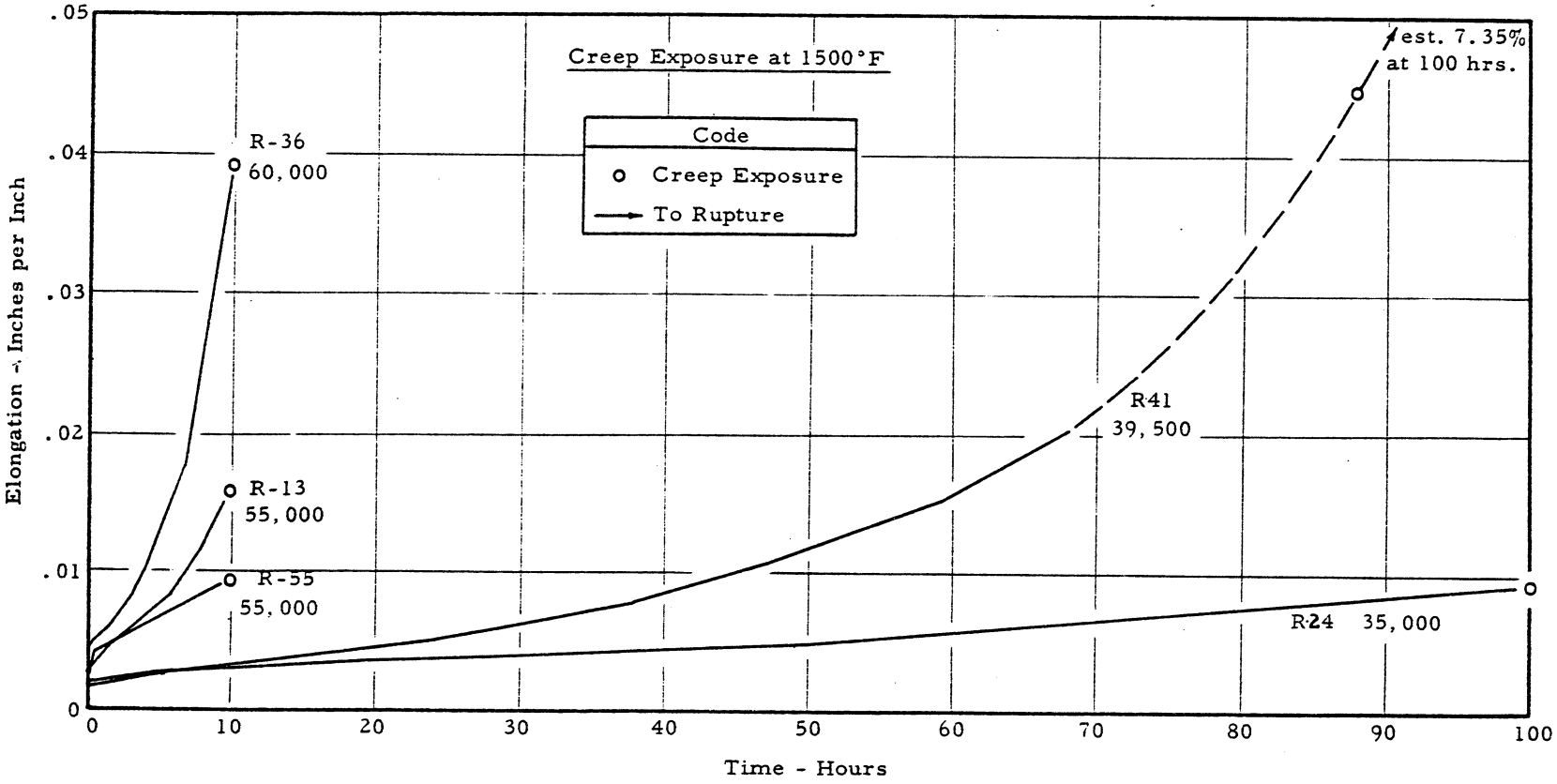

Figure 22 Time-Elongation Curves for Rene' 41 at 1500°F

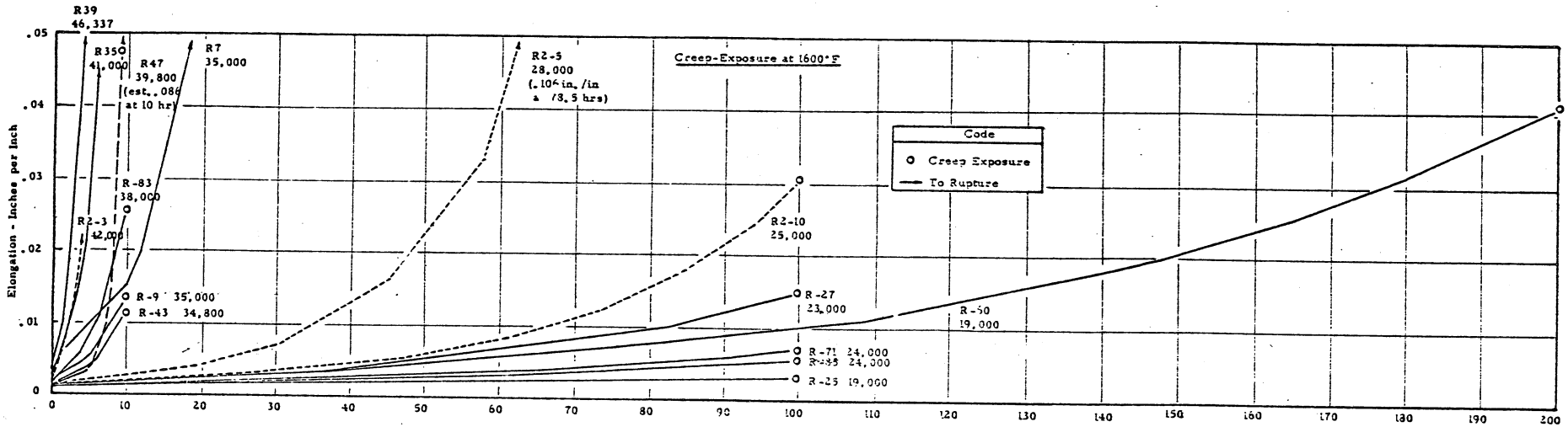

Figure 23 Time-Elongation Curves for Rene' 41 at 1600°F

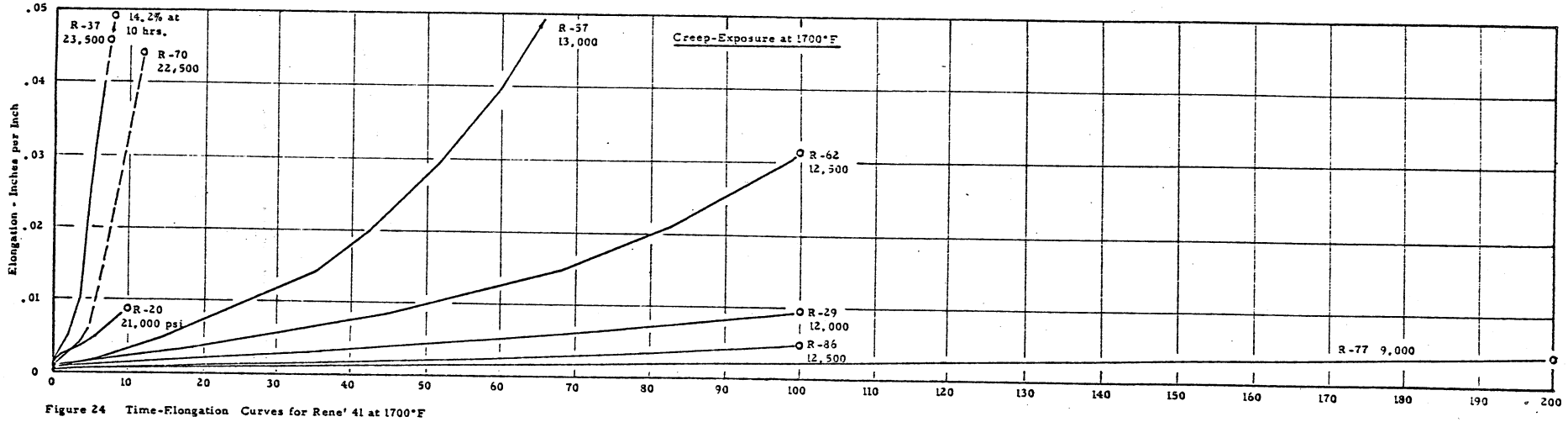

Figure 24 Time-Elongation Curves for Rene' 41 at 1700°F

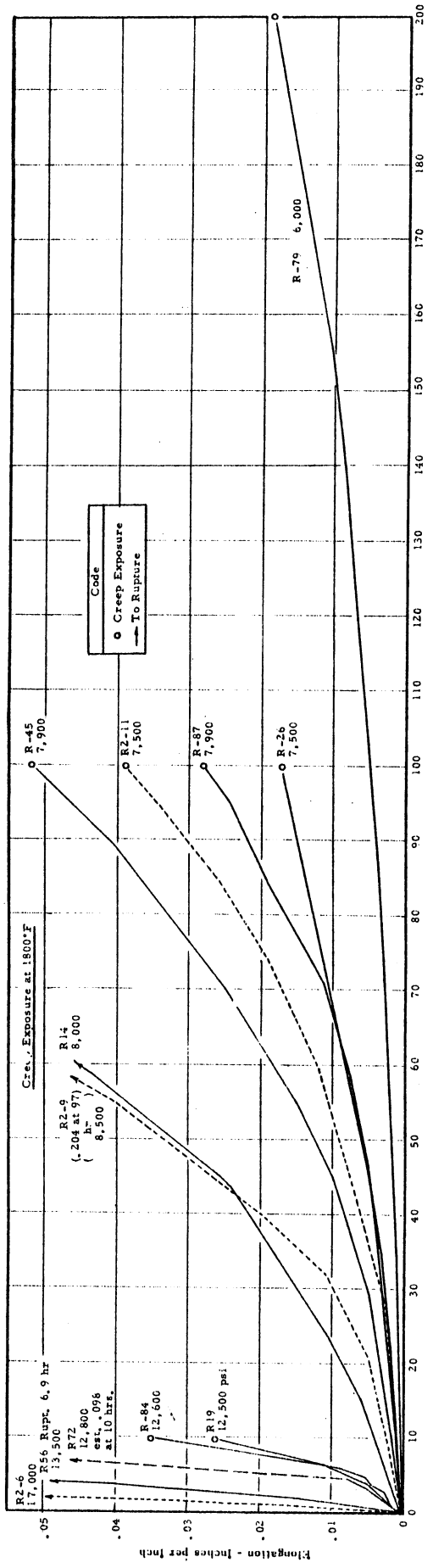

Figure 25 Time-Elongation Curves for Rene' 41 at 1800°F

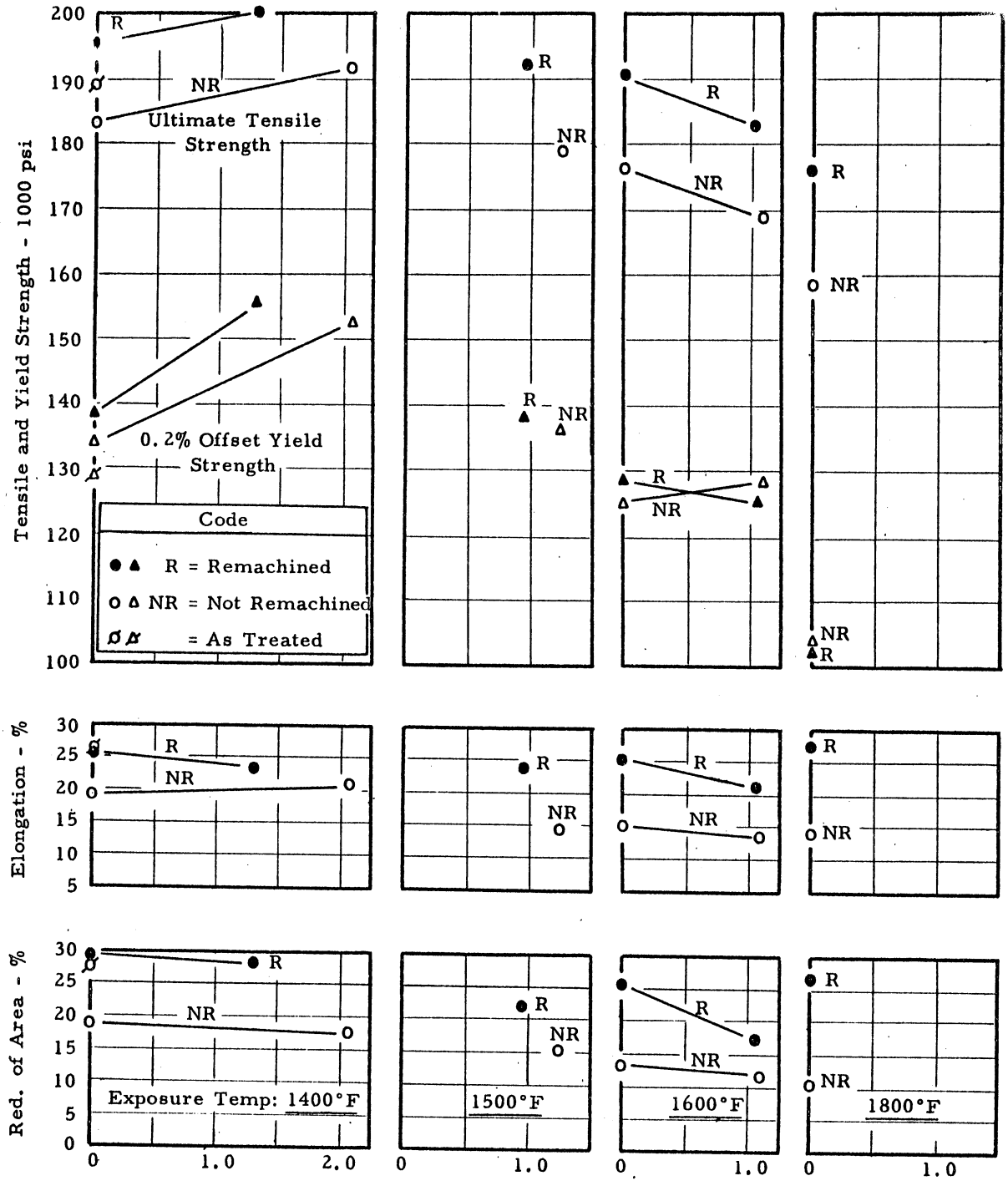

Figure 26 Effect of Remachining on Room Temperature Tensile Properties of Rene' 41 Subjected to Indicated Creep-Exposure. (Remachining Removed Approximately 0.025-inches from Diameter of Gage Section)

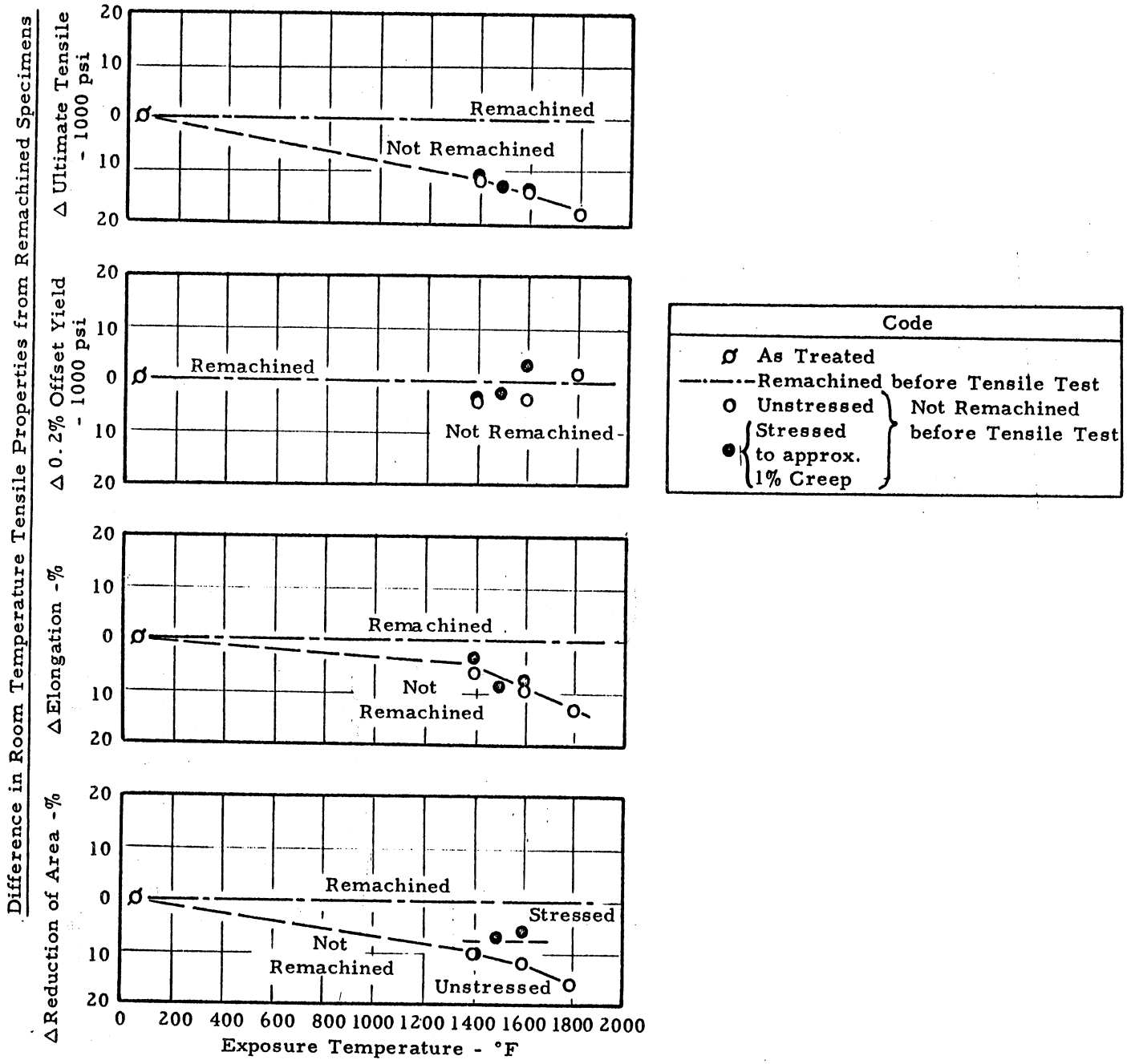

Figure 27 Effect of Exposure Temperature on Difference in Room Temperature Tensile Properties Caused by Remachining Rene' 41 after 10 Hours Exposure at 1400° to 1800°F Either Unstressed or to Approximately One Percent Creep Strain.

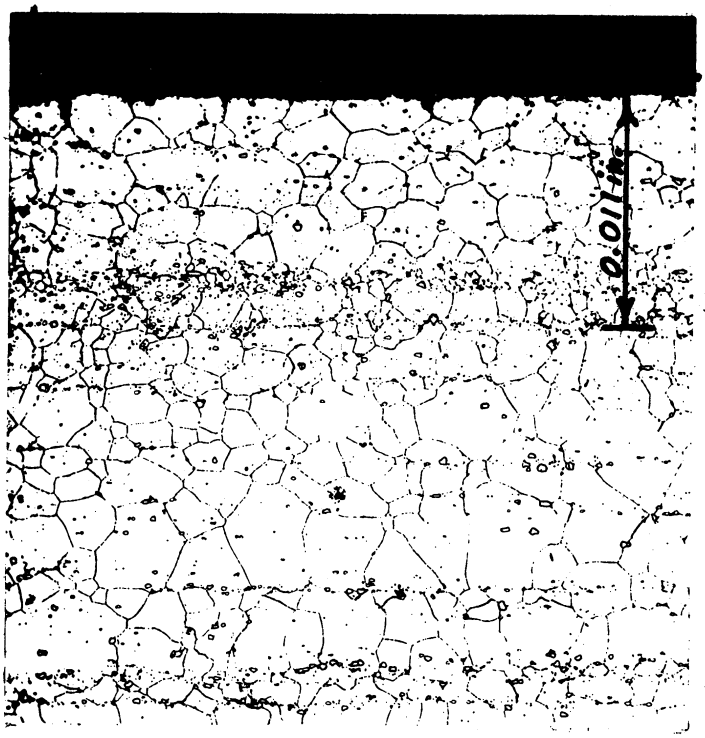

Figure 28 Specimen R-9 - Original Surface (Exposed 10 hrs at 1600°F to 1.13 percent creep. Not re-machined prior to tensile test. Dimension indicated shows amount correspondingly machined from Specimen R-43)

Ductility in Subsequent Room Temperature Test

Elongation: 8.9%

Red. of Area: 11.5%

G-etch
100x

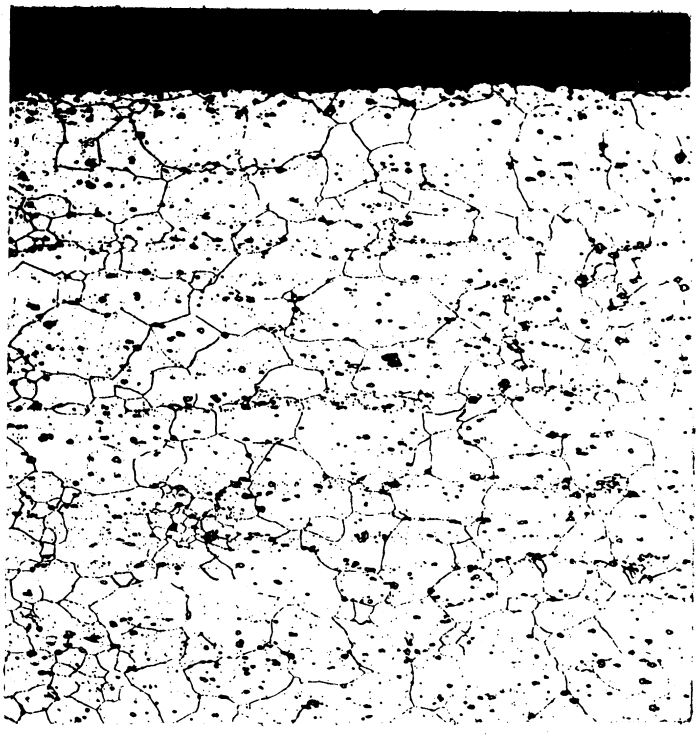

Figure 29 Specimen R-43 - Remachined before tensile test. (Exposed 10 hrs at 1600°F to 1.07 percent creep. 0.022-inches machined from diameter prior to tensile test)

Ductility in Subsequent Room Temperature Test

Elongation: 16.5%

Red. of Area: 17.8%

G-etch
100x

Figures 28-29 Optical Micrographs of Longitudinal Sections Showing Edges of Unmachined and Remachined Creep-Exposure Specimens of Rene' 41 Alloy After Room Temperature Tensile Tests

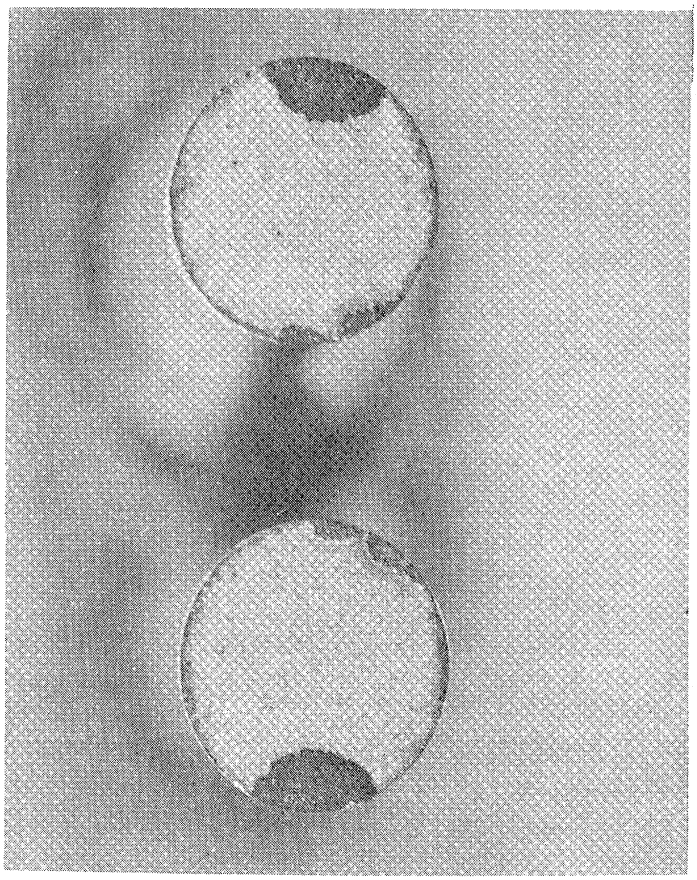

Figure 30 Specimen R-63 (Oxidized Areas on Fracture Surface) Creep-Exposure 10 Hours at 1300°F to 4.60% Deformation
(0.033-inches machined from dia. prior to tensile test)
Elongation: 0.4%
Red. of Area: 0.7%

4.7x

Figure 31 Specimen R-12 (Longitudinal Section to Show Surface Attack) Exposed Without Stress 10 Hours at 1800°F
(Not remachined before tensile test)
Elongation: 9.5%
Red. of Area: 10.5%

Corresponding Remachined Specimen
Elongation: 22.6%
Red. of Area: 26.5%

1000x

Figures 30-31 Optical Micrographs Showing Surface Attack on Rene' 41

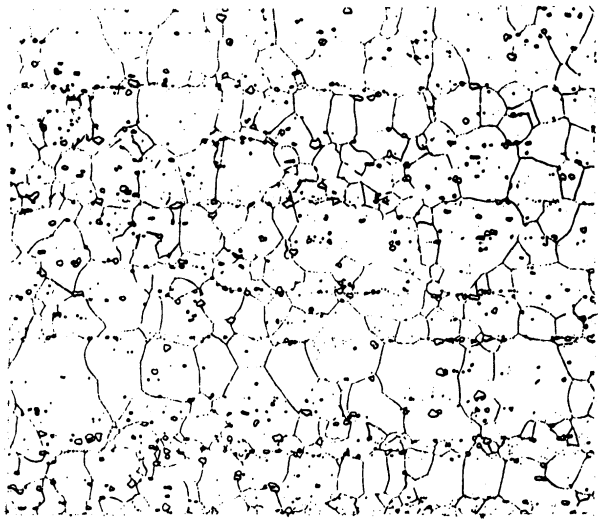

Figure 32 100x

Figure 33 1000x

Rene' 41 As-Treated (Condition "R")
Tensile Properties
UTS = 189,800 psi
0.2% YS = 129,733 psi
El = 20.5%
RA = 27.9%

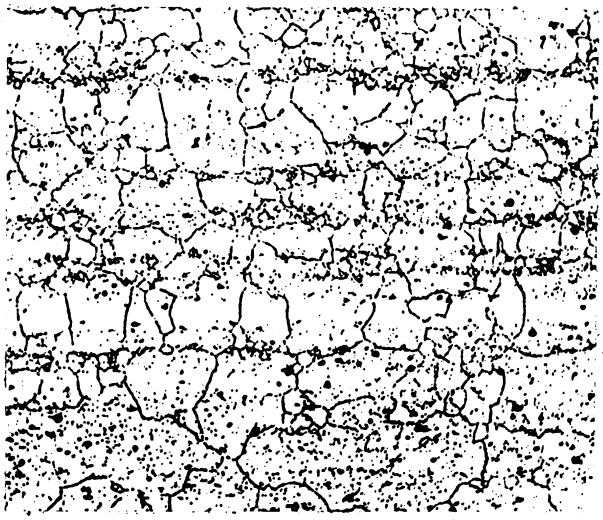

Figure 34 100x

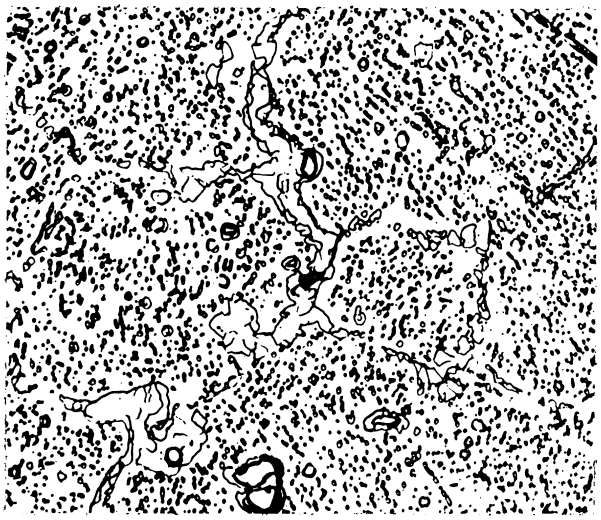

Figure 35 1000x

Spec. R-45 Creep-Exposure at 1800°F
100 hrs - 7900 psi - to
5.17% deformation
Tensile Properties (remachined)
UTS = 139,500 psi
0.2% YS = 119,000 psi
El = 3.5%
RA = 4.1%

Figures 32-35 Optical Micrographs of Rene' 41 Before and After Creep-Exposure

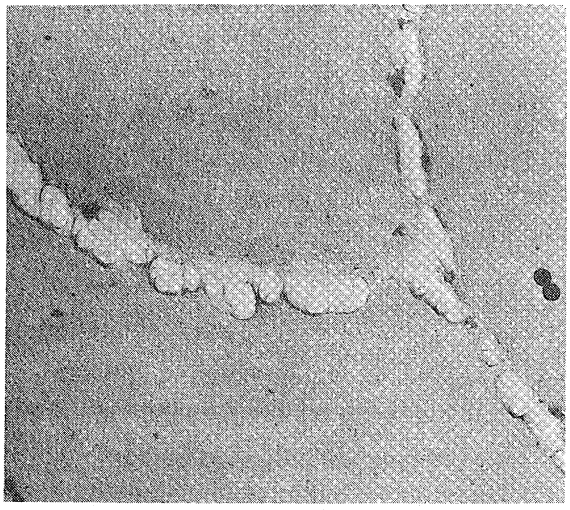

Figure 36 8200x
As Heat Treated
(Condition "R")

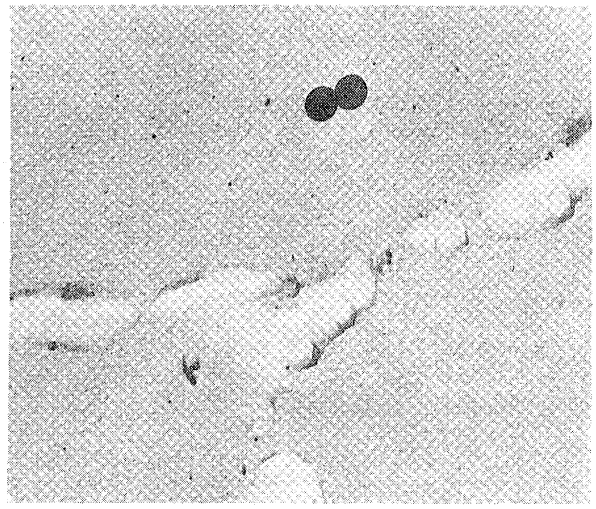

Figure 37 16000x
As Heat Treated
(Condition "R")

Elong. 20.5%
Red. Area 27.9%

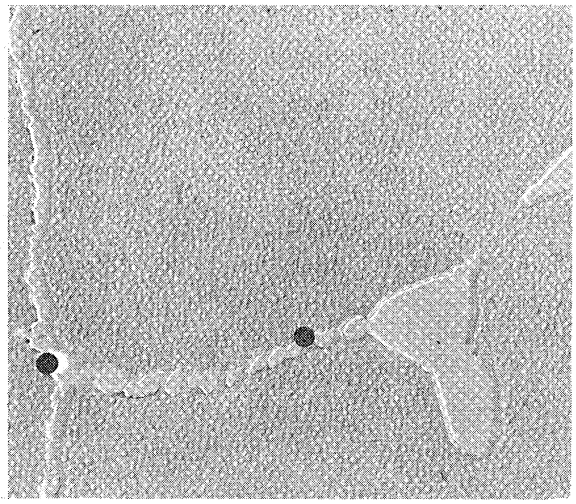

Figure 38 8200x
Specimen R-24 Creep-Exposure 100 Hours at 1500°F to 0.71% Deformation
Elong. 10.5%
Red. Area 15.7%

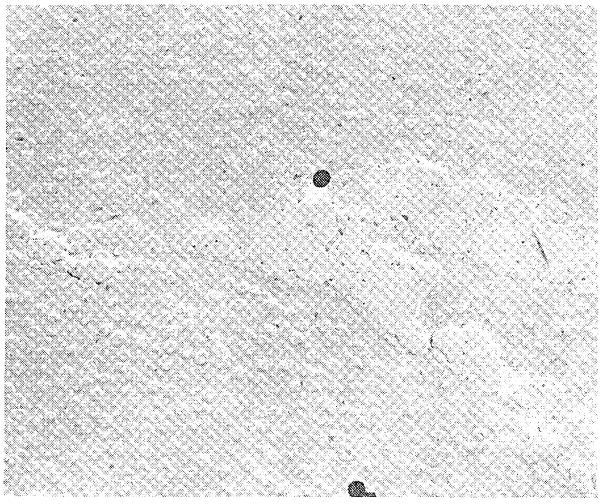

Figure 39 8200x
Specimen D-1 Exposed 436 Hours at 1550°F in Dilatometer Furnace

Ductilities indicated for room temperature tensile test after creep-exposure

Figures 36-39 Electron Micrographs of Rene' 41 After Creep-Exposure

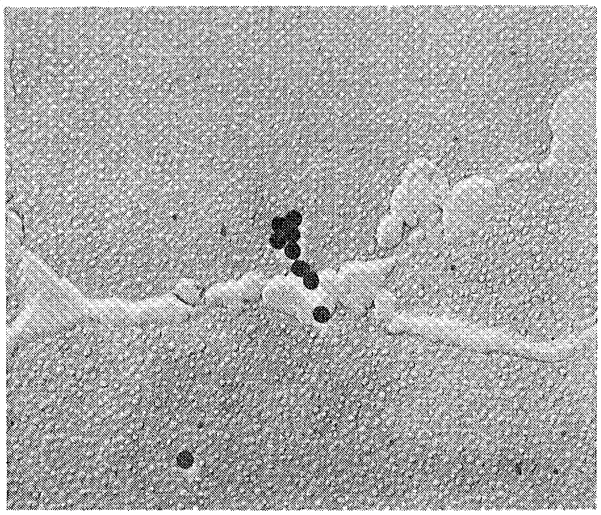

Figure 40 8200x
Specimen R-52 Exposed Without Stress 10 Hours at 1600°F

Elong. 20.4%
Red. Area 25.9%

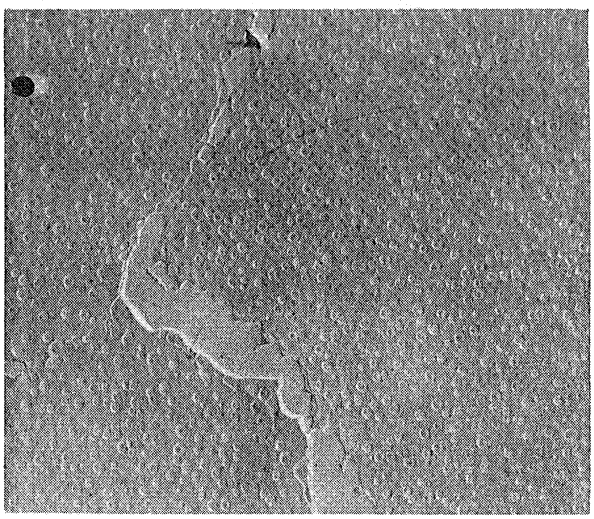

Figure 41 8200x
Specimen R-27 Creep-Exposure 100 Hours at 1600°F to 1.35% Deformation

Elong. 10.3%
Red. Area 11.7%

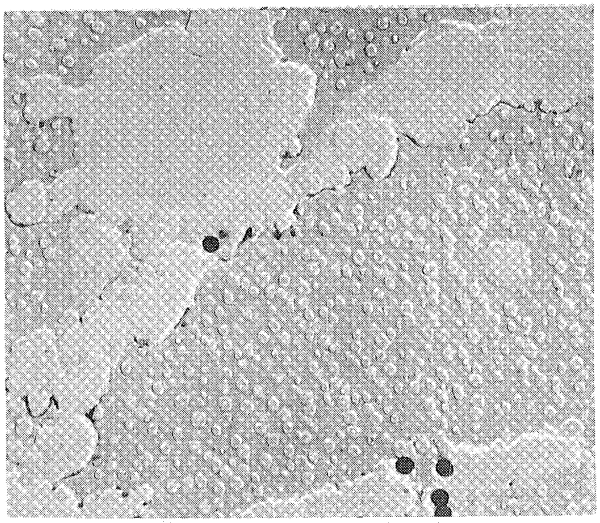

Figure 42 8200x
Specimen R-60 Creep-Exposure 200 Hours at 1600°F to 4.05% Deformation

Elong. 6.8%
Red. Area 7.9%

Ductilities indicated for room temperature tensile test after creep-exposure

Figures 40-42 Electron Micrographs of Rene' 41 After Creep-Exposure

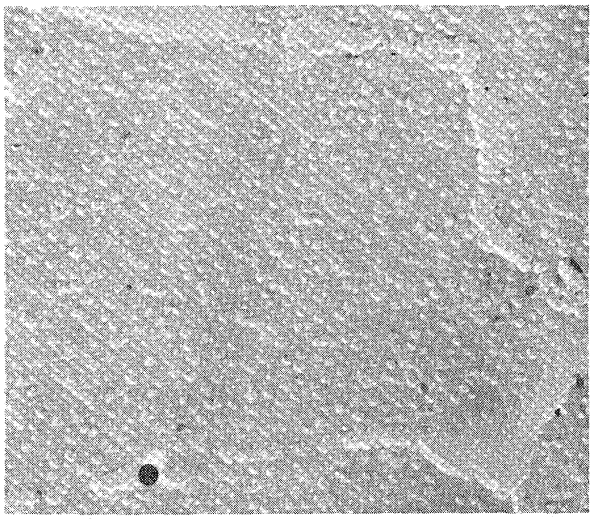

Figure 43 8200x
Specimen R-42 Exposed Without Stress 10 Hours at 1700°F

Elong. 22.9%
Red. Area 26.5%

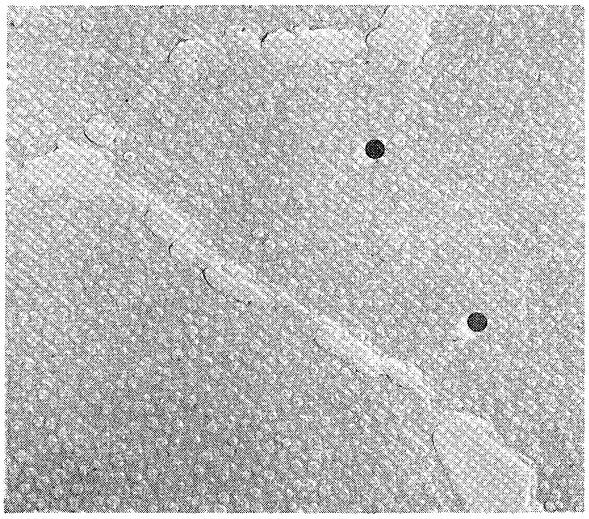

Figure 44 8200x
Specimen R-37 Creep-Exposure 10 Hours at 1700°F to 14.2% Deformation

Elong. 11.3%
Red. Area 12.0%

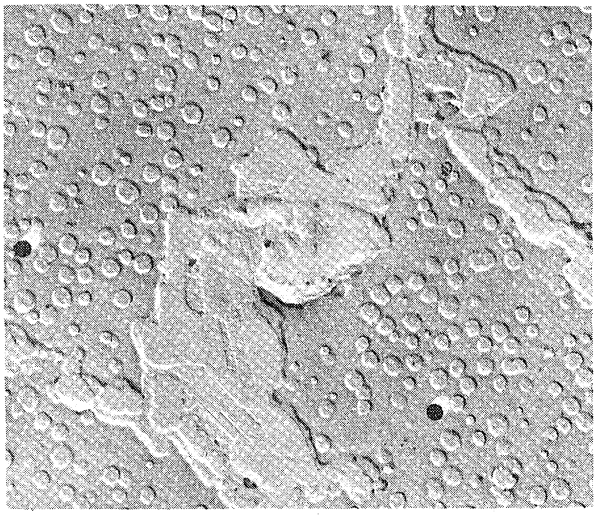

Figure 45 8200x
Specimen R-62 Creep-Exposure 100 Hours at 1700°F to 3.04% Deformation

Elong. 8.2%
Red. Area 8.0%

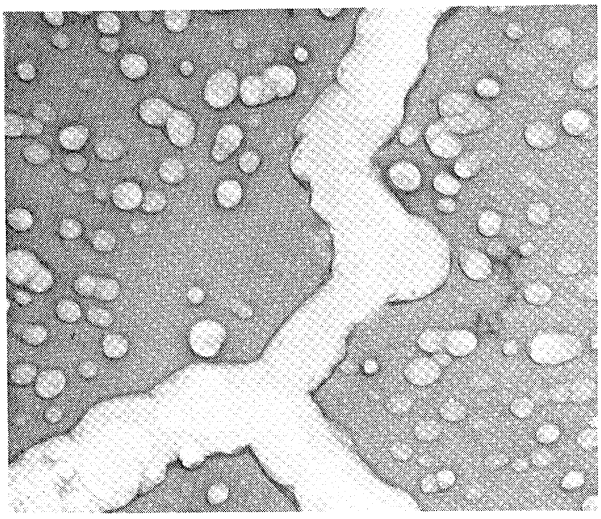

Figure 46 8200x
Specimen R-77 Creep-Exposure 200 Hours at 1700°F to 0.41% Deformation

Elong. 2.7%
Red. Area 5.7%

Ductilities indicated for room temperature tensile test after creep-exposure

Figures 43-46 Electron Micrographs of Rene' 41 After Creep-Exposure

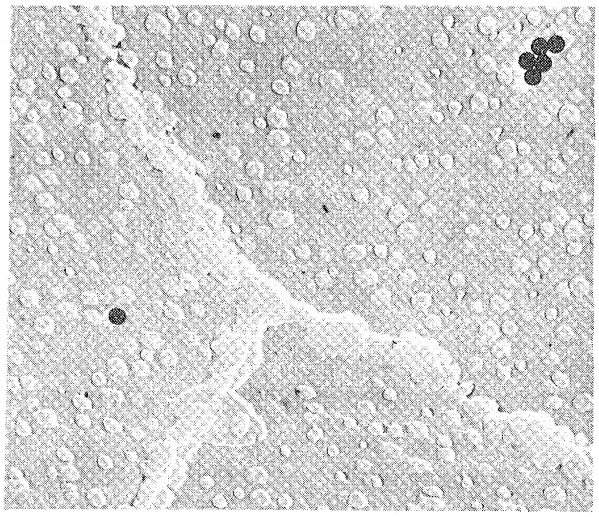

Figure 47 8200x
Specimen R-61 Exposed Without Stress 10 Hours at 1800°F

Elong. 22.6%
Red. Area 26.5%

Figure 48 8200x
Specimen R-45 Creep-Exposure 100 Hours at 1800°F to 5.17% Deformation

Elong. 3.5%
Red. Area 4.1%

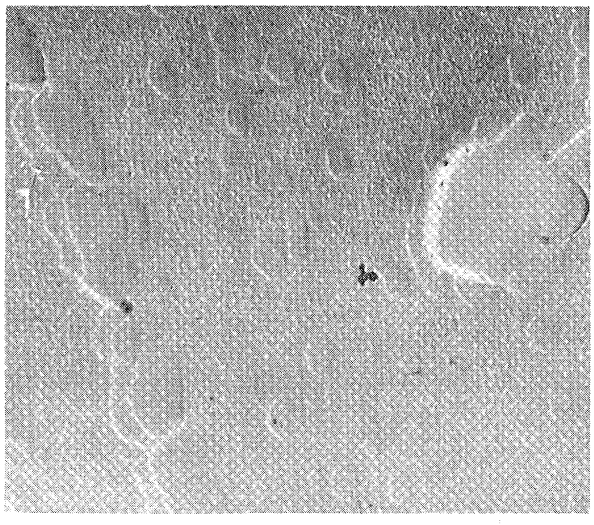

Figure 49 8200x
Specimen R-79 Creep-Exposure 200 Hours at 1800°F to 1.80% Deformation

Elong. 2.2%
Red. Area 5.7%

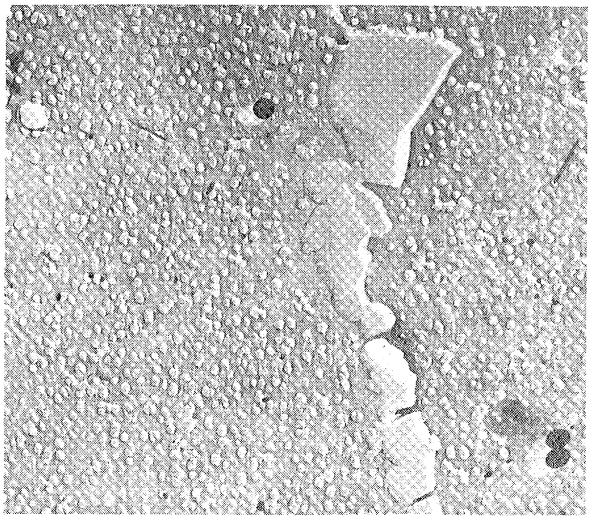

Figure 50 8200x
Specimen R-46 Exposed Without Stress 10 Hours at 1900°F

Elong. 20.6%
Red. Area 26.0%

Ductilities indicated for room temperature tensile test after creep-exposure

Figures 47-50 Electron Micrographs of Rene' 41 After Creep-Exposure

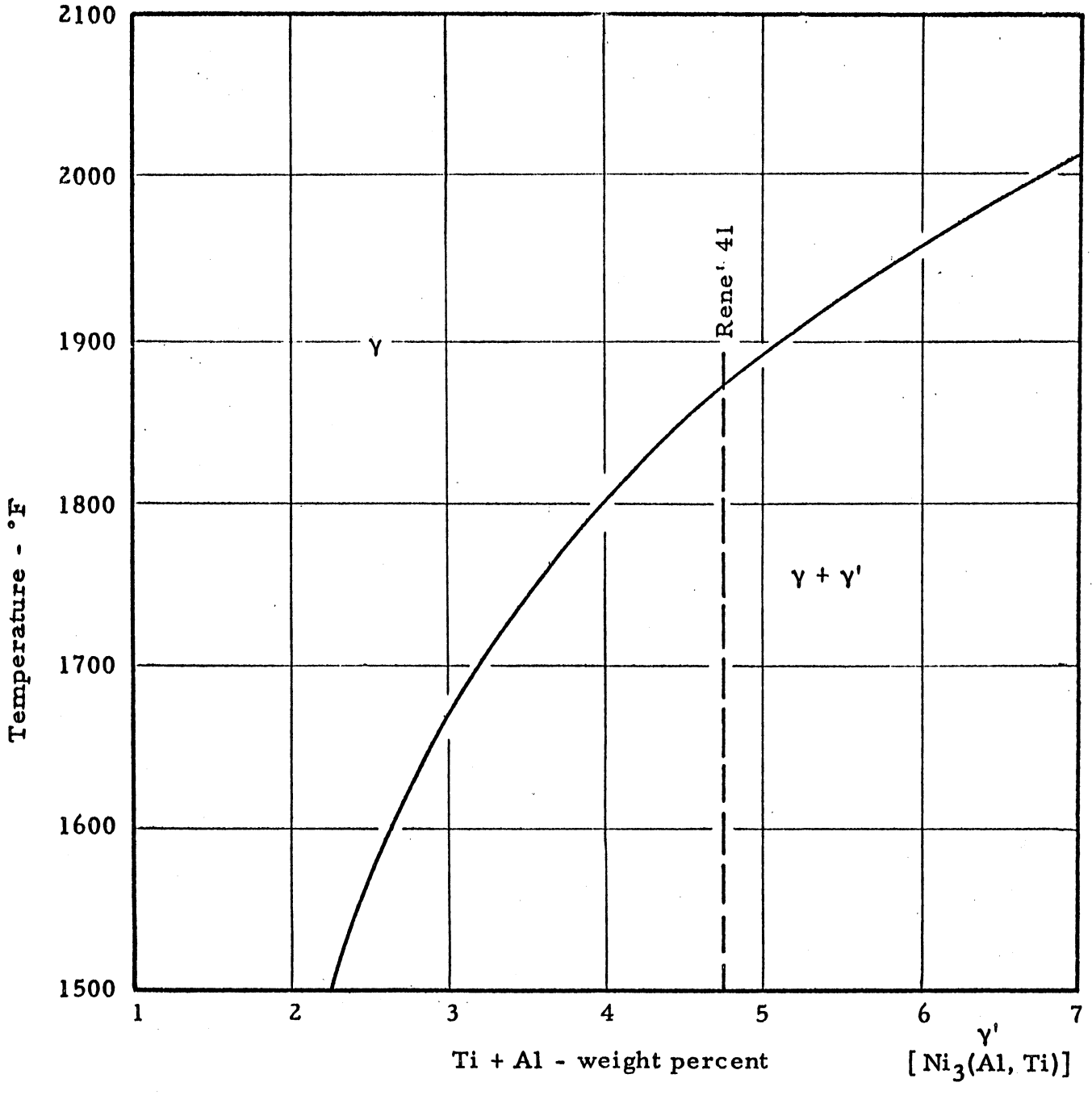

Figure 51 Effect of Ti + Al Content on Solution Temperature of γ'
(Curve of Betteridge and Franklin (Ref. 12)

Figure 52 8200x
Normal Etch

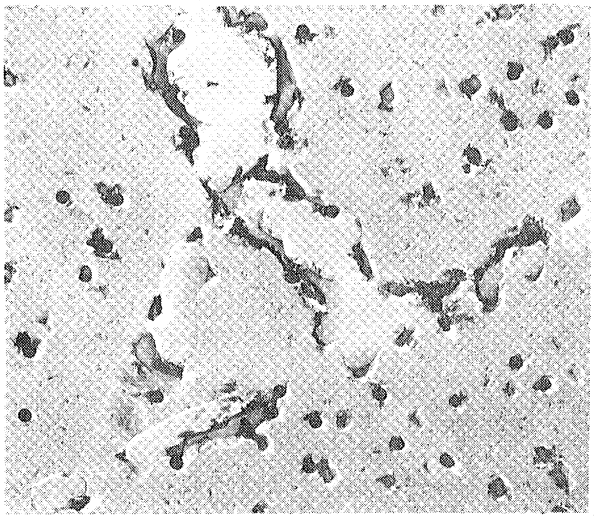

Figure 53 8200x
Selective Etch to Remove γ'

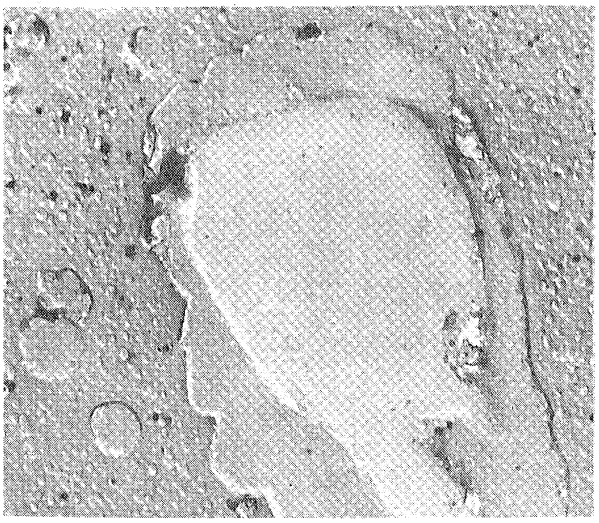

Figure 54 16000x
Normal Etch

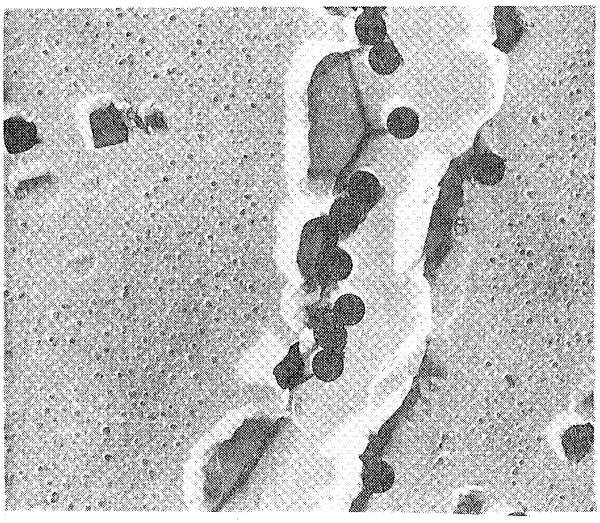

Figure 55 16000x
Selective Etch to Remove γ'

All Pictures are Specimen R-26
Creep-Exposed 100 Hours at 1800°F
to 1.70% Deformation

Figures 52-55 Electron Micrographs of Specimen R-26 Selectively Etched to Show γ' Location

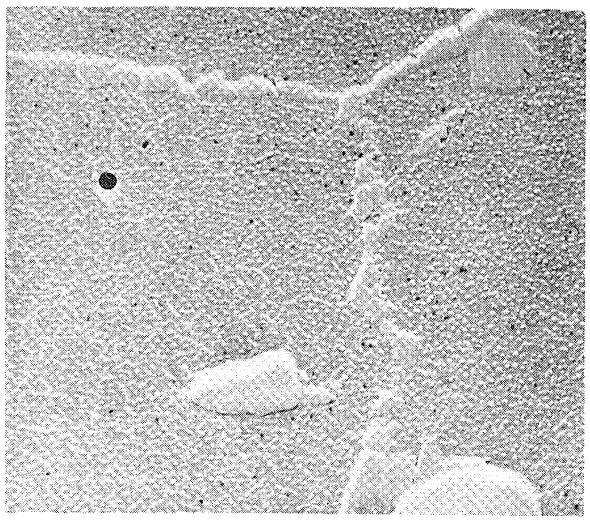

Figure 56 8200x
As Heat Treated
(Condition "R2")

Elong. 25.3%
Red. Area 28.6%

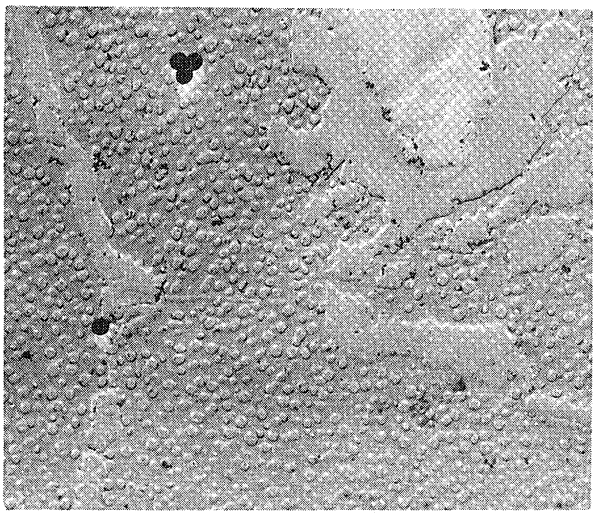

Figure 57 8200x
Specimen R2-10 Creep-Exposure
100 Hours at 1600°F to 2.92%
Deformation

Elong. 9.0%
Red. Area 9.9%

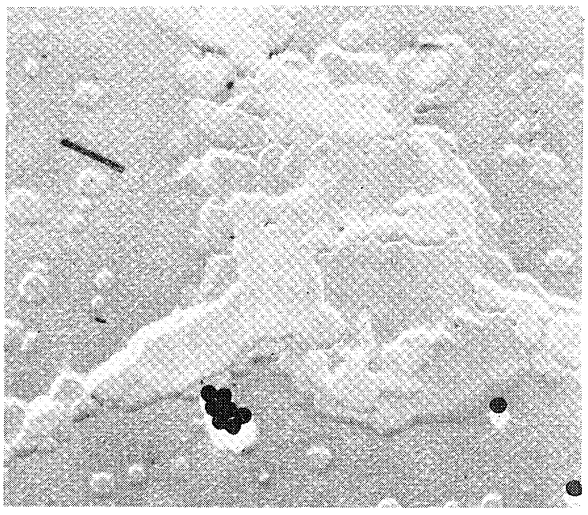

Figure 58 8200x
Specimen R2-8 Exposed Without
Stress 100 Hours at 1800°F

Elong. 5.0%
Red. Area 4.9%

Ductilities indicated for room temperature tensile tests after creep-exposure

Figures 56-58 Electron Micrographs of Rene' 41 in Condition "R2"